Genomic influences on platelet function

A thesis submitted in partial fulfilment of the degree of

Doctor of Philosophy

University of London

2014-2018

Melissa Anne Hayman

The William Harvey Research Institute
Barts and the London School of Medicine and Dentistry
Queen Mary University of London
London, United Kingdom

Statement of originality

I, Melissa Hayman, confirm that the research included within this thesis is my own work or that where it has been carried out in collaboration with, or supported by others, that this is duly acknowledged below and my contribution indicated. Previously published material is also acknowledged below.

I attest that I have exercised reasonable care to ensure that the work is original, and does not to the best of my knowledge break any UK law, infringe any third party's copyright or other Intellectual Property Right, or contain any confidential material.

I accept that the College has the right to use plagiarism detection software to check the electronic version of the thesis.

I confirm that this thesis has not been previously submitted for the award of a degree by this or any other university.

Signature: M. A. Hayman
Date: 28/02/2018

Acknowledgements

Firstly, I'd like to thank Tim for your expert supervision and for enabling me to complete my PhD within your research group. Thanks for always having an enormous amount of time for me on both a personal and professional level. I am hugely grateful for all of the opportunities I was given whilst in your group and had an overall thoroughly fantastic PhD experience.

Thanks to all past and present TW lab members whom I had the pleasure of working alongside in the lab - Thomas, Plinio, Trauma Paul, Mari, Original Paul and Ivana, for your invaluable help and wonderful company. We had some fabulously memorable, big night's/day's/week's out together.

A special thank you to Mel for all of your support. Not only were you excellent at sorting out my professional and scientific problems but also brilliant at giving me calm and rational grown-up life advice.

To my best pals Harriet and Gareth - I wouldn't have had half as much fun without the pair of you and I feel very lucky to have found such wonderful friends in both of you.

To my non-scientific partner Phill thank you for enduring the psychological stress of listening to me practice the same presentation repeatedly each night for two weeks. In the instances where I may have been displaying melodramatic tendencies - unlikely, I know - thank you for your ability to diffuse those episodes.

Finally, thanks to my family for their unwavering belief in my ability to complete my PhD and for very politely showing interest in my work.

Details of collaborations

Liquid chromatography tandem mass spectrometry (LCMS/MS) analysis of eicosanoid production (chapter 4 and 6) was carried out and analysed by Dr. Matthew Edin and Dr. Darryl Zeldin at The National Institute of Environmental Health Science, North Carolina, USA

DNA sequencing and bioinformatics analysis of the PTGS1 mutated family was carried out in Cambridge, UK in accordance with the BRIDGE-BPD study protocol.

RNA-Seq and bioinformatics analysis for the $cPLA_{2\alpha}$ mutated patient samples was carried out by Dr. Charles Mein at the QMUL Genome Centre.

Details of publications

Papers

Knowles RB, Lawrence MJ, Ferreira PM, **Hayman MA**, D'Silva LA, Stanford SN, Sabra A, Tucker AT, Hawkins KM, Williams PR, Warner TD, Evans PA. *Platelet reactivity influences clot structure as assessed by fractal analysis of viscoelastic properties*. Platelets. 2017 May 15:1-9. doi: 10.1080/09537104.2017.1306039

Armstrong PC, Hoefer T, Knowles RB, Tucker AT, **Hayman MA**, Ferreira PM, Chan MV, Warner TD*. Newly Formed Reticulated Platelets Undermine Pharmacokinetically Short-Lived Antiplatelet Therapies.* Arteriosclerosis Thrombosis and Vascular Biology 2017 May;37(5):949-956. doi:10.1161/ATVBAHA.116.308763. Epub 2017 Mar

Abstracts

MA Hayman, PC *Armstrong, MV Chan, TD Warner. Functional Analyses of Reticulated Platelets. FASEB J* August 2017; 31 (8)

MA Hayman, PC Armstrong, TD Warner. *Comparison of reticulated and non-reticulated platelet function and releasates.* Research and Practice in Thrombosis and Haemostasis July 2017: 1 (S1)

MA Hayman, PC Armstrong, TD Warner. *Isolation and functional analysis of reticulated platelets.* pA2 online 2016 http://www.pa2online.org

MA Hayman, MV Chan, PC Armstrong, NS Kirkby, PB Munroe, TD Warner. *A Systematic Comparison of Protocols for the Isolation of Platelets From Whole Blood For RNA Analyses.* pA2 online 2015 http://www.pa2online.org

RB Knowles, MV Chan, PCJ Armstrong, CC Shih, **MA Hayman**, I Vojnovic, AT Tucker, AD Timmis, TD Warner. *The efficacy of $P2Y_{12}$ receptor antagonist therapy is strongly moderated by the endothelial derived mediators prostacyclin and nitric oxide.* pA2 online 2015 http://www.pa2online.org

MA Hayman, MV Chan, NS Kirkby, RB Knowles, PB Munroe, TD Warner. *The Effect of Dual Anti-Platelet Therapy on Platelet Gene Expression.* pA2 online 2014 http://www.pa2online.org

Abstract

The study of platelet messenger and micro-RNAs is of increasing interest owing to the fact that platelets contain the machinery to splice and translate mRNA into proteins in response to inhibitory or activating signals. However, the relatively small size (roughly 4000-5000 transcripts) and short half-life of the platelet transcriptome makes this a technically challenging aspect of platelet biology to investigate.

The aims of these thesis investigations were therefore to optimise protocols for the isolation of platelets for downstream RNA analyses and function testing, to investigate the functional capabilities of platelet subpopulations rich in RNA, and to understand the functional and transcriptomic impact of gene mutations predicted to influence platelet function.

I found that the optimal method for isolating platelets from whole blood is to use simple single step centrifugation to obtain platelet rich plasma. This method is as effective as more involved methods at reducing white blood cell contamination whilst causing minimal platelet activation. Using this method in combination with flow cytometric cell sorting techniques I was able to isolate the newly formed reticulated platelet sub-population and to confirm the link between reticulation status and increased RNA content. Furthermore, using a range of platelet function assays I demonstrated that reticulated platelets are more reactive than non-reticulated platelets. By obtaining blood samples from a patient with a PLA2G4A mutation I was able to show that loss of $cPLA_{2\alpha}$ enzymatic activity alters both platelet function and the expression of certain mRNA transcripts. My investigations using samples from a range of patients with bleeding tendencies show the benefit of combining deep platelet phenotyping with next generation sequencing to understand the causation of bleeding disorders.

Together these investigations highlight the utility of genomic DNA and platelet specific mRNA studies in providing novel insights in to pathways regulating platelet reactivity.

Table of contents

List of figures and tables

Abbreviations

AA	arachidonic acid
ACD	acid citrate dextrose
ADP	adenosine diphosphate
ANOVA	analysis of variance
AMP	adenosine monophosphate
ATP	adenosine triphosphate
BPD	bleeding and platelet disorder
BSA	bovine serum albumin
CAD	coronary artery disease
cAMP	cyclic adenosine monophosphate
cDNA	complimentary deoxyribonucleic acid
$cPLA_{2\alpha}$	cytosolic phospholipase A2 alpha
CMUSE	cryptogenic multifocal ulcerous stenosing enteritis
COX	cyclooxygenase
EDTA	ethylenediaminetetraacetic acid
EET	epoxyeicosatrienoic acid
FACS	fluorescence activated cell sorting
GAPP	genotyping and phenotyping of platelets
GPCR	g-protein coupled receptor
GDP	guanosine diphosphate
GTP	guanosine triphosphate
HETE	hydroxyeicosatetraenoic acid
$iPLA_{2\alpha}$	calcium independent phospholipase A2 alpha

LOX	lipoxygenase
LTA	light transmission aggregometry
MACS	magnetic activated cell sorting
miRNA	micro ribonucleic acid
mRNA	messenger ribonucleic acid
NIHR	national institute of health research
NSAIDS	non-steroidal anti-inflammatory drugs
NSTEMI	non-ST-segment elevation myocardial infarction
OCS	open cananicular system
PBS	phosphate buffered saline
PFA	paraformaldehyde
PG	prostaglandin
PGI_2	prostacyclin
PI3K	phosphoinositide 3-kinase
PLC	phospholipase C
PPP	platelet rich plasma
PRP	platelet poor plasma
qRT-PCR	quantitative real time polymerase chain reaction
RBC	red blood cell
RNA	ribonucleic acid
RNA-Seq	ribonucleic acid sequencing
RPKM	reads per kilobase million
SEM	standard error of the mean
SLE	systemic lupus erythematosus
$sPLA_{2\alpha}$	secretory phospholipase A2 alpha

STEMI	ST-segment elevation myocardial infarction
TO	thiazole orange
TRAP-6 amide	thrombin receptor activator peptide 6 amide
TXA_2	thromboxane A2
vWD	von Willebrands disease
vWF	von Willebrands factor
WBC	white blood cell
WP	washed platelets

Chapter 1 - Introduction

1.1 The cardiovascular system and haemostasis

The cardiovascular system consists of the heart, a muscular pump, and a closed system of vessels that include arteries, veins and capillaries. During mammalian development the cardiovascular system is the first organ system to reach a functional state with a heartbeat detectable four weeks after fertilisation [1]. In the adult human, the principle function of the cardiovascular system is to transport substrates required for biochemical processes and to remove their potentially harmful waste products [2]. The complex integrated control mechanisms of the cardiovascular system ensure that adequate blood supply is maintained irrespective of differences in physiological demand.

Central to the maintenance of the cardiovascular system is the process of haemostasis. This series of integrated biochemical and cellular events can be grouped into the three stages of vascular spasm, platelet plug formation (primary haemostasis) and coagulation (secondary haemostasis) [3]. Together these stages function to maintain the balance between blood in its resting liquid state and blood in its gel-like solid state required for the formation of blood clots in response to vessel wall injury [4]. Deviations in this balance can lead to haemorrhage or thrombosis.

Cardiovascular disease (CVD) encompasses all diseases affecting the heart or circulatory system and is the leading cause of death worldwide [5,6]. In the United Kingdom alone CVD affects over 7 million people costing the National Health Service in excess of £11 billion each year [7]. Consequently, research to better understand the pathophysiology of such diseases in order to design novel therapeutic strategies is a major focus within the life science community.

1.2 The platelet

Central to the process of haemostasis and to the development of many cardiovascular pathologies are platelets.

After the advent of the achromatic lens microscope in 1826, physicians Albert Donne, George Gulliver, William Addison and Max Schultze [8] independently produced the earliest recorded observations of platelets in whole blood describing them using terms such as 'globular masses', 'colourless corpuscles' or 'spherules'. It wasn't until 1874 that William Osler [9] published work clearly recognising platelets as independent cellular bodies [10]; this pivotal discovery provided the foundations for the work of Giulio Bizzozero who was the first investigator to assign function to the platelet [11,12]. In 1882, in a series of in vitro and in vivo experiments Bizzozero documented the role of platelets in coagulation; specifically noting their adherence to vessel walls and interactions with fibrin. Collectively these investigators provided the scientific community with the fundamentals of platelet biology [13].

1.2.1 Platelet production and clearance

Twelve years prior to his publications regarding platelets Bizzozero had been the first to discover megakaryocytes but had failed to recognise them as the platelet's cell of origin. It took until 1906 for James Homer Wright to use his newly developed Wright's stain to characterise the relationship between megakaryocytes and platelets by visualising their granules and thus seeing the similarities in their size and shape [14].

Megakaryocytes are highly specialised, large myeloid cells found mainly in the bone marrow and are the parent cell to platelets. During maturation megakaryocytes begin to increase in volume and fill their cytoplasm with

membrane systems, organelles, granules, proteins and mitochondria essential to the process of platelet production [15].

Many modes of platelet production from megakaryocytes have been proposed but it is the pro-platelet theory that is the most well established and rigorously supported by both in vitro and in vivo experiments [16,17]. In this model mature megakaryocytes produce pseudopods that traffic the proteins and organelles from the megakaryocyte, through the microtubule systems and into structures known as pro-platelets. Pro-platelets are long cytoplasmic extensions of the megakaryocyte cell body; these branched structures can be seen microscopically to extend into the sinusoidal blood vessels of the bone marrow and to contain multiple platelet-sized swellings that become the site for platelet release [18,19]. The ends of pro-platelets repeatedly bend and branch, thus greatly amplifying the surface upon which platelets can be produced [20]. Eventually pro-platelets are released as individual platelets through the narrowing of the pro-platelet extensions and exposure to shear forces in the bloodstream (Figure 1.1).

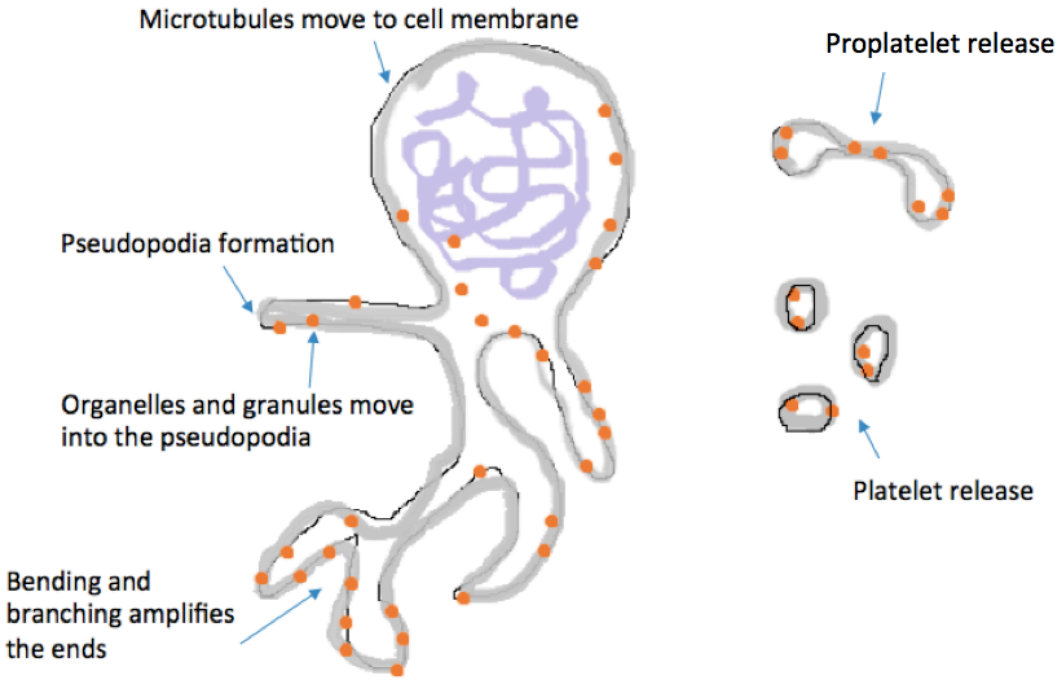

Figure 1.1 Pro-platelet model of platelet formation

Before platelets are released, microtubules firstly disassemble and move towards the plasma membrane and eventually fill the pseudopodia pushed out by the megakaryocyte. Organelles and granules are trafficked into the extending pseudopodia and branching occurs to increase the amount of pro-platelet containing ends. Eventually, pro-platelets, organelles and granules become trapped in close proximity and are released from the main megakaryocyte body. Subsequent microtubule movements result in platelet release. Figure adapted from *Thon J, 2010* [19].

A normal human platelet count falls within the range of 150-400x10^9 cells/L in the circulating blood and is kept constant by maintaining the balance between production and clearance [21]. Platelets in the circulation have a lifespan of 8-11 days; consequentially each day roughly 10% of the total platelet population is renewed. As with the theories of production, there are also multiple hypotheses offered for the control of platelet lifespan and senescence. In more recent investigations the role of the intrinsic apoptosis pathway in the regulation of platelet lifespan has gained more acceptance. Platelets have been shown to express a number of pro-apoptotic proteins including Bak and Bax and pro-survival proteins including Bcl-2, Bcl-xL and Mcl-1 [22]. A shift in the balance towards the pro-apoptotic group will allow Bak and Bax to cause enough mitochondrial damage to trigger caspase activation and initiation of apoptosis [23]. In disease states such as immune thrombocytopenic purpura, characterized by excessive platelet destruction, an antibody-mediated method of platelet clearance is favored. In such cases IgG autoantibodies bind to the platelet surface resulting in opsonisation and subsequent Fc receptor-mediated phagocytosis by macrophages in the spleen [24].

1.2.2 Platelet structure

Platelets are small, anuclear cell fragments measuring on average 2-5 μm with a mean cell volume of 6-10 fL. The outer platelet plasma membrane is a standard phospholipid bilayer and is the site for surface receptor expression. These surface receptors are numerous and play an essential role in determining platelet reactivity and responsiveness to external signals. Connected to the plasma membrane is the open canalicular system (OCS) of channels extending deep into the cytoplasm and functioning to transport substances into the platelet cytoplasm and out of the secretory granules [25]. There are two types of secretory granules within the platelet cytoplasm, α and dense, which release their

contents to mediate a variety of platelet functions in response to platelet activation. Granule content is outlined in Tables 1.1 and 1.2. In addition to the OCS there is also a dense tubular system (DTS) of channels derived from the smooth endoplasmic reticulum of the parent megakaryocyte that primarily functions to facilitate movement of calcium and enzymes needed to support activation [26].

Platelets also have a highly specialised cytoskeleton which rapidly reorganises itself upon platelet activation to facilitate shape change from a smooth discoid cell to a structure of irregular pseudopodia projections [27]. The resulting increase in platelet surface area facilitates additional platelet-cell interactions.

α-granule content	
Adhesion molecules	P-selectin, vWF, thrombospondin, fibrinogen, GP IIB/IIIa, fibronectin, GP IV, PECAM-1
Chemokines	Platelet factor 4, β-thromboglobulin, CCL3, CCL5, CCL7, CCL17, CXCL5, CXCL8
Coagulation components	Factor V, Factor XIII
Fibrinolytic components	Plasminogen, α2-macroglobulin,
Growth factors	Fibroblast growth factor, epidermal growth factor, insulin like growth factor, hepatocyte growth factor, transforming growth factor beta, platelet derived growth factor
Immunological	Factor D, IgG

Table 1.1 Major components found within α-granules
Table adapted from Platelets 3rd edition, [28]

Dense granule content	
Ions	Calcium, magnesium, pyrophosphate, polyphosphate
Nucleotides	ATP, ADP, GTP
Transmitters	Serotonin, histamine

Table 1.2 Major components found within dense granules
Table adapted from Platelets 3rd edition, [28]

1.3 Platelet activation, adhesion and aggregation

The primary role of platelets is to limit blood loss after vessel injury through the formation of a thrombus. In order for platelets to stick to the site of injury they must first come into very close contact with the vessel wall and remain there until platelet-endothelium interactions are permitted. Due to the relative size of platelets and red blood cells (RBC's), under normal blood flow platelets are influenced by the motion of RBC's and are pushed towards the vessel wall (Figure 1.2 A). Under these conditions platelets can begin to slowly roll over the surface of the endothelium lining the vessel and interact with endothelial cells through weak interactions between von Willebrand Factor (vWF) and glycoprotein 1bα on the platelet surface [29].

If the vessel wall is damaged significantly, as in the case of atherosclerotic plaque rupture, sub-endothelial matrix proteins such as collagen become exposed [30]. Platelets readily adhere to collagen through the glycoprotein receptors Ia-IIa (integrin $\alpha_2\beta_1$) and VI [31]. Signalling through glycoprotein VI results in an increase in intracellular calcium [32] leading to platelet activation, shape change and the release of mediators such as thromboxane A_2 and adenosine diphosphate (ADP) which act through the prostanoid (TP) or $P2Y_{12}$ and $P2Y_1$ receptors respectively, to further recruit other platelets into the forming platelet plug. These platelet-platelet interactions, known as platelet aggregates, are largely mediated through the glycoprotein IIb-IIIa receptor that binds vWF and fibrinogen attracting yet more platelets to the site of plug formation [33] (Figure 1.2 B). A summary of these events can be found in Figure 1.2.

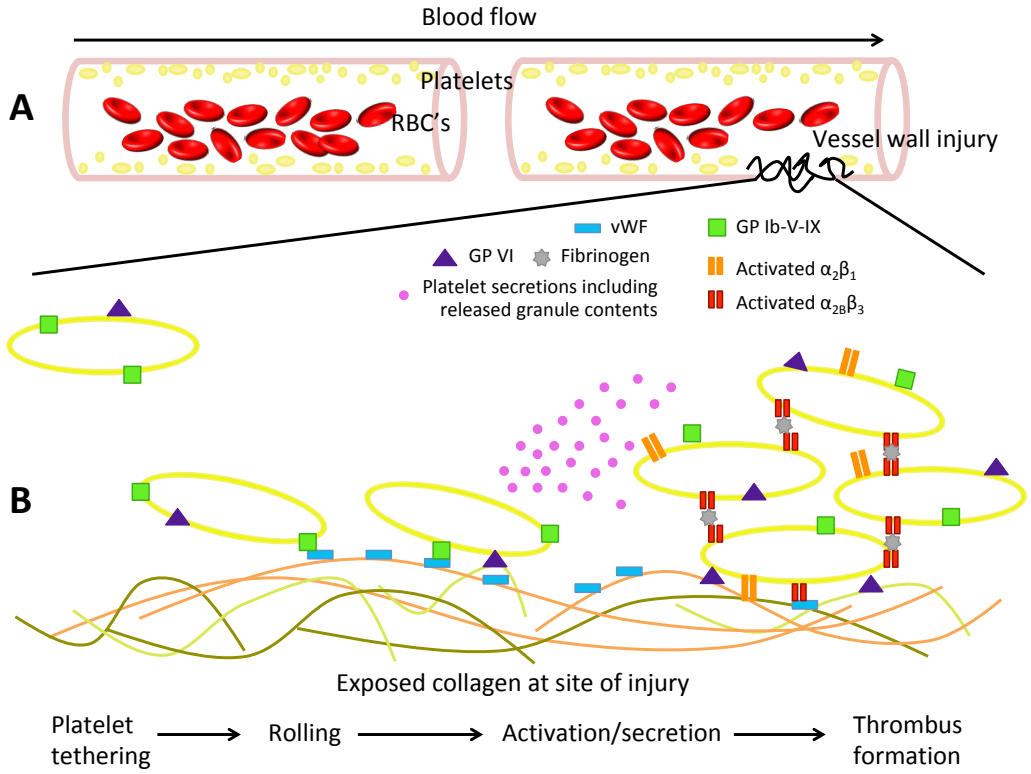

Figure 1.2 A schematic representation of platelet interactions with the vessel wall following injury

The velocity of flowing blood in relation to the stationary vessel wall results shear forces that will allow larger blood cells to move through the centre of the centre of the flow. This in turn will force platelets that are smaller and less dense to the edge of the flow close to the vessel wall (A). In high shear conditions initial tethering of platelets to collagen occurs through the GP 1b-V-IV mediated by vWF. Stronger adhesion is achieved through collagen binding to GPVI and integrin $\alpha_{2b}\beta_3$. This results in platelet activation, shape change and granule release. Fibrinogen mediated platelet aggregation occurs though binding to activated $\alpha_{2b}\beta_3$ and the growing thrombus is stabilised through strong interactions between collagen and vWF with the activated $\alpha_{2b}\beta_3$ and $\alpha_2\beta_1$ integrins (B). Figure adapted from *Gibbins,J, 2004* [34].

1.4 Platelet activators and inhibitors

In addition to collagen, platelets can respond to a wide range of other endogenously produced activating and inhibitory mediators, which act upon their large repertoire of cell surface receptors, to facilitate various physiological functions. These mediators, and their synthetically produced equivalents, can be taken advantage of experimentally to assess platelet reactivity and are utilised in many standard platelet function assays. A summary of the activators and inhibitors used in this thesis can be found in Figure 1.3.

This section will discuss those most relevant to this investigation, all of which signal through G-protein coupled receptors (GPCRs). GPCRs are formed from a single polypeptide chain with seven transmembrane domains and interact with G-proteins within the plasma membrane. These G-proteins, formed from an alpha, a beta and a gamma subunit, bind guanosine triphosphate when active (GTP) or guanosine disphosphate when inactive (GDP). When a signalling molecule binds to the GPCRs active site a conformational change occurs allowing GTP to replace GDP on the alpha subunit. The receptor is not active until the alpha subunit bound to GTP dissociates from the beta-gamma dimer to interact with other membrane proteins, enzymes, second messengers or ion channels to stimulate intracellular signalling pathways [35,36].

1.4.1 Thrombin

Thrombin, formed through conversion of prothrombin by the actions of the prothrombinase (complex consisting of Factors Xa and Va), is an enzyme with an essential role in haemostasis. With specific reference to platelets, thrombin acts upon the protease-activated receptors 1 and 4 (PAR-1 and PAR-4). PAR receptors are a type of GPCR that first requires the cleavage of a tethered peptide ligand that can go on to bind to the receptor to activate signalling [37]. Synthetically produced thrombin related

activating peptide-6 (TRAP-6) mimics the portion of the PAR1 receptor revealed by thrombin cleavage and so acts as a PAR1 agonist. PAR receptors signal through G_q proteins to stimulate phospholipase C (PLC) and inositol triphosphate (IP3) to increase intracellular calcium levels. The receptors also signal through G_i proteins to alter PI3K/Akt pathways and through $G_{12/13}$ proteins to alter rho kinase signalling pathways to ultimately influence platelet shape change [38].

1.4.2 ADP

Stored within platelet dense granules ADP is actively released from the platelet secondary to platelet plug formation initiated by collagen and thrombin signalling. ADP functions as a platelet agonist by binding to the $P2Y_1$ and $P2Y_{12}$ receptors. $P2Y_1$ activates PLC and IP3 via the G_q protein to increase calcium ion concentrations that initiate platelet aggregation and shape alteration whereas $P2Y_{12}$ inhibits adenylyl cyclase to consequently decrease intracellular cAMP levels via the G_i protein leading to an enhanced stability of the aggregate and further granule content secretion [39,40]. In addition $P2Y_1$ and $P2Y_{12}$ receptors work in concert with the glycoprotein IIb/IIIa (integrin α2bβ3) fibrinogen receptor to activate phospholipase A_2 (PLA_2) which catalyses the liberation of arachidonic acid from membrane phospholipids; a crucial step in the formation of the platelet agonist thromboxane A_2 [41].

1.4.3 Epinephrine

Platelet activation in response to epinephrine is mediated through the activity of α_2-adrenergic receptors coupled to G_i proteins that inhibit cAMP formation by suppressing adenylyl cyclase activity. Reducing cAMP formation effectively alleviates a block on platelet signaling that is ordinarily in place to prevent inappropriate platelet activity [42].

1.4.4 Arachidonic acid and Thromboxane A_2

Through the activity of cyclooxygenase (COX), arachidonic acid (AA) is converted to prostaglandin H_2 that is further converted to thromboxane A_2 (TxA_2) by thromboxane synthase [43]. TxA_2 binds to the thromboxane-prostanoid (TP) receptor and signals through the Gq and Gi proteins. Activation of this receptor leads to phosphorylation of myosin light chain kinase through the activity of PLC as well as an increase in intracellular calcium through the activity of IP3 [44]. U46619 is a synthetic TP receptor agonist and is used experimentally to give further information in addition to results obtained using AA [45]. It enables investigators to discriminate between effects due to inhibition of endogenous TxA_2, as in the case of aspirin, or due to changes in TP receptor function; aspirin will block responses to AA but not those to U46619.

1.4.5 Prostacyclin (PGI_2)

Also produced from AA metabolism through the actions of COX and prostacyclin synthase enzymes, PGI_2 is a platelet inhibitor [46]. PGI_2 exerts its inhibitory effects through the platelet prostacyclin receptor (IP) coupled to G_s proteins leading to an increase in adenylate cyclase and consequentially a rise in cAMP. cAMP activates protein kinase A which phosphorylates several different proteins ultimately resulting in myosin light chain kinase inhibition and subsequent prevention of platelet granule secretion [47].

1.4.6 Prostaglandin E_1 (PGE_1)

PGE_1 is produced in the body through the metabolism of dihomo-γ-linolenic acid by COX enzymes. PGE_1 also binds to the IP receptor on platelets to again raise intracellular cAMP concentrations activate protein kinase A and to inhibit PLC activity to subsequently

reduce calcium release from intracellular stores [48,49]. This prostanoid is a longer lasting inhibitor of platelet aggregation in vitro than PGI_2.

1.4.7 Apyrase

The apyrase enzyme functions as a platelet inhibitor by facilitating the breakdown of ADP to AMP, thus preventing the proaggregatory effects of ADP acting upon platelet $P2Y_{12}$ and $P2Y_1$ receptors [50].

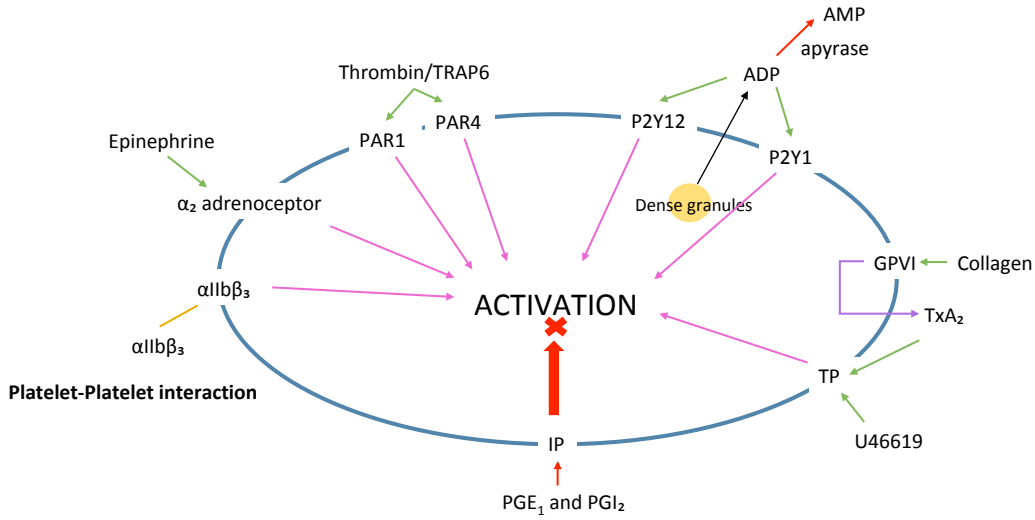

Figure 1.3 Platelet surface receptors and agonist activation pathways

Figure showing the various mechanisms of platelet activation including agonists and their receptors as well as the site of action for common antiplatelet therapies adapted from Patrono, C et al, 2011 [51].

1.5 Platelet RNA

For decades it was generally thought that a platelet's organelle, granule, protein and RNA content were all derived exclusively from the parent megakaryocyte and delivered to the platelet during its production. In addition due to lacking a nucleus platelets have no transcriptional abilities and their synthetic capabilities were assumed to be non-existent. As a consequence the studies of platelet RNA were greatly outnumbered by investigations focussed upon features of platelet biology, such as granules and surface receptors, which were more clearly associated to platelet function.

However in more recent years, and linked to the advent of affordable next generation sequencing technologies, interest in platelet RNA has increased with investigators having now characterised platelet RNA in much finer detail, understanding better, it's structure, regulation and fundamental role in protein synthesis.

1.5.1 Platelet messenger RNA (mRNA)

Messenger RNA (mRNA) is a subtype of RNA that is used as a single stranded template for the DNA from which it was transcribed. mRNA molecules are classically delivered from the nucleus of a cell to ribosomes within the cytoplasm to be translated into protein molecules. The complete set of expressed mRNAs belonging to a cell is called its transcriptome. Owing to the fact that they are anuclear the platelet transcriptome is largely derived from the megakaryocytes that produce them. In a study conducted by Cecchetti et al it was shown, using next generation RNA sequencing techniques and focussing upon examples from the matrix metalloproteinases family, that megakaryocytes selectively sort thousands of mRNA transcripts for transport into the platelet [52]. Furthermore the abundance of a transcript in a megakaryocyte is not predictive of the abundance of that same transcript within the

platelet. As a consequence the platelet transcriptome is only a partial reflection of the megakaryocyte transcriptome.

As expected of a cell lacking a nucleus, the quantity of mRNA within platelets is very small with estimates suggesting that a single platelet contains 10,000 times less mRNA than a single leukocyte [53]. Studies profiling the human platelet transcriptome have revealed that platelets possess a small but diverse range of 6000-10000 transcripts [54,55]. Structurally platelet mRNAs closely resemble those of nucleated cells having both a 5' 7-methylguanosine cap and a 3'poly(A) tail with polyadenylation sequences [56]. mRNA translation is initiated when access to these structures is permitted by eukaryotic initiation factor-4E [57] and aided by mRNA binding proteins also found within the platelet [58].

Not only do platelets contain mRNA they have also been shown to retain pre-mRNA and functionally critical components of a spliceosome, presumably accumulated during pro-platelet formation from megakaryocytes. A spliceosome is a complex molecular machine, associated with the nucleus, required to remove non-coding introns from pre-mRNA to produce translatable mRNA ready for transport into the cytoplasm [59]. Despite lacking a nucleus this process has been shown to occur in platelets in a signal dependent manner in response to activating stimuli such as thrombin [60]. This process is thought to be an important feature of platelet biology as it further enhances a platelet's ability to diversify its functional properties.

Following on from the production of mature mRNA, platelets are known to be capable of protein synthesis and to contain both ribosomes and rough endoplasmic reticulum. These observations were first made in the 1960s and 70s through experiments with radioactively labeled amino acids [61] and electron microscopy [62]. Improvements in protein separation techniques in the 1980s enabled investigators to show that platelets synthesized proteins including glycoprotein Ib, glycoprotein IIb/IIIa,

fibrinogen, albumin, thrombospondin and vWF [63]. Such protein production is now known to occur in a signal dependent manner usually in response to an activating stimulus. In one example, Weyrich et al showed that platelets activated by thrombin translate B-cell lymphoma 3 mRNA into protein via mammalian target of rapamycin (mTOR) signaling pathways [64]. In addition this group was also the first to show that activated platelets possess the ability to use mRNA splicing events as a mechanism of regulating the synthesis of proteins including interleukin 1β and tissue factor [65]. There is also some limited evidence supporting the idea that platelets continually produce protein throughout their lifespan even in the absence of agonist stimulation [66]. Platelet biologists should consider these translational capabilities carefully as they reinforce the idea that platelets are important participants in more long-term cellular responses such as those contributing to immune responses.

The quantity of megakaryocyte derived platelet mRNA declines throughout a platelets life span due to the fact that they lack the ability to transcribe new mRNA molecules. It has been estimated using in vivo studies that mouse platelet mRNA has a half-life of 6 hours with a 95% overall reduction in detectable cytoplasmic mRNA by 24 hours [67]. Furthermore experiments using platelet like particles grown from human megakaryocytes in culture have been shown to contain mRNA which rapidly declines in concentration beginning at 4 hours post production and that this decay occurs with a half-life of 5.7 hours [68]. Platelet mRNA decay is an interesting feature of platelet biology which can be used to investigate both platelet age and for the functional relevance of the mRNA itself.

1.5.2 Platelet microRNA (miRNA)

In addition to mRNA platelets also contain a host of other functional and regulatory small non-coding RNAs including circular RNAs, YRNAs and microRNAs (miRNA), which may function to regulate platelet protein expression at the mRNA level. miRNAs are typically less than 22 nucleotides in size and have been shown to regulate more than half of all human mRNAs either by enhancing translation, reducing translation or inducing degradation [69,70]. Just like mRNAs, platelets obtain their miRNA repertoire from parent megakaryocytes during platelet formation [71]. To date investigators have detected over 750 miRNAs within platelets which remain stable throughout its life-span in healthy control samples but which can be significantly altered in various disease states [72]. Specific miRNAs have the ability to modify platelet function, for example miRNA-223 has been shown to bind to the 3' untranslated region of human $P2Y_{12}$ receptor mRNA where it could have the potential to regulate receptor expression and thus impact $P2Y_{12}$ mediated platelet activity [73]. Following on from this, reduced platelet miRNA-223 levels have been associated with high on clopidogrel ($P2Y_{12}$ receptor antagonist) platelet reactivity [74,75].

1.5.3 Functional relevance of platelet messenger and micro RNAs

Having now firmly established that platelets possess a diverse and dynamic selection of micro- and messenger-RNAs, have a signal dependent system for protein translation and a mechanism for receiving select megakaryocyte derived transcripts platelet biologists are beginning to question the functional relevance of these RNA species.

Advances in sequencing technologies have lead to the development of newer application such as RNA-Seq which supersede previous techniques such as Sanger sequencing, microarrays and qRT-PCR by enabling more precise detection of transcripts, without the need for a

reference genome, in a high-throughput and cost effective manner [76]. In addition RNA-Seq requires a much smaller concentration of RNA, making it ideal for genetic studies of platelets. This technique enabled researchers to characterise and compare complete human and mouse platelet transcriptomes publishing them in 2011 as a public research tool [54].

A key question remains as to whether the platelet transcriptome is altered in disease states and what relevance this may have to the identification of novel biomarkers or therapeutic targets. In a study from Eicher et al the platelet transcriptomes belonging to patients with ST-segment elevation myocardial infarction (STEMI) versus non-STEMI (NSTEMI) patients were compared. The group identified over ninety differentially expressed genes between the two patient groups. In addition the study also identified genes linked to platelet aggregation in response to agonist stimulation with TRAP-6, collagen and ADP indicating that different activating signals have different impacts upon platelet gene expression [77].

In a study using micro-array techniques Lood et al demonstrated that platelets taken from patients with systemic lupus erythematosus (SLE) expressed higher levels of both genes and proteins linked to the type-1 interferon pathway. The investigators propose that these differences occur through the actions of interferon-α on megakaryocytes. Pro-inflammatory cytokines belonging to the type-1 interferon pathway have previously been linked to increased platelet aggregation and to the development of acute coronary syndromes. Patients with SLE have an increased risk of cardiovascular disease and thus the investigators proposed that platelet expression of type-1 interferon genes could be used as a novel biomarker for the development of cardiovascular disease in patients with SLE [78].

Using platelets obtained from patients with sickle cell anemia researchers sought to investigate the link between thromboembolism/ hypercoagulability and sickle cell disease. By comparing the platelet

transcriptomes of those with sickle cell anemia to healthy controls the study revealed differential expressions for over 100 genes. Further pathway analysis indicated a global activation of genes involved in arginine uptake and catabolism. Arginine is converted to nitric oxide, an important platelet inhibitor and so if arginine catabolism is increased then this may provide a possible mechanism for the increased platelet reactivity and hypercoagulable state present in sickle cell anaemia patients [79].

Platelets also possess the ability to transfer their nucleic acid material to other cell types. The group of Jane Freedman, for instance, showed using both in vitro and in vivo models that platelet-like particles produced from cultured megakaryocytes (MEG-01) transfer RNA to both monocytes (THP-1 cell line) and endothelial cells (HUVEC cell line) when co-cultured. Furthermore, they showed by transfecting MEG-01 cells with a GFP vector that PLP recipient cells received GFP both as a mature protein and mRNA that was subsequently translated [80–82]. The authors of these studies suggest that such mechanisms of platelet RNA uptake provide novels mechanisms by which platelets may regulate vascular homeostasis and systemic immune responses. In another study using similar transfection and co-culturing techniques, investigators propose a mechanism of platelet-mediated liver regeneration which centres on the ability of hepatocytes to internalise platelets which then subsequently transfer functional RNA [83].

Platelet miRNAs have also been shown in numerous investigations to regulate the expression of genes in other cells within the circulation [84]. For example, platelet derived microparticles containing Argonaute 2/miRNA-223 complexes were shown to regulate the expression of mRNA and protein levels of two endothelial cell genes (FBXW7 and EFNA1) following internalisation [85,86]. In a clinical study using RNA-Seq, Gidlof et al demonstrated that platelets from patients with myocardial infarction display a significant loss of eight miRNAs compared to control platelets. Furthermore they showed that miRNAs

shed from activated platelets can be taken up by endothelial cells to alter the expression of genes including ICAM1, an adhesion molecule mediating leukocyte-endothelial cell interactions [87].

Additionally platelets also have the ability to uptake circulating RNA from other cell types. This activity is currently being utilized in the field of cancer diagnostics where platelets have been shown to take up tumour-derived vesicles containing tumour specific RNA released into the circulation [88]. Researchers have established a platelet RNA-Seq protocol enabling them to distinguish 228 patients with tumours from 55 healthy controls with 96% accuracy [89].

Together these studies provide evidence for the ability of circulating platelets to change their transcriptomes in response to extracellular signalling in disease states and have helped to expand our knowledge of platelet thrombotic and non-thrombotic functions. Moreover, the research provides an interesting role for platelet RNA as a mediator of intracellular communication and proposes the use of platelet RNA as a diagnostic biomarker [90].

1.6 Newly formed, reticulated, platelets

The total platelet population consists of multiple sub-populations each with distinct functional properties [91–93]. Of particular interest to this thesis investigation is the newly formed, or reticulated, population owing to the fact that these platelets are thought to contain an abundance of megakaryocyte derived mRNA. The reticulated population is thought to account for just 10% of the total platelet population. This estimate is based on the knowledge that platelet lifespan is around 10 days and platelet mRNA half-life is around 12-24 hours [67]. As such each day 10% of the platelet population is renewed [94]. Consequently these newly formed reticulated platelets are sometimes referred to as immature platelets.

The other defining feature of this platelet population is that they are thought to be more reactive than their non-reticulated counterparts and as such have been linked to multiple disease states. Notably, elevated populations of reticulated platelets have been linked to a higher incidence of acute coronary syndromes [95] as well as to high on treatment platelet reactivity in various patient groups receiving standard dual antiplatelet therapies [96,97]. Indeed our own group has shown previously that, because of the short pharmacokinetic half-lives and single daily dosing of aspirin and thienopyridine antiplatelet therapies, there exists a point within the day that newly formed reticulated platelets emerge uninhibited. This highly reactive uninhibited platelet population then act as seeds for the formation of platelet aggregates [98]. This study provides a possible cause for the lack of efficacy of antiplatelet therapies which could be particularly pertinent to patient groups known to have an increased platelet turnover as is seen in diabetes [99] and chronic kidney disease [100].

Theses two defining features of reticulated platelets - increased reactivity and abundance of RNA – make this subpopulation interesting to researchers investigating the platelet transcriptome and the biological function of platelet RNA as well as to those looking to identify novel drug

targets or biomarkers of disease. The assessment of the reticulated platelet population is made possible by using either flow cytometry or the fully automated Sysmex haematological system. Both of these methods detect reticulated platelets based on the florescence intensity of nucleic acid binding dyes such as thiazole orange; reticulated platelets have abundance of cytosolic RNA and so will stain brightly with these dyes compared to other platelet populations [101]. Flow cytometric measurements usually report reticulated platelet numbers within a predefined gate [102–104] whereas the Sysmex system reports reticulated platelets as the immature platelet fraction (%) or as the immature platelet count [105–107]. The Sysmex system is used widely in clinical settings and in patient studies where it is favoured over flow cytometry owing to its standardisation, reproducibility, high throughput, efficiency and low cost.

As the field moves forward it will be important to ascertain the cellular and molecular mechanisms linking reticulated platelets to pathological disease processes as well as to fully characterise their functional capabilities.

1.7 Platelet mediated bleeding disorders

The term bleeding disorder is an umbrella term used to describe a group of conditions that share the common feature of inappropriate bleeding due to ineffective clot formation. Patients with bleeding disorders usually present with some or all of the following symptoms; bleeding into joints or soft tissue, menorrhagia, epistaxis, excessive bruising and extended bleeding after minor injuries, dental procedures or surgeries [108]. Bleeding disorders are often inherited [109], however some can occur secondary to other conditions such as anaemia, liver cirrhosis, leukaemia, vitamin K deficiency or thrombocytopenia. Other bleeding disorders can occur as side effects caused by medications such as warfarin [110] and aspirin [111].

Haemophilia (frequency of 1 in 10,000 in UK) [112,113] and von Willebrands disease (frequency of 1 in 100 in UK) [114] are the two most commonly diagnosed bleeding disorders and account for 95% of all inherited deficiencies of coagulation factors [115]. Bleeding disorders attributable to defects in platelet function are considerably more rare and are often under-recognised due to difficulties in diagnosis. Platelet disorders are usually inherited in an autosomal recessive manner and present with milder symptoms of bleeding [116–119]. The best characterised inherited platelet disorders are outlined in the following paragraphs. A list of all genes associated with inherited bleeding disorders can be seen in Table 1.3.

Bernard Soulier syndrome is an inherited platelet disorder characterised by giant platelets, thrombocytopenia and prolonged bleeding time. This syndrome is caused by quantitative or qualitative defects in the glycoprotein Ib-IX-V complex that binds vWF. As a consequence this syndrome is often diagnosed by the absence of ristocetin induced platelet agglutination [120,121].

Glanzmann thrombasthenia is a platelet surface receptor defect of glycoprotein IIb/IIIa (integrin α2bβ3) that mediates platelet interactions

with adhesive protein such as vWF and fibrinogen. As such the primary platelet defect is a reduction in platelet aggregate formation [122–124]. Molecular defects to the $P2Y_{12}$ receptor [125], TP thromboxane receptor and GPVI [126] and a2b1 collagen receptors have also been documented for a very limited number of cases [127].

Wiskott-Aldrich syndrome is caused by mutations to the WAS gene which encodes for the WAS protein [128]. This protein plays a key role in signal transductions processes in many cell types; as such symptoms of this syndrome are varied. The platelet dysfunction attributable to this syndrome is decreased aggregation in response to ADP, collagen and epinephrine as well as reduction in dense granule number [129,130].

Storage pool disease is the collective term given to a number of platelet disorders featuring deficiencies of granule number, granule content and granule release resulting in reduced platelet aggregation. Grey platelet syndrome [131], Quebec platelet disorder [132], Paris-Trousseau syndrome [133], Hermansky-Pudlak syndrome [134] and Chediak-Higashi syndrome [135] are all examples of platelet storage pool disorders.

Although the incidence of these syndromes is low, their characterisation has helped further our understanding of the molecular mechanisms supporting platelet function [136,137]. Prior to the advent of DNA sequencing the gold standard assay for platelet function testing - light transmission aggregometry – was the most informative test used for the identification of platelet mediated bleeding disorders. In more recent years however advances in DNA and RNA sequencing technologies have significantly increased the rate of diagnosis of rare bleeding conditions. As a consequence large multicentre collaborative studies between clinicians and platelet biologists have been established to investigate links between bleeding phenotypes and genotypes [138–142]. Three relevant examples of such studies are the ThromboGenomics study, the BRIDGE consortium's bleeding and platelet disorders (BRIDGE-BPD) study and The Genotyping and Phenotyping of Platelets (GAPP) study. The

ThromboGenomics study uses a targeted approach for the identification of bleeding disorders associated to gene variants. This study recruits patients internationally but requires individuals who have a strong clinical phenotype for the 98 candidate gene approach to be informative [139]. The BRIDGE-BPD study, setup by the NIHR as one of its rare diseases projects, aims to discover novel and established genetic variants linked to unexplained bleeding disorders [143]. This study uses high throughput sequencing techniques to search for variants in a large cohort of patients recruited throughout the UK and in Europe. Similarly the GAPP study is a collaborative investigation carried out by research groups in Bristol, Nottingham and Sheffield who collect samples from patients referred to haemophilia care centres in the UK. Using whole exome sequencing and platelet phenotyping the study aims to discover causative variants in each individual recruited onto the study [140,141]. Together such studies are helping to improve the lives of those living with bleeding disorders by offering clinical monitoring and treatment options where appropriate.

Gene Symbol	Bleeding Disorder
SERPINF2	Alpha 2-antiplasmin deficiency
LMAN1 + MCFD2	Combined factor V and VII deficiency
F5	Factor V deficiency
F7	Factor VII deficiency
F10	Factor X deficiency
F11	Factor XI deficiency
F13A1	Factor XIII deficiency
F13B	Factor XIII deficiency
FGA	Fibrinogen deficiency
FGG	Fibrinogen deficiency
FGB	Fibrinogen deficiency
F8	Haemophilia A
F9	Haemophilia B
GGCX	Multiple coagulation factor deficiency type 1
VKORC1	Multiple coagulation factor deficiency type 2
SERPINE1	Plasminogen activator inhibitor 1 deficiency
PLG	Plasminogen deficiency
F2	Prothrombin deficiency
VWF	von Willebrand disease
P2Y12	ADP receptor defect
HOXA11	Amegakaryocytic thrombocytopenia with radioulnar synostosis
MECOM	Amegakaryocytic thrombocytopenia with radioulnar synostosis
VIPAS39	Arthrogryposis-renal dysfunction-cholestasis syndrome
VPS33B	Arthrogryposis-renal dysfunction-cholestasis syndrome
ANKRD26	Autosomal dominant thrombocytopenia
CYCS	Autosomal dominant thrombocytopenia
GP1BA	Bernard-Soulier syndrome or mild thrombocytopenia
GPIBB	Bernard-Soulier syndrome or mild thrombocytopenia
GP9	Bernard-Soulier syndrome or mild thrombocytopenia
GP6	Bleeding disorder due to glycoprotein VI deficiency
LYST	Chediak-Higashi syndrome
MPL	Congenital amegakaryocytic thrombocytopenia
PLA2G4A	Deficiency of group IVA phospholipase A2
NBEA	Dense granule abnormality
CHST14	Ehlers Danlos syndrome, musculocontractural type
STXBP2	Familial haemophagocytic lymphohistiocytosis type 5
RUNX1	Familial platelet disorder with predisposition to AML
TBXAS1	Ghosal syndrome
ITGA2B	Glanzmann thrombasthenia
ITGB3	Glanzmann thrombasthenia
NBEAL2	Grey platelet syndrome
GFI1B	Grey platelet-like syndrome

Table 1.3 continued

Gene Symbol	Bleeding Disorder
HPS1	Hermansky-Pudlak syndrome
HPS2 (AP3BI)	Hermansky-Pudlak syndrome
HPS3	Hermansky-Pudlak syndrome
HPS4	Hermansky-Pudlak syndrome
HPS5	Hermansky-Pudlak syndrome
HPS6	Hermansky-Pudlak syndrome
HPS7 (DTNBP1)	Hermansky-Pudlak syndrome
HPS8 (BLOC1S3)	Hermansky-Pudlak syndrome
HPS9 (BLOC1S6)	Hermansky-Pudlak syndrome
FERMT3	Leucocyte adhesion deficiency type 3
ACTN1	Macrothrombocytopenia
FLNA	Macrothrombocytopenia
TUBB1	Macrothrombocytopenia, beta tubulin 1 related
MYH9	May-Hegglin and other MYH9-related disorders
GNE	Myopathy associated with thrombocytopenia
FLI1	Paris-Trousseau thrombocytopenia and Jacobson syndrome
RASGRP2	Platelet-type bleeding disorder 18
GPIBA	Platelet-type von Willebrand disease
PLAU	Quebec platelet disorder
ANO6	Scott syndrome
STIM1	Stormorken syndrome
ORAI1	Stormorken syndrome
RBM8A	Thrombocytopenia absent radius syndrome
DIAPH1	Thrombocytopenia and sensorineural hearing loss
ETV6	Thrombocytopenia and susceptibility to cancer
THPO	Thrombocytopenia and thrombocythaemia 1
TBXA2R	Thromboxane A2 receptor defect
WAS	Wiskott-Aldrich syndrome
GATA1	X-linked macrothrombocytopenia with dyserythropoiesis

Table 1.3 International Society of Thrombosis and Haemostasis list of genes linked to bleeding disorders

Table adapted from Sivapalaratnam, S et al, 2017 [144].

1.8 Summary

Platelets play an essential role in maintaining the fine balance between haemostasis and thrombosis within the human body. Tipping this balance in favour of thrombosis can result in myocardial infarction or ischemic stroke; two of the most common causes of death worldwide. As a consequence, great efforts have been made to understand better platelet biology with the hope of identifying novel therapeutic targets. Much of this work has focussed upon the characterisation of platelet receptors and their signalling pathways and many clinically approved antiplatelet therapies are based upon the inhibition of specific platelet surface receptors. Other antiplatelet therapies target the signalling molecules produced by platelets and the intracellular pathways through which they act.

Much research has focussed upon the mediators and pathways regulating platelet activation whereas until recently very little attention has been given to the role of RNA, mainly because platelets lack nuclei. However, in more recent years aided by advances in sequencing technologies investigators have begun to characterise the relatively small amounts of RNA within the platelet cytoplasm and to make associations between certain RNA species and disease outcomes.

While laboratory research continues to delineate the many molecular controls of platelet function, cohorts of patients with bleeding disorders are being recruited into large multinational studies aiming to provide full genome sequencing for those patients. Not only will this provide patients with a genetic diagnosis for their bleeding symptoms but it will also shed light on the relationship between the platelet genotype and the platelet phenotype linking laboratory investigations to physiological function and disease outcomes.

1.9 Hypothesis and Aims

This thesis will investigate the hypothesis that the characterisation and description of changes to genomic material, in the form of both platelet specific mRNA and as whole genomic DNA, coupled with in depth functional analyses can provide deeper definition of platelet reactivity, thrombotic risk and pro-thrombotic pathways.

To that end the particular experimental aims are:

1. To establish a robust protocol for the extraction of a pure platelet population from whole blood, taking into account the need to perform platelet function testing and RNA extraction.
2. To further isolate newly formed reticulated platelets, using the most appropriate method established above, and to subsequently investigate their mRNA content and function.
3. To obtain a platelet sample from a patient who has a mutation known to alter platelet function and to characterise those platelets in terms of function and mRNA content.
4. To obtain blood and urine samples from families with known bleeding disorders, who have had their genomes sequenced, and provide in depth platelet function testing to understand better the functional consequences of those genetic variants.

Chapter 2 - Materials

384 wel qRT-PCR plate	Life Technologies, UK
96 well flat-bottom half-area microtitre plates	Fisher Scientific, UK
Abscorbic acid	VWR, UK
ABsolute qPCR ROX mix	ThermoScientific, UK
Acid-citrate-dextrose	Sigma-Aldrich, UK
Acrodisc syringe filter	Sigma-Aldrich, UK
ADP	Labmedics, Salford, UK
Agilent 2100 Bioanalyser	Agilent Technology, Germany
Agilent 2200 Tapestation	Agilent Technology, Germany
Alexa488 anti-mouse	eBioscience, UK
Alexa647 anti-rabbit	eBioscience, UK
Anti-human CD45 PerCP-Cyanine5.5	eBioscience, UK
Anti-human CD61 FITC	eBioscience, UK
Anti-human CD62 PE	eBioscience, UK
Anti-mouse tubulin	Sigma-Aldrich, UK
Anti-rabbit COX-1	New England Biolabs, USA
Anti-human CD61 APC	eBioscience, UK
Applied Biosystems ABI 7900HT instrument	Agilent Technology, Germany
Apyrase	Sigma-Aldrich, UK
Arachidonic acid	Sigma-Aldrich, UK
Automated pipetting system CAS-1200	Corbett robotics, UK
BD FACSAria Fusion cell sorter	BD Biosciences, USA
Bio/Data PAP-8E aggregometer	Alpha Laboratories, UK
Bioshake plate IQ shaker	Quantifoil, Germany
Bovine serum albumin	Sigma-Aldrich, UK
$CaCl_2$	Sigma-Aldrich, UK
CellQuest software	BD Biosciences, USA
Chart version 4.2 software	AD Instruments, UK
Chronolume ATP	Labmedics, UK
Chronolume luciferin-luciferase reagent	Labmedics, UK
Chronolog 560C lumi aggregometer	Chronolog, USA
Diclofenac	Barts Hospital Pharmacy, UK
Donkey serum	Sigma-Aldrich, UK
EDTA	Sigma-Aldrich, UK

Epinephrine	Labmedics, UK
Ethanol	VWR, UK
FACSCalibur flow cytometer	BD Biosciences, USA
Fibrinogen	Sigma-Aldrich, UK
Fix lyse solution	ThermoFisher Scientific, UK
FlowJo software	TreeStar Inc, USA
Formalin	Sigma-Aldrich, UK
Gelatin	Sigma-Aldrich, UK
Genome Suite software	Partek Inc, USA
Glucose	Sigma-Aldrich, UK
GraphPad Prism version 6 software	GraphPad Inc, USA
Heparin	Sigma-Aldrich, UK
HEPES	Sigma-Aldrich, UK
Horm collagen suspension	Takeda, Linz, Austria
Human serum albumin	Sigma-Aldrich, UK
IBMX	Sigma-Aldrich, UK
IDEAS software	Merck-Millipore, UK
Illumina TopHat v2 software	Illiumina, Cambridge, UK
Illumina Nextera XT Sample Kit	Illiumina, Cambridge, UK
Illumina NextSeq®500 High-output kit	Illiumina, Cambridge, UK
Illumina NextSeq sequencer	Illiumina, Cambridge, UK
Imagestream^X Mark II	Merck-Millipore, UK
Isotonic glucose	Takeda, Linz, Austria
KCl	Sigma-Aldrich, UK
LD MACS separation columns	Miltenyi Biotec, Surrey, UK
Lepirudin	Sigma-Aldrich, UK
LSM 710 confocal microscope	Zeiss, Germany
MACS beads anti-CD45	Miltenyi Biotec, Surrey, UK
Methanol	VWR, UK
$MgCl_2$	Sigma-Aldrich, UK
Na_2HPO_4	Sigma-Aldrich, UK
NaCl	Sigma-Aldrich, UK
Nanodrop 2000 spectrophotometer	ThermoScientific, USA
Nanodrop 8000 spectrophotometer	ThermoScientific, USA

Paraformaldehyde	VWR, UK
PAXgene RNA tubes	PreAnalytiX, Switzerland
PGE_1	Sigma-Aldrich, UK
Phosphate buffered saline (PBS)	Sigma-Aldrich, UK
ProLong Diamond antifade mountant	ThermoFisher Scientific, UK
Prostacyclin (PGI_2)	Enzo Life Sciences, UK
PureLink RNA minikit	ThermoFisher Scientific, UK
Qubit 2.0 Fluorometer	ThermoFisher Scientific, UK
Ristocetin	Helena Biosciences, UK
RNeasy minikit	Qiagen, UK
Saline	Baxter, UK
SDS qRT-PCR software	ThermoFisher Scientific, UK
SMARTer cDNA synthesis kit	Clontech Laboratories, USA
SuperScript III first-strand synthesis system	Life Technologies, UK
TaqMan anti-human FAM-labelled probes	Life Technologies, UK
Tecan infinite® M200 plate reader	Tecan, Switzerland
Tecan Sunrise plate reader	Tecan, Switzerland
Thiazole orange	Sigma-Aldrich, UK
TRAP-6 amide	Bachem, UK
Tri-sodium citrate	Sigma-Aldrich, UK
Triton	Sigma-Aldrich, UK
TRIzol	ThermoFisher Scientific, UK
U46619	Cayman Chemical, USA
ZEN 2009 software	Zeiss, Germany

Chapter 3 - Comparison of protocols for the isolation of platelets from whole blood for downstream functional and RNA analyses

3.1 Introduction

Platelets whilst anucleate are now known both to contain transcriptional machinery, messenger RNAs and micro RNAs derived from their parent megakaryocytes and to be transcriptionally active (1). This recent realisation has encouraged studies to characterise platelet messenger and micro RNAs. However the low abundance of RNA within individual platelets and the contamination of samples with other cell types, in particular white blood cells (WBCs), present major complications for downstream RNA applications. Because of this there are many diverse protocols for the isolation of platelets from whole blood but currently no consensus as to which is best. In addition there is little information available regarding the choice of anticoagulant or blood collection method and whether this could impact measurements of platelet function.

Within the blood platelets outnumber white blood cells (WBCs) 100 to 1. However, the RNA content of a white cell is much greater than that of a platelet with estimates being that a single WBC has 12,500 times more RNA than a single platelet [53]. It is also worth noting that only about 10% of the total platelet population contains any RNA at all and those that do, have a relatively small selection of around 4000-5000 transcripts [54,55,145]. Collectively, this makes detecting platelet specific RNA in whole blood technically challenging. Despite these technical challenges, the adoption of newer transcriptome sequencing tools, including RNA-Seq, which circumvent the need for large RNA inputs have enabled the characterization of the platelet transcriptome in healthy volunteers [54,146]. Moreover these techniques have facilitated the detection of changes to the platelet transcriptome in response to disease, most notably myocardial infarction [77]. Other groups are investigating the link between platelet micro-RNA containing vesicles and cancer metastases [147]. Together these studies have helped to reinforce the idea that platelet message, in the form of RNA expression, has valuable meaning, is relevant to multiple areas of research and could aid the discovery of novel biomarkers of disease [148].

In the studies outlined above, researchers have isolated pure platelet populations from whole blood using a variety of techniques, but there appears to be no agreement as to which is best. The most suitable isolation method must take in to consideration not only the ability to remove contaminating blood cells but also the ability to minimise consequent platelet activation. For example syringe filtering of platelet rich plasma to remove WBCs requires the platelets to be forced through a filter under pressure. The exposure of platelets to such forces may cause their activation, which could in turn bias towards a particular platelet sub-population or remove young platelets with an abundance of mRNA as they considered to be more reactive [149]. Such activation events may therefore affect overall determinations of platelet RNA in individual samples. Moreover a suitable technique that is scalable to the large cohort sizes required in population studies would be particularly attractive.

In this chapter I compare a range of platelet isolation protocols for their abilities to remove contaminating WBCs from platelet samples whilst minimising platelet activation.

3.2 Methodology

3.2.1 Human blood collection

St. Thomas' Hospital Research Ethics committee approved all experiments using human blood (reference, 07/Q0702/24). Volunteers gave written consent and were screened by obtaining measures of heart rate, temperature and blood pressure in conjunction with a medical history questionnaire. Donors were also required to have abstained from any pharmacological agents known to alter platelet function, must be non-smokers and must be under the age of 40.

Blood samples were obtained by venepuncture of the antecubital vein into vacutainers or syringes loaded with tri-sodium citrate (3.2% w/v), acid-citrate-dextrose (ACD) or lepirudin (250 μg/mL) to achieve an anticoagulant to whole blood ratio of 1:9. For whole blood RNA analyses blood samples were taken directly into a PAXgene Blood RNA tubes.

3.2.2 Preparation of platelet rich plasma (PRP) and platelet poor plasma (PPP)

Whole blood samples were centrifuged at 175 x g for 15 min at 25°C to produce PRP which was then kept in the water bath at 37°C until use. PRP was further centrifuged at 12000 x g for 2 min at 25°C to obtain PPP (Figure 3.1).

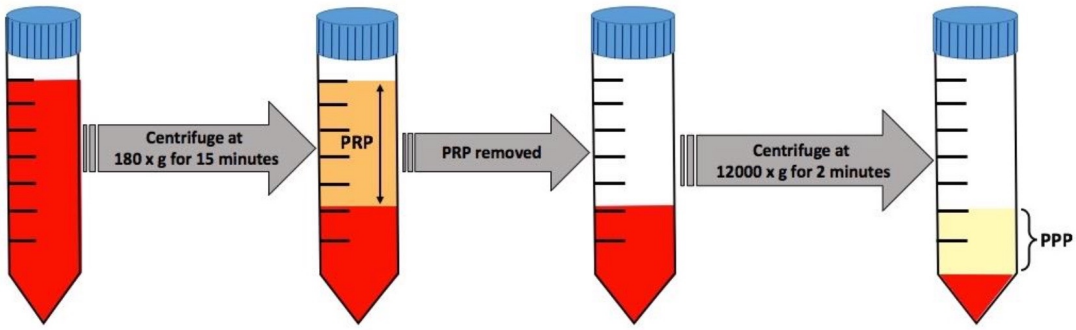

Figure 3.1 Centrifugation of whole blood

Schematic diagram outlining the process of centrifuging whole blood to obtain platelet rich plasma (PRP) and platelet poor plasma (PPP).

3.2.3 Preparation of washed platelets

PRP was centrifuged with the addition of PGI_2 (2 µg/ml) and apyrase (0.02 U/ml), at 1000 x g for 10 min resulted in a platelet pellet that was re-suspended in modified Tyrode's-HEPES buffer (NaCl, 134 mM; KCl, 2.9 mM; Na_2HPO_4, 0.34 mM; $NaHCO_3$, 12 mM; HEPES, 20 mM; $MgCl_2$, 1 mM), supplemented with glucose (0.1% w/v), bovine serum albumin (BSA; 0.35% w/v) and apyrase (0.02 U/ml). PGI_2 (2 µg/ml) was added and the platelets were centrifuged again at 1000 x g for 10 min. Supernatant was removed and the pellet was resuspended in modified Tyrode's-HEPES buffer to yield washed platelets.

3.2.4 Preparation of syringe filtered platelets

Apyrase (0.02 U/mL) was added to a volume of washed platelets which were then loaded into a syringe and forced, by hand, through an 5 µm Acrodisc® syringe filter.

3.2.5 Preparation of magnetically activated cell sorted (MACS) platelets

Washed platelets were incubated with (MACS + beads) or without (MACS - beads) anti-CD45 magnetic beads for 15 min at 4°C. LD MACS separation columns were mounted on a MACS separation stand and primed with MACS buffer before the platelets were added. The washed platelets were then passed through these columns twice and the flow-through was collected (Figure 3.2).

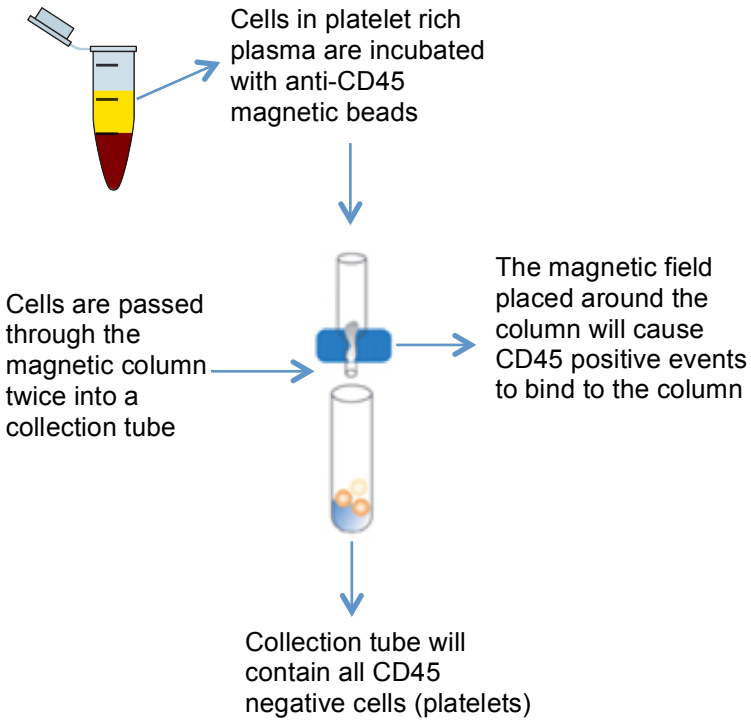

Figure 3.2 Magnetic activated cell sorting of platelets

A schematic diagram showing the labelling and processing of PRP to remove contaminating CD45 positive events, using magnetic separation techniques.

3.2.6 Light transmission aggregometry (LTA)

LTA is considered to be the gold standard for platelet aggregation testing. It is based upon the principles first outlined by Gustav Born in the 1960s [150]. In this study 225 µL of PRP was added to each cuvette that was then placed in one of eight channels in a Bio/Data PAP-8E turbidometric aggregometer. PRP was stirred, by placing a stir bar in the bottom, and incubated at 37°C. All channels were blanked using a cuvette containing 250 µL PPP and a stir bar. 25 µL of agonist at 10 times the final required concentration was added to the appropriate PRP containing cuvettes. PBS was used as a diluent for ADP and TRAP-6 amide, isotonic glucose for collagen, and 0.1% ascorbic acid/PBS for arachidonic acid. When agonists were added causing the platelets to aggregate the platelet suspension became less turbid, decreasing light scatter and thus increasing light transmission as detected by the photocell.

3.2.7 Optimul plate assay

Flat-bottom half area microtitre plates were precoated with hydrogenated gleatin in PBS before the addition of agonists. Agonists used were ADP (0.005-40 µM), epinephrine (0.0004-10 µM), TRAP-6 amide (0.03-40 µM), U46619 (0.055-40 µM), arachidonic acid (0.03-40 µM), ristocetin (0.14-4 mg/mL) and Horm collagen (0.01-40 µg/mL). 5 µL of agonist was added to its corresponding well. The plates were then placed in a -80°C freezer for 1 hour before being put into a freeze-dryer at -40°C and left overnight. Plates were then vacuum-sealed and wrapped in aluminum foil until required [151] (Figure 3.3). Upon use, 40 uL of PRP or PPP was added to the appropriate wells, the plate were shaken on a Bioshake plate shaker at 1200 rpm, for 5 min at 37°C and the absorbance was read at 595 nm on a Tecan Sunrise plate reader.

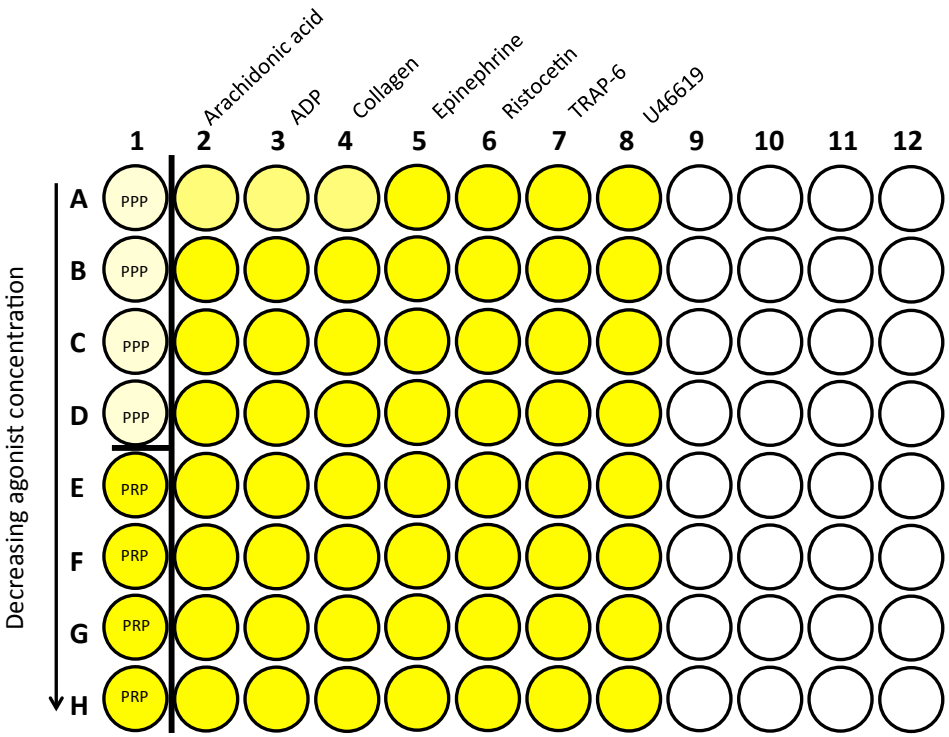

Figure 3.3 Example Optimul plate setup

Agonists freeze dried onto plate in columns 2-8. Column 1 A-D contain PPP representing 100% aggregation, E-H contain PRP representing 0% aggregation.

3.2.8 Flow cytometry quantification of white blood cell contamination

To quantify white blood cell (WBC) contamination samples were incubated with anti-human CD45 PerCP-Cyanine5.5 (1:60) to identify WBCs and anti-human CD61 APC (1:25) to identify platelets. Both antibodies were diluted in saline and samples were incubated for 30 min in the dark at 4°C and fixed in 990 µL 1% formalin in saline. Data was then acquired on a FACSCalibur flow cytometer using CellQuest software. CD45-positive events were recorded and expressed per 100,000 CD61-positive events using FlowJo software.

3.2.9 Flow cytometric assessment of platelet activation

To assess platelet activation, platelet preparations (PRP, washed platelets, or FACS sorted platelets) were stimulated with TRAP-6 25 μM and shaken in a 96-well plate at 1200 rpm for 5 min or left untreated for measurements of basal activation. Samples were then incubated for 30 min in the dark at 4°C with CD61 APC (1:160) as the platelet identifier and CD62P PE (1:80) as the indicator of activation, and then fixed using 500 μL 1% formalin in saline. Flow cytometry was then used to quantify either the number of CD62P positive events per 100,000 CD61 positive events or to obtain mean fluorescence intensity values for the total CD62P positive events. Data was acquired on a FACSCalibur flow cytometer using CellQuest software.

3.2.10 Whole blood RNA extraction

2.5 mL of blood was collected directly into PAXgene Blood RNA tubes containing 6.9 mL of reagent designed to lyse all cell types, prevent ex vivo gene regulation events and protect RNA molecules from RNase and other enzymatic degradation processes. The stabilisation of RNA molecules allowed samples to be frozen at -80°C for up to 96 months.

Prior to RNA extraction PAXgene Blood Tubes containing sample were removed from the -80°C freezer and left to thaw at room temperature for a minimum of 2 hrs. The tubes were then spun at 4000 x g for 10 min, the supernatant removed and pellet resuspended in RNase free water before being spun again at 4000 x g for 10 min. The pellet was then resuspended in optimised buffers and proteinase K to enable protein digestion. Samples were then centrifuged through a shredder spin column to remove debris. 350 μL ethanol was then added to the flow through to enable binding when placed into an RNA spin column. When centrifuged inside this spin column RNA selectively binds to the silica membrane whereas contaminants are washed through. A series of wash

steps were then implemented to further remove any contaminants. DNase I was added between washes to remove any remaining DNA. After washing RNA was eluted from the silica membranes with the addition of elution buffer. RNA was finally denatured by heating to 65°C for 5 min and stored at -20°C until required for its downstream applications. All reagents and materials were supplied in the PAXgene Blood RNA kit.

3.2.11 Platelet RNA extraction

RNA was extracted from platelets using the RNeasy mini kit and the protocol was based on manufacturers instructions. Centrifuging PRP at 1000 x g rpm for 10 min pelleted platelets, the supernatant was discarded. The cell pellet was then resuspened in 350 µL Buffer RLT, the pellet was disrupted by pipetting. This was then centrifuged for 3 min at 15000 x g. Supernatant was removed and to it 350 µL 70% ethanol was added to optimise binding conditions. 700 µL of the sample was transferred into an RNeasy Mini spin column containing the silica membrane to which the RNA binds, placed in a 2 mL collection tube and centrifuged for 1 min at 15000 x g. The flow through was discarded. 700 µL of Buffer RW1 was then added to the membrane and centrifuged as in the previous step. The flow through was discarded. 500 µL Buffer RPE was then added to the membrane and centrifuged as in the previous step, this was repeated twice. The spin column was then placed in a new 2 mL collection tube and spun for 1 min at 15000 x g to dry the membrane. To finally elute the RNA, the spin column was place into a new 2 mL collection tube, 30 µL of RNase free water was added and the column was spun for 1 min at 15000 x g. RNA was stored at -80°C until required.

3.2.12 cDNA synthesis

cDNA was synthesised from the extracted RNA using SuperScript III first-strand synthesis system for RT-PCR. Each sample had its own reaction tube. To these nuclease free-micro centrifuge tubes 8 µL of RNA, 1 µL of 50 µM oligo(dT) and 1 µL of 10 mM dNTP mix was added. The tubes were then incubated at 65°C for 5 min before being placed on ice for 5 min. To each of these tubes 10 µL of cDNA synthesis mix was added. cDNA synthesis mix was composed of 2 µL 10X RT buffer, 4 µL 25 mM $MgCl_2$, 2 µL 0.1 M DTT, 1 µL 40 U/µL RNaseOUT, 1 µL 200 U/µL SuperScript III RT. The tubes were then incubated at 50°C for 50 min followed by 85°C for 5 min before then being chilled on ice. 1 µL of RNase H was then added to each tube and incubated at 37°C for 20 min. cDNA was stored at -20°C until required.

3.2.13 Nanodrop quantification of RNA concentration

RNA concentrations were determined using the Nanodrop 2000 spectrophotometer. Prior to sample loading the instrument was cleaned and blanked against a deionised water control. 1 µL of RNA sample was pipetted onto the lower optical pedestal allowing the software to automatically calculate the RNA concentration.

3.2.14 Quantitative real tme PCR (qRT-PCR)

Target genes were rationally selected as candidates based on their associations to either white blood cells (ANPEP, PTPRC, MPO) or platelets (GP6, PF4, P2RY12). House keeping genes used were ACTB, TUBB1, 18S and GAPDH. TaqMan anti-human FAM-labelled probes were obtained from Life Technologies (ANPEP, Hs00174265_m1; PTPRC, Hs04189704_m1; MPO, Hs00924296_m1; GP6, Hs00212574_m1; PF4, Hs00427220_g1; P2RY12, Hs01881698_s1;

ACTB, Hs01060665_g1; TUBB1, Hs00258236; 18s, Hs99999901_s1 and GAPDH, Hs02758991_g1).

8 µL of the probe containing mix of 55 µL gene specific TaqMan probe, 295 µL of RNase free water and 550 µL of ABsolute qPCR ROX mix plus 2 µL cDNA were added to each well of a 384 well qPCR plate using an automated pipetting system. qRT-PCR was performed on a Applied Biosystems ABI 7900HT instrument. The cycle consisted of an initiation phase of 15 min at 95°C, followed by an amplification phase of 15 sec at 95°C then 1 min at 60°C for 40 cycles and then a dissociation phase of 15 sec at 95°C followed by 15 sec at 60°C followed by 15 min at 95°C. Data was collected using SDS software and analysed using the formula 2^-(GEOMEAN (composite Ct of platelet genes) – GEOMEAN (composite Ct of white blood cell genes). An example of how Ct values are derived can be seen in Figure 3.4.

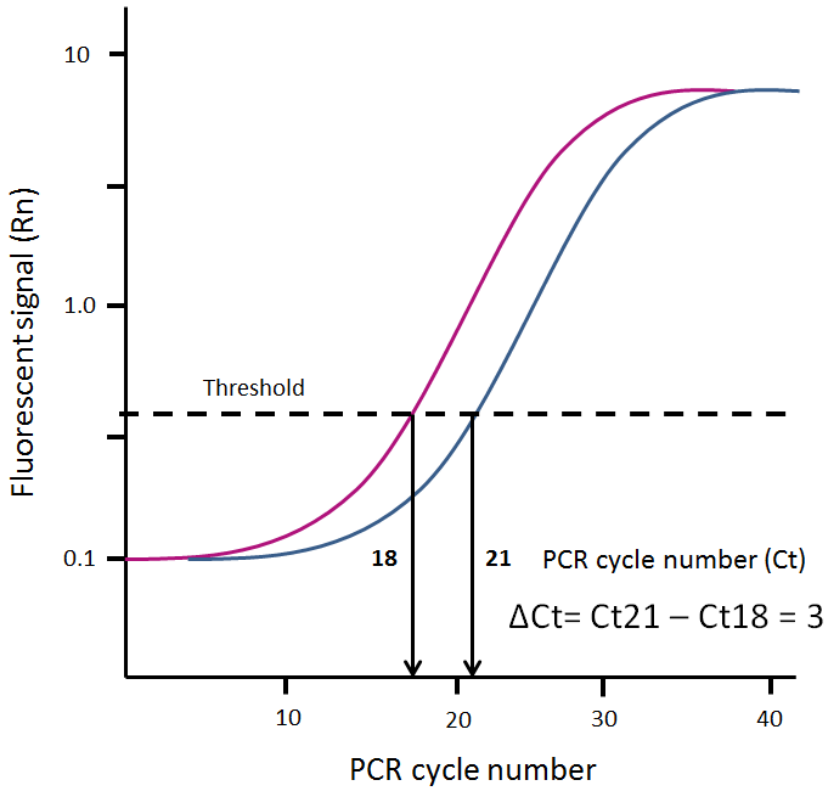

Figure 3.4 Hypothetical amplification plot

Hypothetical amplification plot showing how Ct values are obtained. The Ct value of a particular gene corresponds to the number of cycles it takes for that gene's fluorescence signal to surpass an arbitrary threshold set by the analysis software. From this example there is a three cycle difference between the pink and blue genes [152].

3.2.15 Statistical analysis

All statistical analyses were conducted used GraphPad Prism v6 and described in each results section.

3.3 Results

3.3.1 Assessing the impact of anticoagulants and blood collection methods on platelet aggregation using traditional light transmission (LTA) aggregometry and the Optimul plate assay

A blood sample was collected by venepuncture into either a syringe or vacutainer containing the anticoagulants ACD, lepirudin or citrate. PRP was produced from these samples and platelet responses assessed using LTA and the Optimul plate assay. In traditional LTA experiments there was no significant difference between syringes versus vacutainers (Figure 3.5) or between ACD versus lepirudin versus citrate (Figure 3.6) for any of the agonists used: AA 1 mM (A), ADP 20 µM (B), collagen 10 µg/mL (C) or TRAP-6 25 µM (D). In the Optimul plate assays there were no significant differences between responses of platelets collected in different anticoagulants in either syringe (Figure 3.7) or vacutainer (Figure 3.8) for the agonists AA (A), ADP (B), collagen (C), epinephrine (D), ristocetin (E), TRAP-6 (F) or U46619 (G) at multiple concentrations. Log EC50 values and the 95% confidence intervals of the log EC50 values can be seen for the syringe collected samples in Table 3.1 and for vacutainer collected samples in Table 3.2. Non-linear regression curves were fitted using GraphPad Prism software for each agonist using the following constraints; bottom ≥ 0 and top ≤ 100.

Comment on the fact that all the ‘not calculated’ 95% confidence interval values occurred exclusively in the lepirudin samples indicating the lack of reproducibility of results when using this anticoagulant.

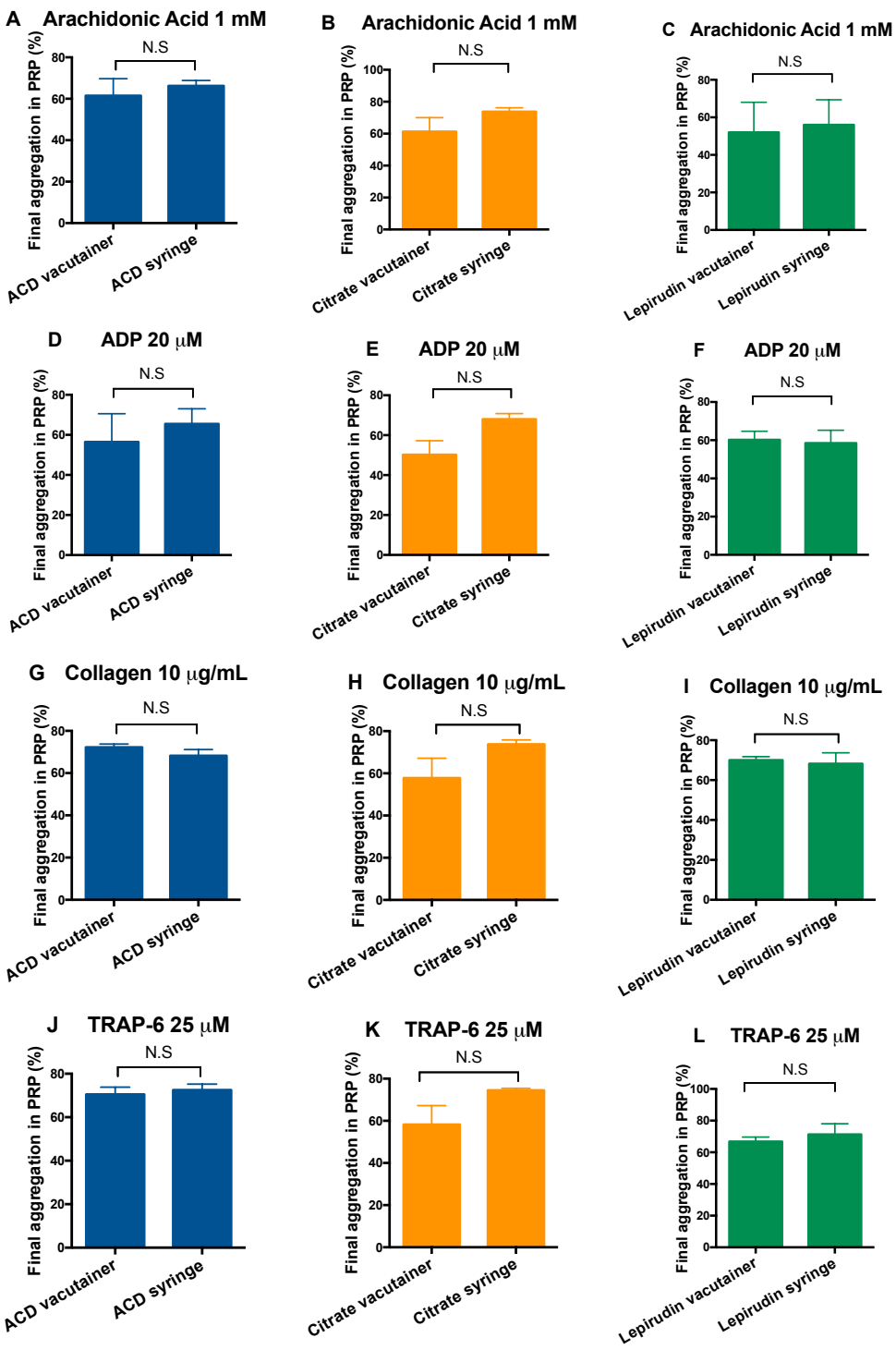

Figure 3.5 The effects of syringe versus vacutainer blood collection on platelet aggregation assessed using LTA

LTA aggregation data presented as final percentage aggregation. Results displayed as mean ± SEM (n=4). Significance was assessed using a t-test (p=<0.05).

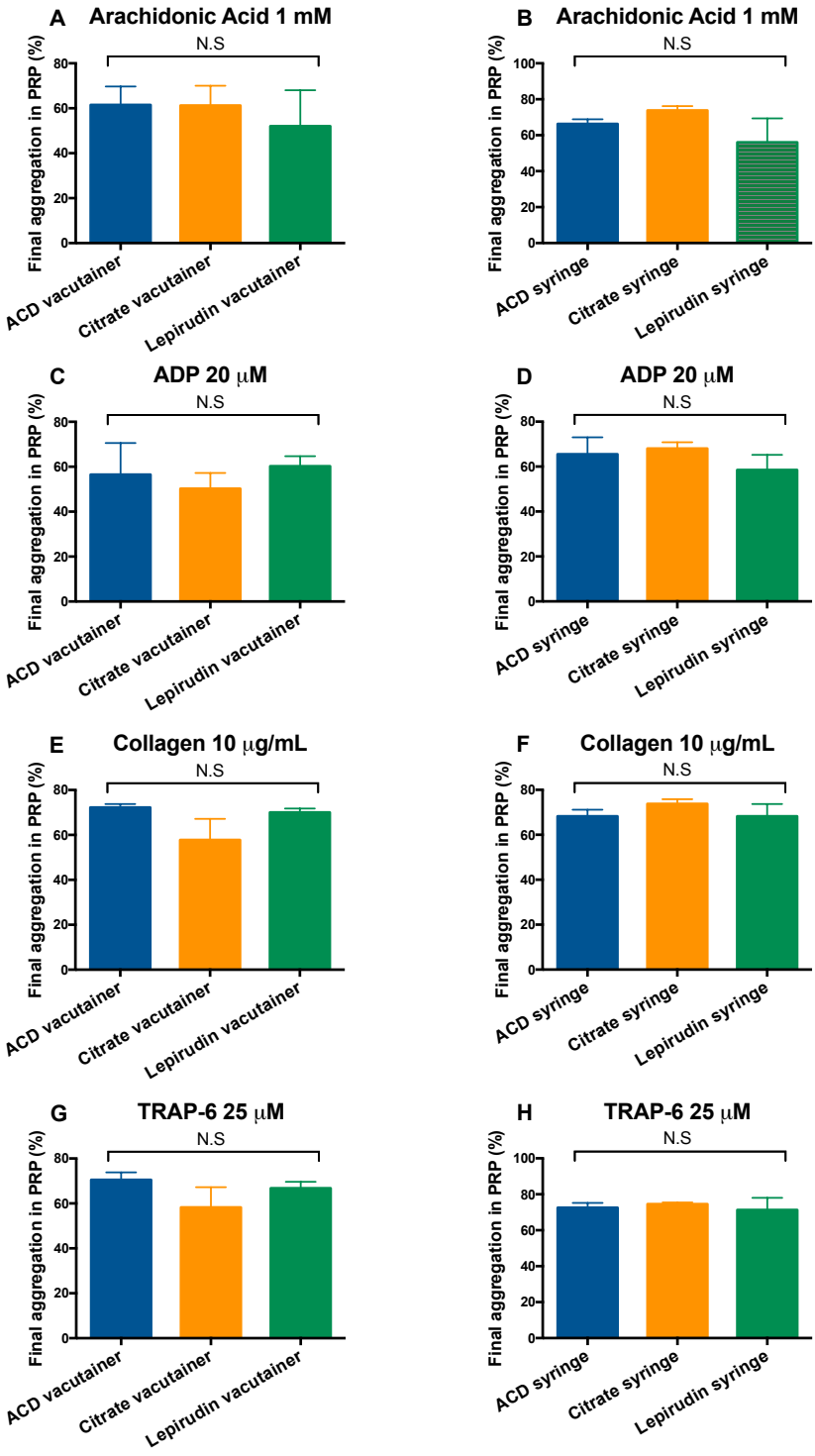

Figure 3.6 The effects of different anticoagulants on platelet aggregation assessed using LTA

LTA aggregation data presented as final percentage aggregation. Results displayed as mean ± SEM (n=4). Significance was assessed using a one-way ANOVA with Tukey's multiple comparisons test (p=<0.05).

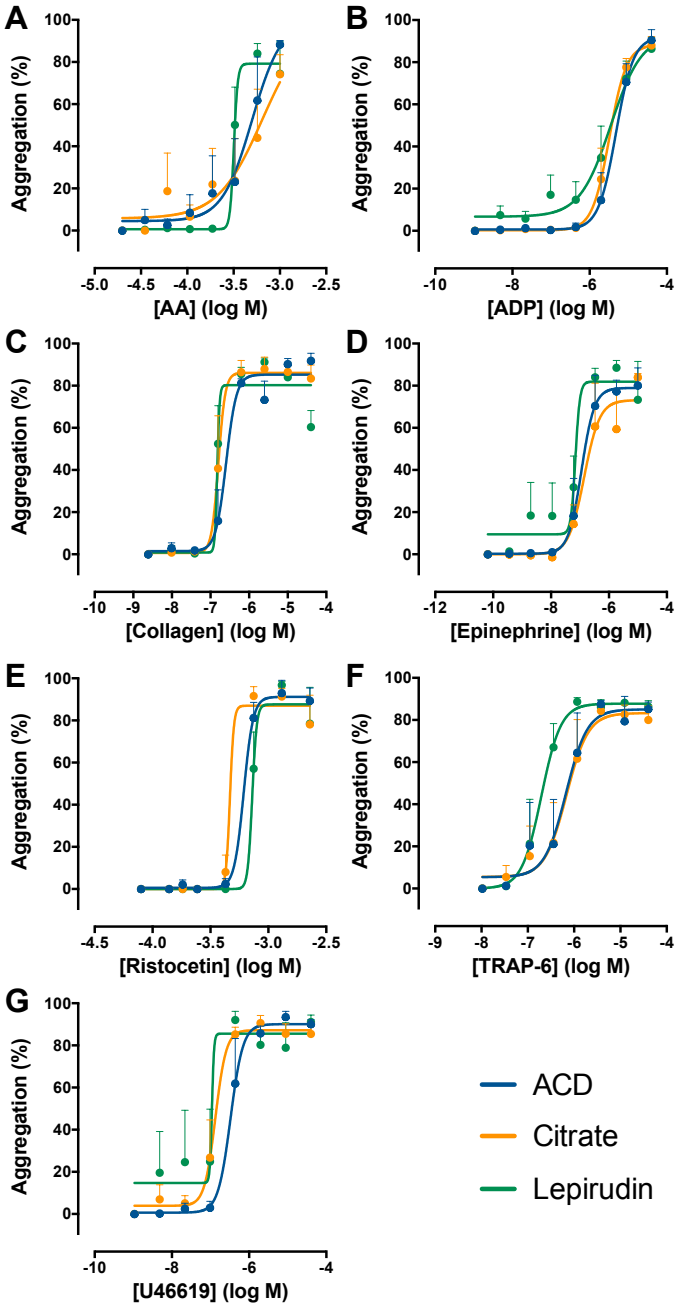

Figure 3.7 The effects of different anticoagulants on platelet aggregation assessed by the Optimul plate assay - syringe collected blood

Optimul plate platelet aggregation data presented as percentage aggregation for PRP samples obtained from syringe collected whole blood. Results displayed as mean ± SEM (n=4). Significance was assessed using a two-way ANOVA and Tukey's multiple comparisons test (p=<0.05).

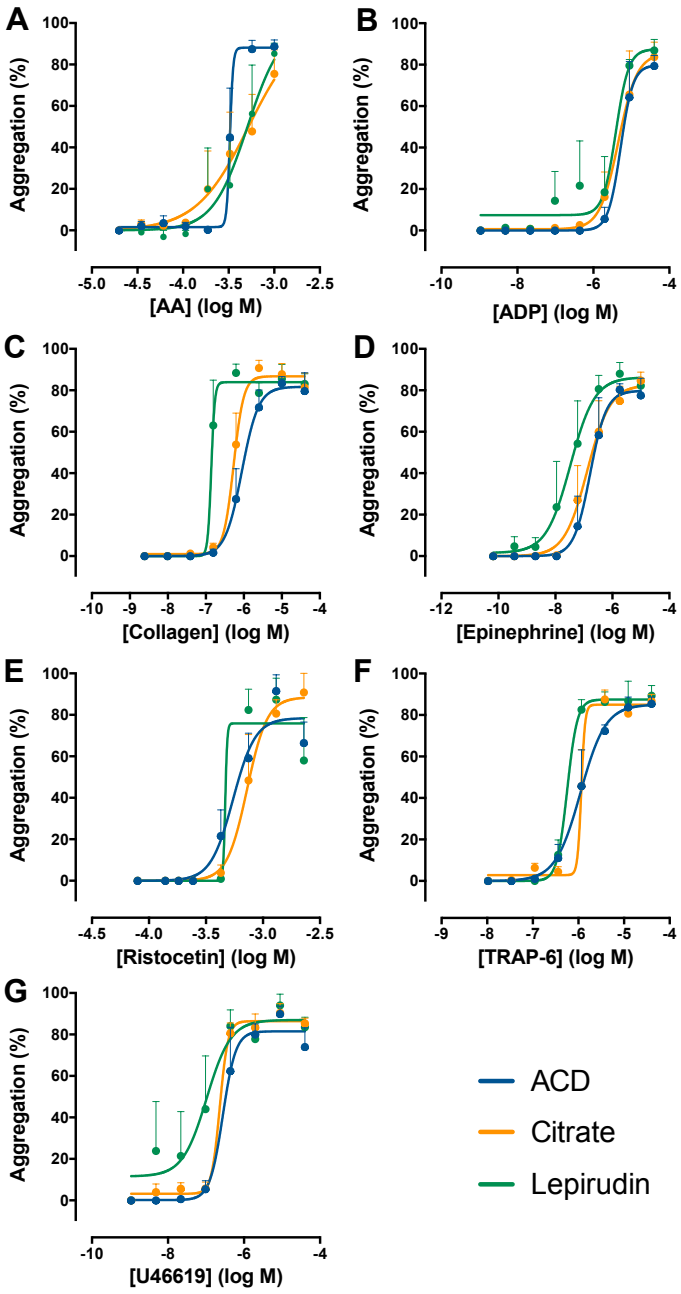

Figure 3.8 The effects of different anticoagulants on platelet aggregation assessed by the Optimul plate assay – vacutainer collected blood

Optimul plate platelet aggregation data presented as percentage aggregation for PRP samples obtained from syringe collected whole blood. Results displayed as mean ± SEM (n=4). Significance was assessed using a two-way ANOVA and Tukey's multiple comparisons test (p=<0.05).

Agonist	Anticoagulant	Log EC50 value	95% confidence interval of Log EC50
Arachidonic acid	ACD	-3.30	-3.645 to -2.958
	Citrate	-3.19	-4.681 to -1.696
	Lepirudin	-3.50	Not calculated
ADP	ACD	-5.32	-5.485 to -5.152
	Citrate	-5.49	-5.661 to -5.315
	Lepirudin	-5.45	-5.909 to -4.999
Collagen	ACD	-6.60	-6.807 to -6.384
	Citrate	-6.80	-7.061 to -6.529
	Lepirudin	-6.83	Not calculated
Epinephrine	ACD	-6.95	-7.251 to -6.650
	Citrate	-6.86	-7.266 to -6.447
	Lepirudin	-7.16	Not calculated
Ristocetin	ACD	-3.21	-3.288 to -3.137
	Citrate	-3.22	-3.281 to -3.167
	Lepirudin	-3.14	Not calculated
TRAP-6	ACD	-6.18	-6.520 to -5.831
	Citrate	-6.16	-6.465 to -5.861
	Lepirudin	-6.71	-6.904 to -6.509
U46619	ACD	-6.48	-6.686 to -6.276
	Citrate	-6.87	-7.145 to -6.603
	Lepirudin	-6.93	Not calculated

Table 3.1 Optimul data log EC50 values and 95% confidence intervals – syringe collected blood

Log EC50 values and 95% confidence intervals for the non-linear regression curves fitted to the Optimul data assessing effects of different anticoagulants on platelet aggregation in syringe collect blood samples.

Agonist	Anticoagulant	Log EC50 value	95% confidence interval of Log EC50
Arachidonic acid	ACD	-3.49	-3.519 to -3.453
	Citrate	-3.28	-4.436 to -2.128
	Lepirudin	-3.29	-3.810 to -2.777
ADP	ACD	-5.28	-5.496 to -5.070
	Citrate	-5.34	-5.633 to -5.048
	Lepirudin	-5.41	-5.814 to -5.006
Collagen	ACD	-6.05	-6.232 to -5.873
	Citrate	-6.27	-6.425 to -6.113
	Lepirudin	-6.86	Not calculated
Epinephrine	ACD	-6.78	-7.081 to -6.477
	Citrate	-6.88	-7.240 to -6.520
	Lepirudin	-7.47	-7.943 to -7.004
Ristocetin	ACD	-3.26	-3.365 to -3.160
	Citrate	-3.14	-3.217 to -3.061
	Lepirudin	-3.33	Not calculated
TRAP-6	ACD	-5.96	-6.141 to -5.769
	Citrate	-5.98	-6.073 to -5.881
	Lepirudin	-6.25	-6.376 to -6.118
U46619	ACD	-6.56	-6.818 to -6.299
	Citrate	-6.64	-6.838 to -6.440
	Lepirudin	-6.98	-7.529 to -6.435

Table 3.2 Optimul data log EC50 values and 95% confidence intervals – vacutainer collected blood

Log EC50 values and 95% confidence intervals for the non-linear regression curves fitted to the Optimul data assessing effects of different anticoagulants on platelet aggregation in vacutainer collect blood samples.

3.3.2 Assessing the impact of anticoagulants and blood collection methods on platelet activation by flow cytometric analysis of P-selectin expression

In addition to measures of platelet aggregation, platelet activation in response to the three anticoagulants and the syringe or vacutainer collected blood samples was measured by quantifying platelet surface expression of P-selectin (CD62P) using a flow cytometric assay. There was no significant difference between syringes versus vacutainers for either PBS vehicle treated PRP or TRAP-6 (25 μM) stimulated PRP (Figure 3.9) or between ACD versus lepirudin versus citrate anticoagulants (Figure 3.10).

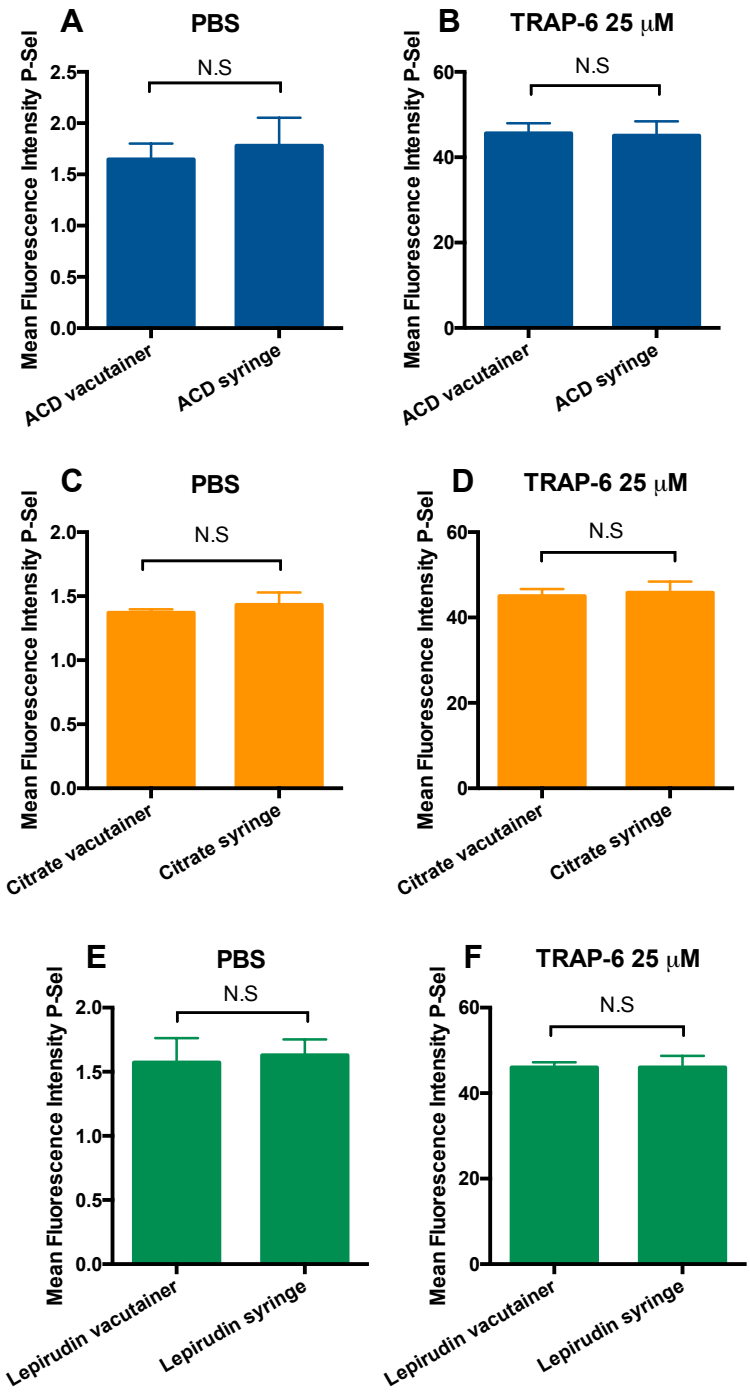

Figure 3.9 The effects of syringe versus vacutainer blood collection on platelet activation

Flow cytometric analysis comparing platelet surface P-selectin (CD62P) expression for PBS (A,C,E) or TRAP-6 (25 μM) (B,D,F) treated PRP. Data presented as mean fluorescence intensity of P-selectin. Results displayed as mean ± SEM (n=4). Significance was assessed using a t-test (p=<0.05).

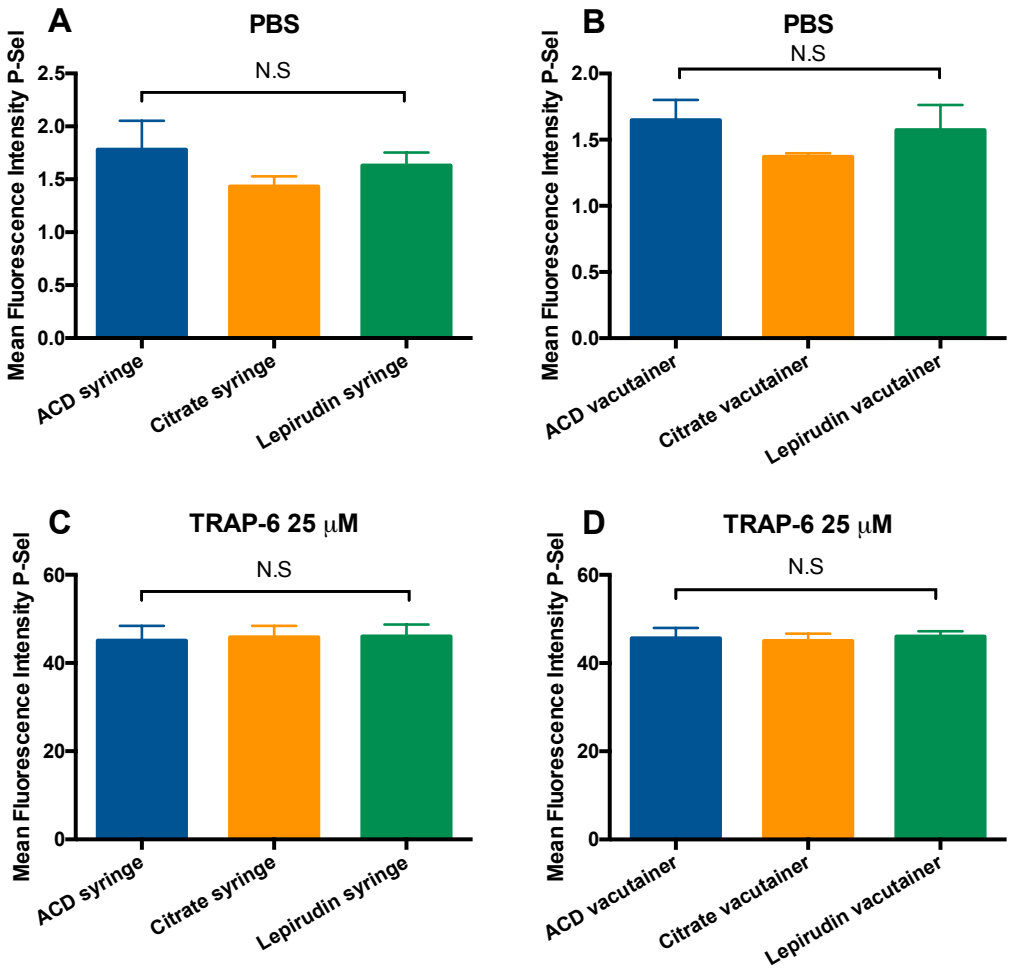

Figure 3.10 The effects of different anticoagulants on platelet activation

Flow cytometric analysis comparing platelet surface P-selectin (CD62P) expression for PBS (A,B) or TRAP-6 (25 μM) treated (C,D) PRP. Data presented as mean fluorescence intensity of P-selectin. Results displayed as mean ± SEM (n=4). Significance was assessed using a one-way ANOVA and Tukey's multiple comparisons test (p=<0.05).

3.3.3 Selection of appropriate antibody dilutions for the identification of platelets and WBCs in PRP samples

In order to maximise target identification and to minimise off target binding when using antibodies in flow cytometric assays it was important to first test a range of antibody dilutions from which optimal dilutions could be selected.

CD61 APC was used as the platelet specific identifier at a dilution range of 1:20, 1:25, 1:40 and 1:80 (Figure 3.11 A-B). CD45 PerCP-Cyanine 5.5 was used as the white blood cell specific identifier at a dilution range of 1:30, 1:60, 1:120, 1:160 (Figure 3.11 C-D). Isotype controls were used to identify non-specific binding. Based on sufficient difference between the isotype control signals, CD61 APC at a dilution of 1:25 and CD45 PerCP-Cyanine 5.5 at a dilution of 1:60 were selected as appropriate dilutions for experiments moving forward.

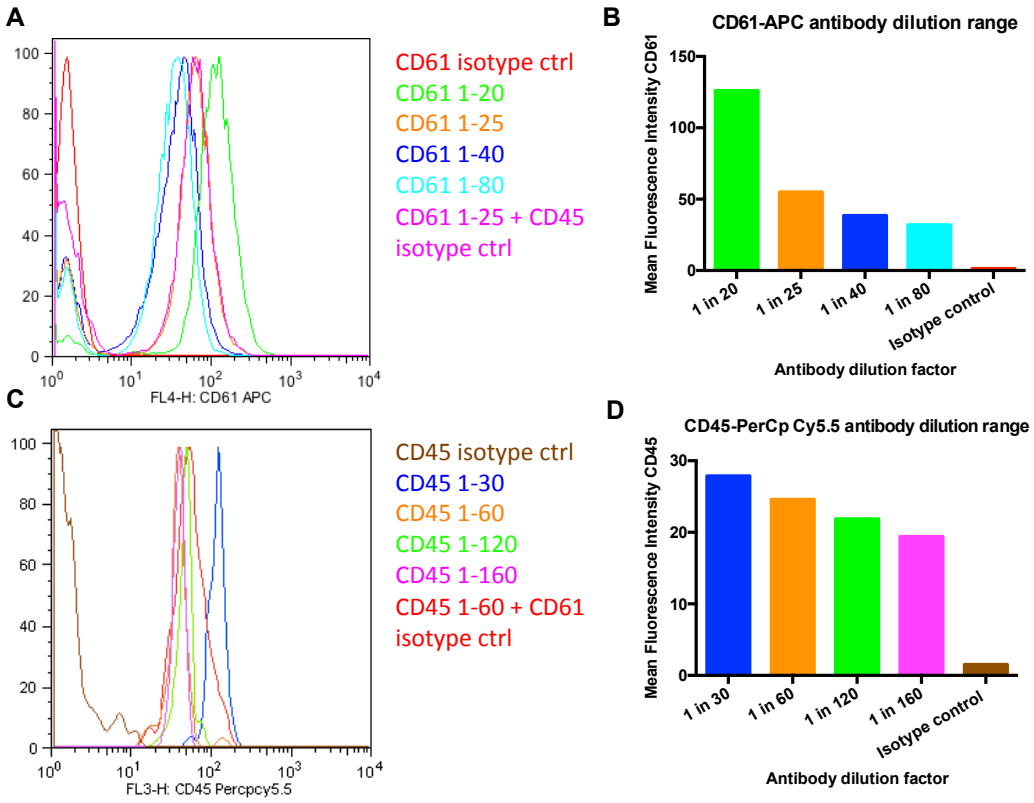

Figure 3.11 Flow cytometric histograms used to identify appropriate antibody dilutions

Representative histograms (A,C) and bar charts (B,D) showing mean fluorescence intensity of CD61 APC or CD45 PerCP-Cyanine 5.5 across a dilution range. Histograms created using FlowJo v8.7 software.

3.3.4 Flow cytometric gating strategies for platelets and WBCs in whole blood or PRP samples

Antibodies for CD61 and CD45 were used to identify platelets (Figure 3.12 B and E) and white blood cells (Figure 3.12 C and F) respectively in samples of either whole blood (Figure 3.12 A-C) or PRP (Figure 3.12 D-F). Gating was based on side scatter and forward scatter or by fluorescence intensity of the identifying antibody. The cell populations of interest are shown inside the pink shapes.

Sample acquisition stop gates we set at either 100,000 or 1,000,000 CD61 positive events and the percentage of CD45 positive events were recorded for each. There was no significant difference in the percentage of CD45 positive events between samples containing 100,000 versus samples containing 1,000,000 CD61 positive events showing that acquiring 100,000 CD61 positive events is sufficient for accurate quantification of WBC contamination (Figure 3.13).

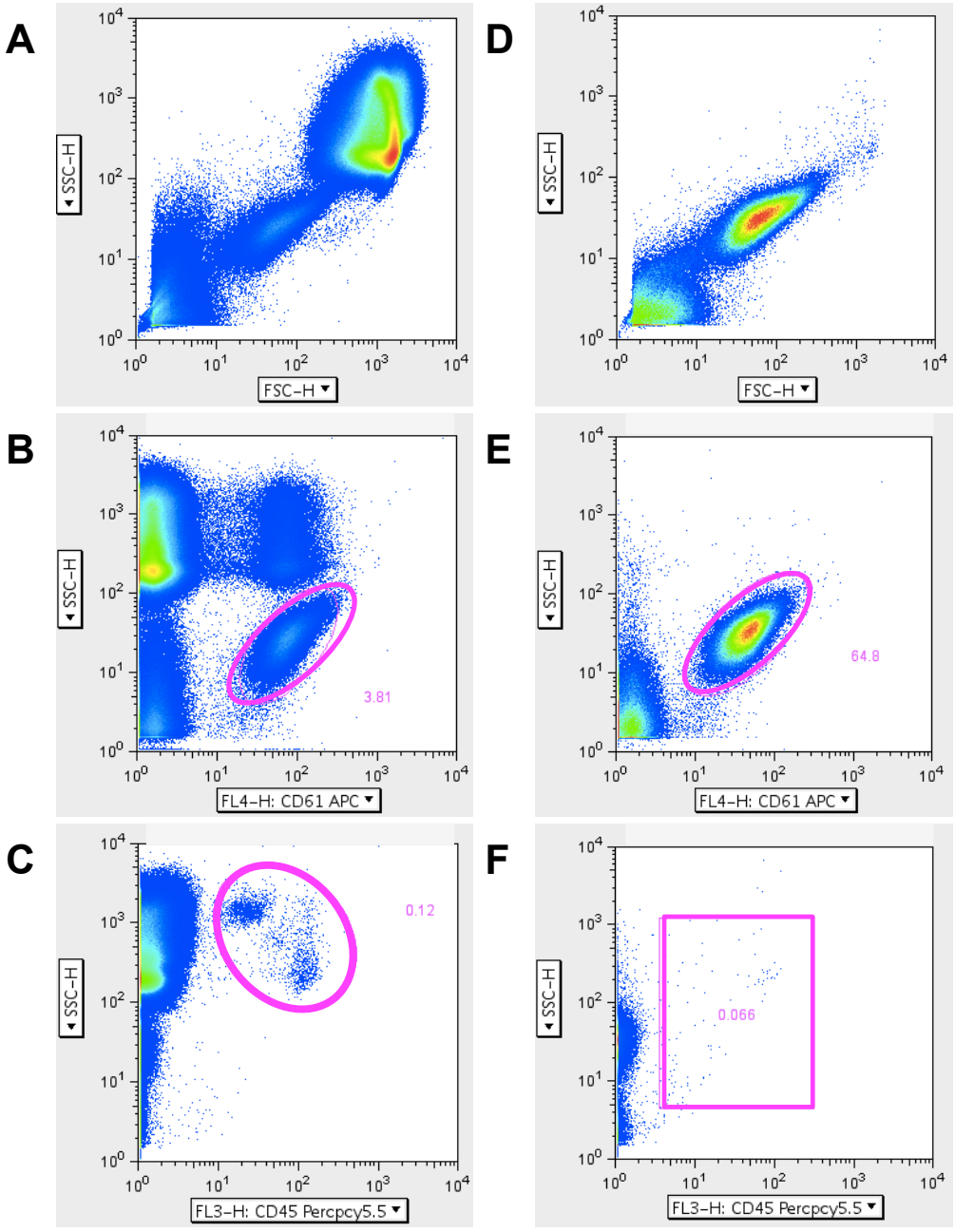

Figure 3.12 Identifying platelets and WBCs in whole blood and PRP using flow cytometry

Representative pseudo-colour plots showing the cellular populations present in both whole blood samples (A-C) or in PRP samples (D-F). Platelets were identified using CD61 APC. WBCs were identified using CD45 PerCP Cyanine 5.5. Pseudo-colour plots created using FlowJo v8.7 software.

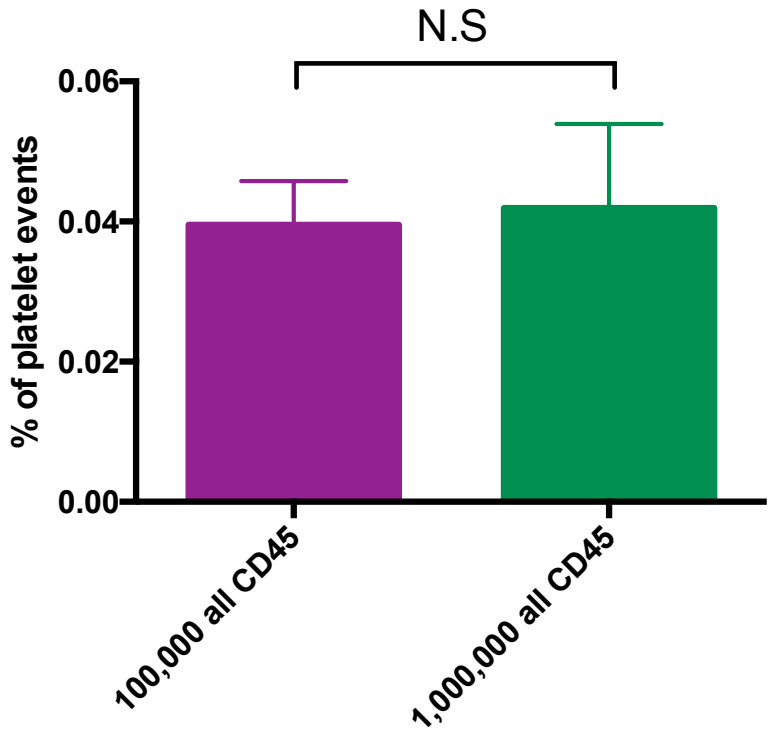

Figure 3.13 Assessing the percentage of CD45 positive events when capturing 100,000 or 1,000,000 CD61 positive events

Flow cytometric analysis comparing the percentage of CD45 events in PRP samples where either 100,000 or 1,000,000 CD61 positive events were captured. Results displayed as mean ± SEM (n=10). Significance was assessed using a t-tes (p=<0.05).

3.3.5 Flow cytometric assessment of WBC contamination for each platelet isolation method

Platelets were isolated from whole blood using various isolation protocols as outlined in Methods 3.2.2-3.2.5. Populations were gated to capture total CD45 positive events. Each isolation method showed significant reductions in CD45-positive events compared to whole blood. In freshly collected blood there were 2416±210 CD45-positive events per 100,000 platelets. All platelet isolation methods produced marked reductions in CD45-positive events (Figure 3.14): PRP 41±6; washed platelets 59±12, washed platelets plus syringe filter 57±12; MACS minus beads, 37±7; MACS plus beads, 36±10 (per 100,000 platelets). No significant differences were seen between the different isolation methods ($p>0.05$).

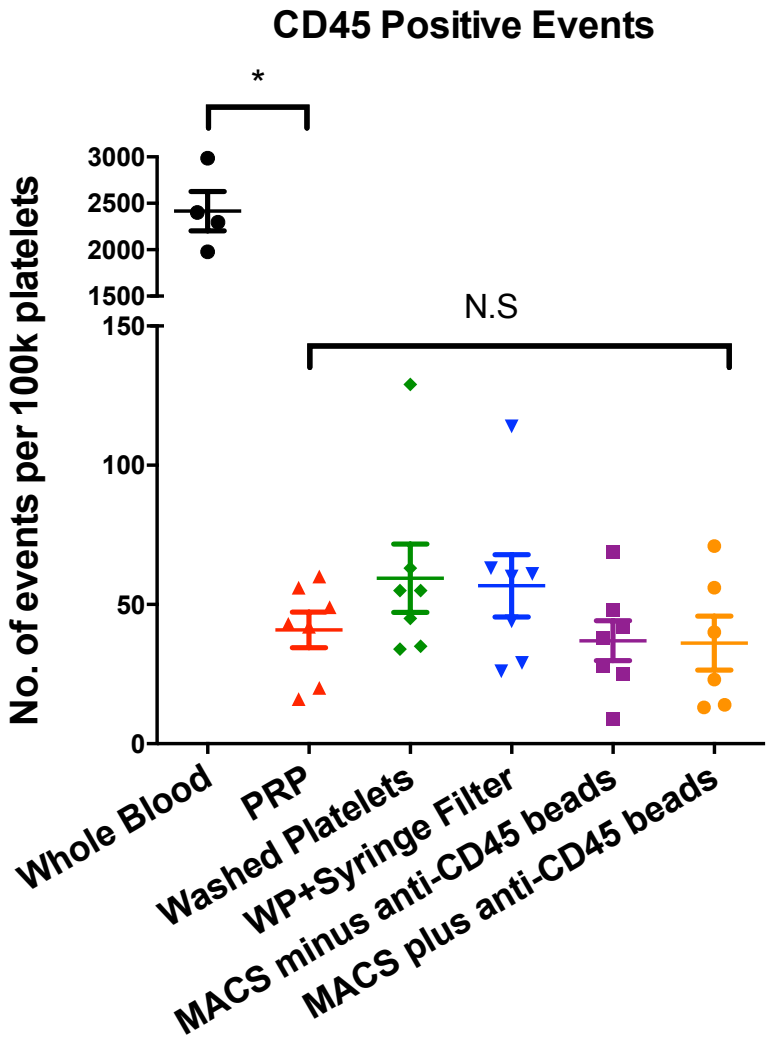

Figure 3.14 FACS quantification of WBC contamination

FACS analysis showing the number of total CD45 positive events per 100,000 CD61 positive events in whole blood, platelet rich plasma (PRP), washed platelets, washed platelets passed through a syringe filter, PRP through MACS columns without CD45 magnetic beads, and PRP through MACS columns with CD45 magnetic beads. Results displayed as mean ± SEM. A one-way ANOVA with Tukeys multiple comparisons test was used to determine significance ($p=<0.05$) n=8.

3.3.6 Nanodrop quantification of RNA concentration obtained using various RNA extraction kits

RNA was extracted from 25-35 mL of PRP obtained from 100 mL of whole blood and pelleted by centrifugation with PGI_2. Three commercially available RNA extraction kits were compared for RNA concentration following extraction measured using the Nanodrop 2000 spectrophotometer. There was no significant difference between the three kits tested (Figure 3.15). As a consequence the RNeasy minikit was used for all proceeding RNA extractions owing to its simplicity of use.

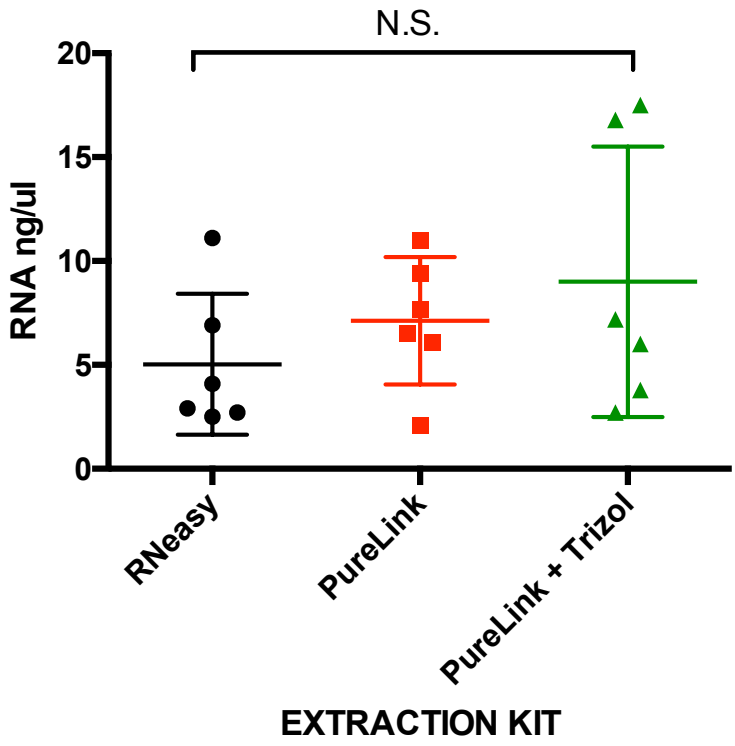

Figure 3.15 Comparison of commercially available RNA extraction kits

Nanodrop quantification of RNA concentrations extracted from PRP using the RNeasy mini kit, PureLink RNA mini kit and the PureLink RNA mini kit plus a TRIzol lysis step. Results displayed as mean ± SEM (n=6). A one-way ANOVA with Tukey's multiple comparisons test was used to determine significance ($p<0.05$).

3.3.7 Optimising minimum PRP volumes for subsequent RNA analysis

In many situations access to patient or healthy volunteer blood samples are limited due to ethical restrictions. For this reason it is important to determine the minimum volume of PRP required for RNA extraction and the production of reliable signals using downstream applications such as qRT-PCR. Figure 3.16 shows that as the volume of PRP increases the average Ct value of each gene decreases. The greater the Ct value the smaller the amount of RNA present in the sample prior to amplification.

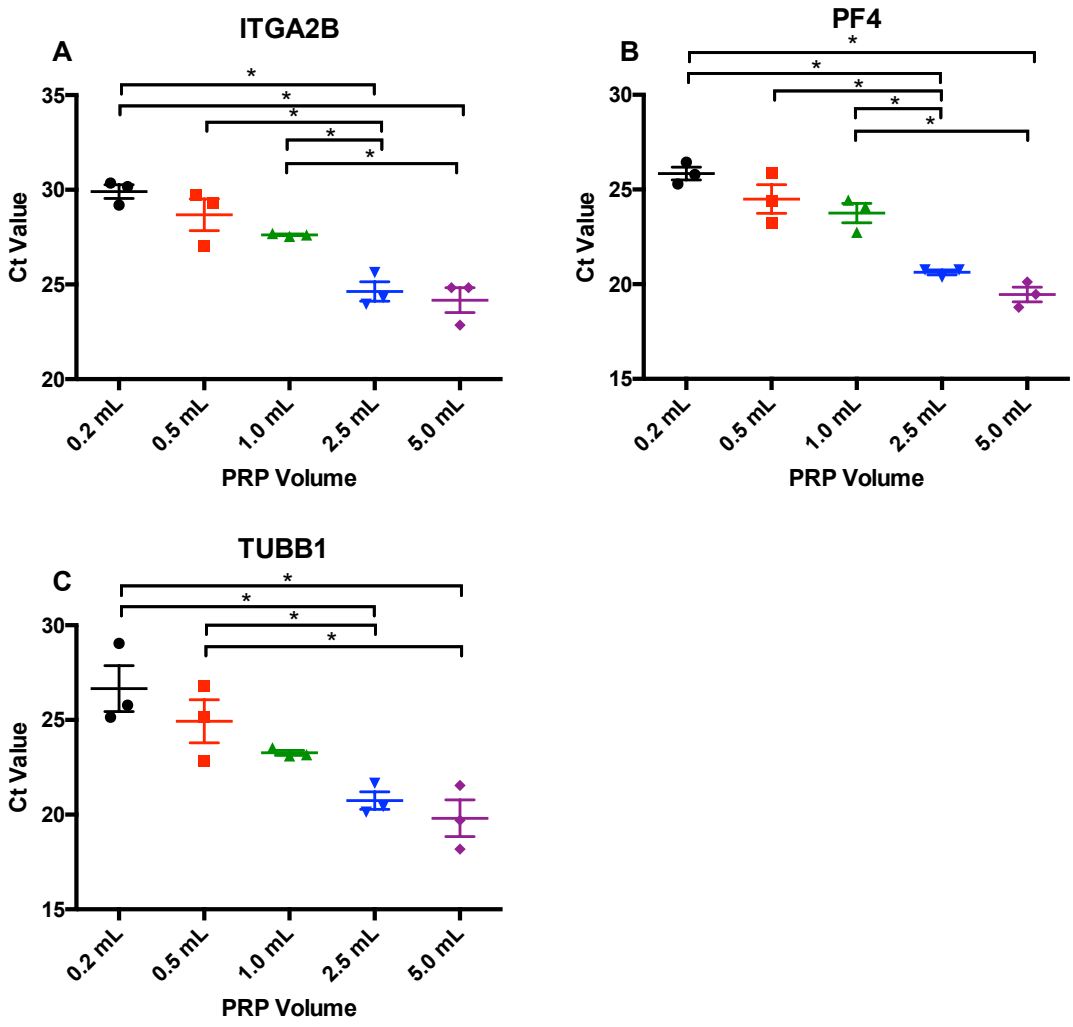

Figure 3.16 qRT-PCR analysis of abundant platelet genes in RNA samples extracted from a range of PRP volumes

qRT-PCR analysis comparing the mean Ct values for three genes which are abundant in platelets; ITGA2B, PF4 and TUBB1 for RNA extracted from 0.2 mL, 0.5 mL, 1.0 mL, 2.5 mL and 5 mL PRP. Each gene was run in triplicate. Results displayed as mean ± SEM (n=3). A one-way ANOVA for each individual gene with Tukeys multiple comparisons test was used to determine significance and represented as bars between groups ($p<0.05$).

3.3.8 qRT-PCR assessment of WBC contamination for each platelet isolation method

The qRT-PCR data further supports the results generated by flow cytometry. Data shows that all platelet isolation protocols significantly increase the expression of platelet specific genes (composite measure of P2RY12, PF4 and GP6 mRNA levels) in comparison to whole blood (Figure 3.17). The greatest change occurs between whole blood and PRP showing a 554-fold increase in platelet specific gene expression compared to white blood cell specific gene expression (Table 3.3). Ct values for each individual gene can be found in Table 3.4.

Platelet extraction method	Fold change in comparison to WB	Fold change in comparison to PRP
Whole blood	N/A	N/A
PRP	554	N/A
Washed platelets	2010	3.6
WP+syringe filtering	3635	6.6
WP+MACS	6031	10.9

Table 3.3 Summary of qRT-PCR data comparing expression of platelet specific genes to WBC specific genes

Table comparing the fold change in the ratio of platelet specific to WBC specific gene expression. Values were then compared to the fold change in relation to whole blood and again to the fold change in comparison to PRP for each platelet extraction method.

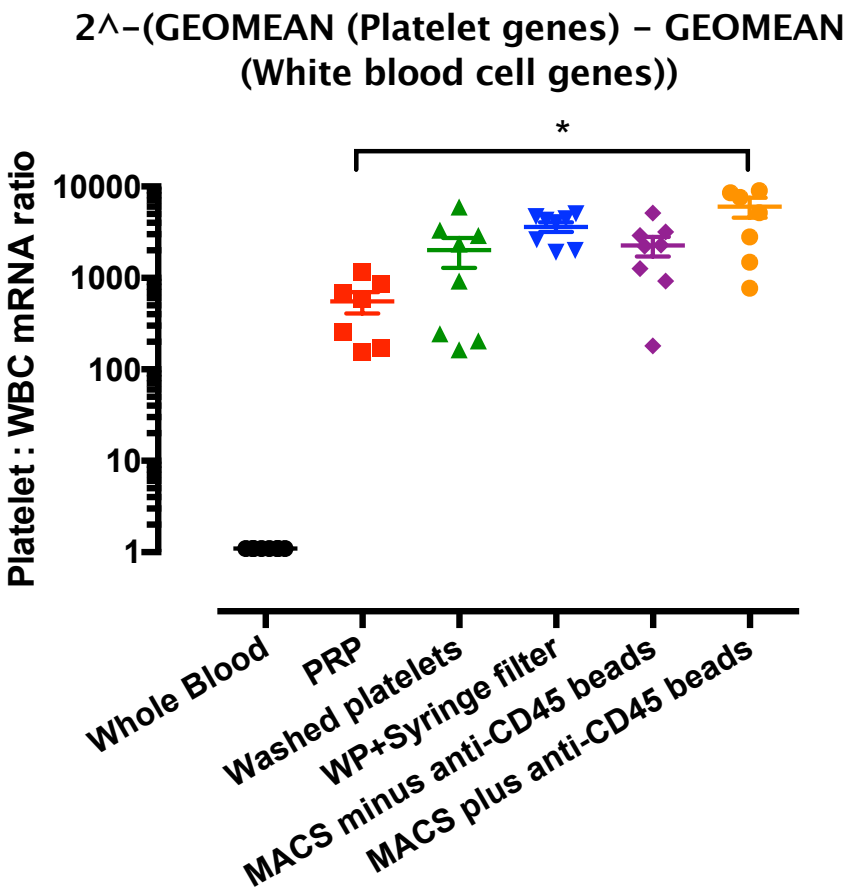

Figure 3.17 qRT-PCR data comparing expression of platelet specific genes to WBC specific genes

qRT-PCR data plotting the ratio of platelet specific gene expression (GP6, PF4, P2RY12) to WBC specific gene expression (ANPEP, MPO, PTPRC). Results were calculated using the formula 2^-(GEOMEAN (Platelet markers)-GEOMEAN (WBC markers)) and significance assessed using column statistics with a one sample t-test comparing all extraction methods to whole blood which was set as the hypothetical value of 1. Results displayed as mean ± SEM (n=6).

Platelet extraction method	Average Ct value for PF4	Average Ct value for GP6	Average Ct value for P2RY12	Average Ct value for ANPEP	Average Ct value for MPO	Average Ct value for PTPRC
Whole blood	26.2	32.2	31.6	26.0	32.7	24.4
PRP	22.4	30.1	29.4	33.5	38.9	30.0
Washed platelets	21.7	28.2	28.1	34.2	37.5	29.0
WP+syringe filtering	23.9	30.9	30.5	39.2	39.6	34.1
WP+MACS	24.7	31.1	30.9	39.7	39.4	36.1

Table 3.4 qRT-PCR data comparing individual gene expression of platelet specific genes to WBC specific genes

Table of raw Ct value data used to generate Figure 3.17. Data table shows the average Ct values for each of the six individual genes used in the calculation 2^-(GEOMEAN (Platelet markers)-GEOMEAN (WBC markers)). Results displayed as mean (n=6).

3.3.9 Assessing the impact of each isolation technique on platelet activation

To assess the impact of the isolation methods on platelet activation levels, flow cytometry was used and the expression of CD62P upon the platelet surface, as an indicator of P-selectin expression and platelet activation, was measured. Syringe filtering of washed platelets (mean=43003) induced significantly higher CD62P expression on platelets compared to PRP (mean=3799; $p<0.05$; Figure 3.18).

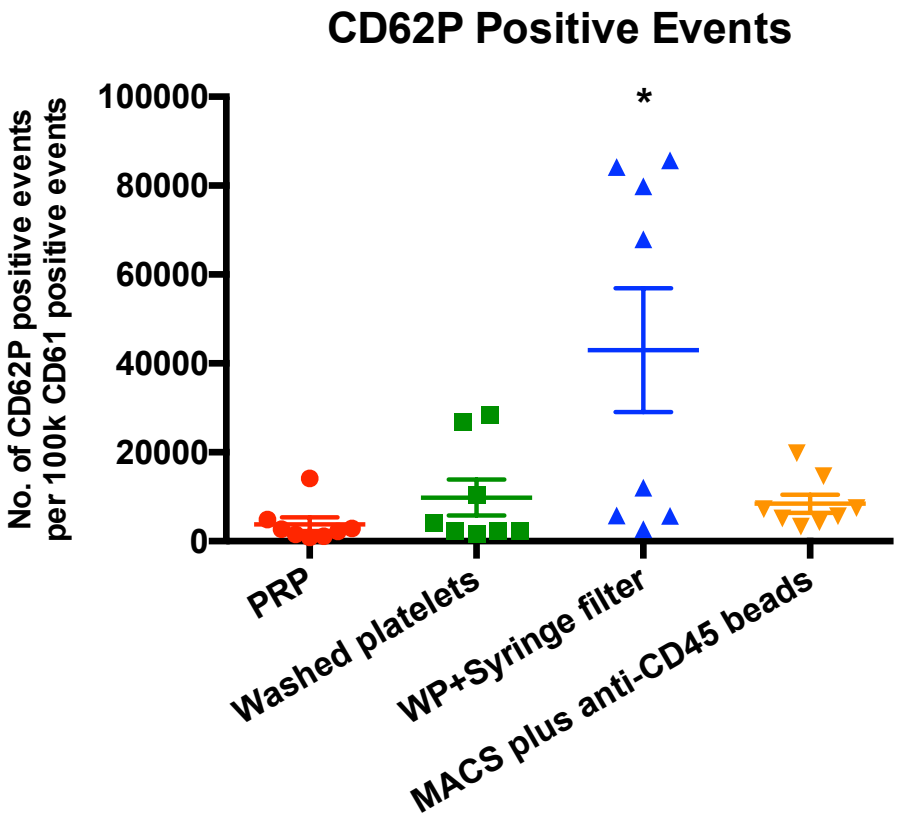

Figure 3.18 FACS analysis quantification of platelet activation

FACS analysis data of the number of CD62P positive cells found following different isolation methods per 100,000 CD61 positive events. Results displayed as mean ± SEM (n=8). A one-way ANOVA with Tukey's multiple comparisons test was used to determine significance ($p=<0.05$).

3.4 Discussion

Ex vivo and in vitro investigations of platelet function rely fundamentally on the ability to obtain an anticoagulated blood sample. The choice of anticoagulant used is key; the chosen agent must prevent the formation of a blood clot whilst preserving platelet function. Furthermore platelets are readily activated during the blood sampling procedure and so the selection of needle gauge, tourniquet release point and receptacle into which the blood is taken must be considered carefully in respect to the specific aspects of platelet function being investigated.

The inter-laboratory variability and lack of agreement on a standardised blood taking protocol for the assessment of platelet function in platelet rich plasma makes comparisons of data generated by different research groups challenging [153].

In this chapter I compared the use of three anticoagulants commonly used to study platelet function in PRP; acid-citrate-dextrose (ACD), lepirudin and sodium citrate. ACD and sodium citrate function as anticoagulants by chelating extracellular calcium. Calcium is an essential cofactor required for multiple processes occurring as part of the coagulation cascade. A drawback to using this type of anticoagulant is that calcium is also essential for platelet secretion and aggregation responses, thus calcium depletion may lead to altered in vitro reactivity [154]. In contrast lepirudin, a yeast derived recombinant version of hirudin, functions as an anticoagulant by acting as a direct thrombin inhibitor thus preventing the conversion of fibrinogen to fibrin in the coagulation cascade and inhibiting PAR activation. In studies performed using assays to examine platelet function in whole blood it has been reported that platelet aggregation was significantly impaired in citrated blood compared to samples containing thrombin inhibitors [155,156]. However supporting evidence in assays using PRP is lacking. According to results from a worldwide survey on the assessment of platelet function testing conducted by the International Society on Thrombosis and Haemostasis

99% of platelet testing laboratories surveyed used sodium citrate as their routine anticoagulant [157].

In addition I also compared the use of either syringe or vacutainer collection of blood samples. Advantages of using a syringe include being able to take a large volume of blood into a single container, being able to change the rate at which blood is collected and being able to alter the concentration of anticoagulant loaded into the syringe. Advantages of using a vacutainer include standardisation of anticoagulant concentration and blood volume, lower risk of contamination, exposure of blood to a consistent force and being simple to use [158].

Together I assessed these five blood collection variables in terms of their abilities to effect platelet aggregation, as measured using LTA (Figure 3.5 and Figure 3.6) and the Optimul assays (Figure 3.7 and 3.8), and platelet activation measured using a flow cytometric assay (Figure 3.9 and 3.10). I found that there was no significant difference between any of the combinations of anticoagulants or blood taking receptacles investigated within any of the assays used. Furthermore analysis of the 95% confidence intervals of the EC50 values calculated for each agonist response curve revealed large and in some cases incalculable ranges for many of the lepirudin samples (Table 3.1 and 3.2). Such large variability makes this the use of this anticoagulant unsuitable for experiments with small sample sizes. Therefore I collected future blood samples into sodium citrate filled syringes unless stated otherwise.

The ability to obtain a pure platelet population from freshly collected whole blood is essential for downstream platelet RNA expression analyses and for platelet function testing. This chapter compared the ability of four typically used methods to remove contaminating WBCs from isolated platelets. I found that there was a large reduction in both WBC number, as assessed using flow cytometric techniques (Figure 3.14), and WBC specific mRNA expression (Figure 3.17), as assessed by qRT-PCR, when comparing PRP to whole blood. This

reduction was noted as a more than 500-fold enrichment of platelet mRNA relative to WBC mRNA when comparing PRP to whole blood (Table 3.3). There was a further 6.6-fold enrichment by the use of subsequent syringe filtration (Table 3.4). However, there was a concern that this more robust physical manipulation of platelets could cause stimulation. This platelet stimulation could lead to activation of platelet transcription and/or selective activation and loss of particular platelet subpopulations that would confound analyses. To assess this possibility measurements of platelet surface expression of CD62P as a marked of platelet activation were made. Notably, this was unchanged between PRP and whole blood but was markedly increased in syringe filtered washed platelets (Figure 3.18).

In summary, the choice of anticoagulant or blood taking receptacle has negligible effect on measurements of platelet function including aggregation and activation. In addition, simple centrifugation of whole blood to obtain PRP is effective at reducing WBC contamination by a factor of around 500-fold. Additional steps of syringe filtering or magnetic cell separation provide at best a further 10.9-fold enrichment. However, these approaches introduce a very marked increase in sample preparation time and the potential for platelet activation. The simple production of PRP requires much less labour and expense and is highly applicable to large numbers of samples derived from population-based studies. Importantly, it also removes the need for extensive sample manipulation that could modify platelet phenotype and/or bias towards platelet subpopulations.

Chapter 4 - Isolation and functional analysis of newly formed reticulated platelets

4.1 Introduction

The platelet population as a whole is considered to be a heterogeneous mix of various sub-populations each with distinct biological capabilities [98]. Reticulated platelets, that is platelets rich in mRNA from their progenitor megakaryocytes [159], are currently attracting great research interest for two particular reasons. Firstly, because analysis of the mRNA within reticulated platelets may provide a window into the processes of platelet formation and the activity of megakaryocytes within the bone marrow. Secondly, because reticulated platelets may be particularly reactive and so key players in the development of thrombosis.

In normal physiological conditions human platelets survive within the circulation for some 7-10 days following their release from the bone marrow. Despite lacking a nucleus, these platelets contain a host of mRNAs, most of which are derived from the parent megakaryocyte. The residual mRNA from the megakaryocytes largely disappears within the first day or two of platelets entering the circulation meaning that the vast majority of this residual mRNA appears to reside within a small population of recently formed platelets, known as reticulated platelets. As can be reasoned from the difference between the survival of progenitor mRNA and the circulating life span of platelets, these reticulated platelets are estimated to account for around 10% of the total platelet population [94].

Functionally, reticulated platelets are often reported to be more reactive than non-reticulated platelets, however rigorous *in vitro* and *ex vivo* evidence is lacking. Some work has indicated that this population has an increased thrombotic potential due to the observation that reticulated platelets are more readily recruited into forming thrombi [160]. The clinical relevance of this population is also pertinent to the study of dual antiplatelet therapies where they may account for some of the high on treatment platelet reactivity in particular patient groups [96,161]. In particular, there is evidence linking reticulated platelets to high platelet reactivity and

consequent increase in the incidence of acute coronary syndromes and myocardial infarction [95,97,162]. Other diseases associated with increased platelet turnover or an increased reticulated platelet count include diabetes [163], kidney dysfunction [100] and sepsis [164]. Thus this population of platelets may provide an interesting target for novel therapeutics. This chapter therefore aims to establish a protocol for the isolation of reticulated platelets from PRP to subsequently investigate the reactivity of this subpopulation.

4.2 Methodology

4.2.1 Blood collection and preparation of PRP

Blood was obtained from healthy volunteers and PRP/PPP prepared as outlined previously in section 3.2.1 and 3.2.2.

4.2.2 Thiazole orange staining of platelets

Thiazole orange is an intracellular nucleic acid binding fluorescent dye (excitation wavelength of 510 nm and emission wavelength of 530 nm) and was used to determine the presence of RNA within platelets as an indicator of reticulation status. Thiazole orange was made to a concentration of 2 mg/mL in 100% methanol and then diluted to a concentration of 20 µg/mL in saline. 10 µL of thiazole orange (20 µg/mL) was added to 1 mL PRP and incubated at room temperature for 30 min.

4.2.3 Light transmission aggregometry (LTA) agonist stimulation of thiazole orange stained PRP

225 µL of thiazole orange stained PRP was added to add to each test cuvette and stimulated with 25 µL of agonist as described in section 3.2.6 to achieve final concentrations of arachidonic acid 1 mM, ADP 20 µM, collagen 10 µg/mL or TRAP-6 25 µM.

4.2.4 Flow cytometric sorting of reticulated, intermediate and non-reticulated platelets from PRP

Thiazole orange stained PRP was stirred for 5 min in the PAP8E-aggregometer prior to cell sorting. 1 mL of this was then added to 7 mL of HEPES-modified Tyrode's buffer as previously detailed, supplemented with glucose (0.1%), bovine serum albumin (0.35%),

apyrase (0.04 U/ml), PGE_1 (2 μM) and $CaCl_2$ (2 mM) for activation experiments and saline supplemented with apyrase (0.04 U/ml), PGE_1 (2 μM) and IBMX (0.5 mM) for qRT-PCR experiments. Platelets were sorted using a BD FACSAria Fusion based on gating according to thiazole-orange fluorescence. The top 10% of thiazole orange bright cells were gated as reticulated platelets, the middle 50% thiazole orange bright cells were gated as intermediate platelets and the bottom 30% of thiazole orange bright cells were gated as non-reticulated platelets.

4.2.5 qRT-PCR analysis for mRNA of genes of interest present within the three thiazole orange sorted populations

RNA was extracted using the RNeasy minikit as outlined in section 3.2.9 and cDNA synthesised using the SuperScript III synthesis system as outlined in section 3.2.10. Target genes were selected based on their specificity to platelets (ITGA2B Hs01116228_m1, PF4 Hs00427220_g1, TUBB1 Hs00258236_m1) or by their known involvement to pathways important to platelet function (ADCY3 Hs01086502_m1, GP6 Hs00212574_m1, GUCY1A3 Hs01015574_m1, P2RY1 Hs00704965_s1, P2RY12 Hs01881698, PEAR1 Hs01378394, PLA2G4A Hs00233352_m1, PTGIR Hs00168765, PTGS1 Hs003777726_m1, TBXAS1 Hs01022706). Taqman probes were used for all targets.

4.2.6 Flow cytometric assessment of platelet activation

Flow cytometry was used to quantify either the number of CD26P PE (1:80 dilution) positive events per 100,000 CD61 APC (1:160) positive events or to obtain mean fluorescence intensity values for the total CD62P positive events as indicators of platelet activation as described in detail in section 3.2.9. Data was acquired on a FACSCalibur flow cytometer using CellQuest software.

4.2.7 ATP release from agonist stimulated reticulated, intermediate and non-reticulated platelets

ATP release from platelet dense granules can be used as an indication of platelet activation. 2.5 million reticulated, intermediate and non-reticulated platelets were sorted as described in 4.2.4. The cells were pelleted at 1000 *x g* for 10 min with the addition of PGI_2 2 μM and subsequently resuspended in 45 μL of modified Tyrode's-HEPES buffer supplemented with $CaCl_2$ (0.1M) and fibrinogen (1 mg/mL). The platelets (2.5 million in 45 uL) were then placed into wells of a 96-well white, half area, flat bottom microtitre plate and stimulated with TRAP-6 (25 μM) by shaking on a plate shaker for 2 min at 1200 rpm. 25 uL of Chronolume luciferin-luciferase system reagent was then added to each well and shaken slowly for 2 min at 350 rpm. ATP release was subsequently determined by assessing the luminescence emitted by each well using a Tecan Infinite® M200 plate reader and comparing to standard ATP concentrations. A summary of the light emitting reaction is outlined below.

Luciferin + ATP → Luciferyl Adenylate + Inorganic phosphate [PPi]

Luciferyl Adenylate + O_2 → Oxyluciferin + AMP + LIGHT

4.2.8 Liquid chromatography tandem mass spectrometry (LC-MS/MS) analysis of agonist stimulated lipid release from reticulated, intermediate and non-reticulated platelets

10 million reticulated, intermediate and non-reticulated platelets were sorted as described in 4.2.4. The cells were pelleted at 1000 *x g* for 10 min with the addition of PGI_2 2 μM and subsequently resuspened in 900 μL of modified Tyrode's-HEPES buffer supplemented with $CaCl_2$ (0.1M) and fibrinogen (1 mg/mL). Each cell suspension was then divided into three LTA cuvettes and stimulated with PBS, TRAP-6 amide

(25 μM) or collagen (30 mg/mL) in a PAP8E aggregometer for 30 min at 37°C whilst being continually stirred. 30 μL of diclofenac/heparin solution (31.8 mg diclofenac sodium salt, 8.8 mL phosphate buffered solution, 200 μL heparin) was then added to each cuvette to stop the reaction. The contents of the cuvettes were transferred into 1.5 mL eppendorf tubes and centrifuged at 1000 *x g.* Supernatants (200 μL) were removed and stored at -80°C until required.

Samples were sent to Matthew Edin at The National Institute of Environmental Health Science, North Carolina, USA for liquid chromatography tandem mass spectrometry analysis. Samples were spiked with 3ng each PGE_2-d4, d8-11,12-DHET, d8-11,12-EET as internal standards, mixed with equal volume of 0.1% acetic acid in 5% methanol, and extracted by liquid:liquid extraction with 3 ml ethyl acetate. Ethyl acetate was transferred into glass tubes containing 6 μL of 30% glycerol in methanol. Ethyl acetate was evaporated by vacuum centrifugation, and the dried tubes covered with argon and stored at -80°C until analysis. Samples were reconstituted in 50 μL of 30% ethanol. Samples were analyzed in duplicate 10 μL injections. Online liquid chromatography of extracted samples was performed with an Agilent 1200 Series capillary HPLC Separations were achieved using a Halo C18 column (2.7 mm, 10062.1 mm) which was held at 50°C. Mobile phase A was 85:15:0.1 water:acetonitrile:acetic acid. Mobile phase B was 70:30:0.1 acetonitrile:methanol:acetic acid. Flow rate was 400 μL /min. Gradient elution was used; mobile phase percentage B and flow rate were varied as follows: 20% B at 0 min, ramp from 0 to 5 min to 40% B, ramp from 5 to 7 min to 55% B, ramp from 7 to 13 min to 64% B. From 13 to 19 min the column was flushed with 100% B at a flow rate of 550 μL /min. Mass spectroscopy was performed on an MDS Sciex API 3000 equipped with a TurboIonSpray source. Turbo desolvation gas was heated to 425°C at a flow rate of 6 L/min. Negative ion electrospray ionization tandem mass spectrometry with multiple reaction monitoring was used for detection. Quantification was done using Analyst 1.5.1

software comparing relative response ratios for each analyte/internal standard to standard curves for each analyte.

4.2.9 Flow cytometric assessment of the ability of the sorted platelets to aggregate

2.5 million thiazole orange stained reticulated or non-reticulated platelets were sorted from PRP prepared from three separate healthy volunteers on three separate days. Sorted platelet samples were then stained with CD61 FITC (reticulated) or CD61 APC (non-reticulated, both eBioscience, UK) and centrifuged at 1000 *x g* for 10 min with the addition of PGI_2 2 μM to produce platelet pellets. Subsequently pellets were re-suspended in filtered modified Tyrode's-HEPES buffer and recombined in equal proportions. Aggregation was stimulated with TRAP-6 amide (25 μM) in a half-area 96-well plate as previously described and samples subsequently fixed with 1% formalin. Flow cytometric imaging (Imagestream^X Mark II) was then used to analyse non-aggregated single platelets and formed aggregates (283±49 aggregates per sample). Images were individually assessed and scored by three separate individuals using IDEAS software (Amnis, Seattle, WA).

4.2.10 Flow cytometric assessment of reticulated platelet loss from the single platelet population following agonist stimulation

225 μL of thiazole orange stained PRP was added to add to each test cuvette and stimulated with 25 μL of agonist as described in section 3.2.6 to achieve final concentrations of arachidonic acid 1 mM, ADP 20 μM, collagen 10 mg/mL or TRAP-6 2.5 μM as above. Samples were stimulated until 40% aggregation had been reached. Flow cytometry was then used to select for the reticulated platelet population within PRP by gating for the top 10% of thiazole orange bright cells and to then assess the loss of this single platelet population following agonist stimulation and the consequent formation of platelet aggregates. Imaging flow cytometry

using the Imagestream ^{X} Mark II cytometer was used on the same samples to visualise the formation of aggregates.

4.2.11 Statistical analysis

All statistical analyses were conducted used GraphPad Prism v6 (GraphPad Software, Inc, USA) and are described in each results section.

4.3 Results

4.3.1 Assessing the impact of thiazole orange staining on platelet function

LTA as described in 4.2.3 was used to assess the function of thiazole stained platelets. For each agonist used (A; arachidonic acid, B; ADP, C; collagen, D; TRAP-6) there was no significant difference in the percentage aggregation measured between thiazole orange (TO; 20 µg/mL) treated and vehicle (1% methanol in saline) treated PRP (Figure 4.1).

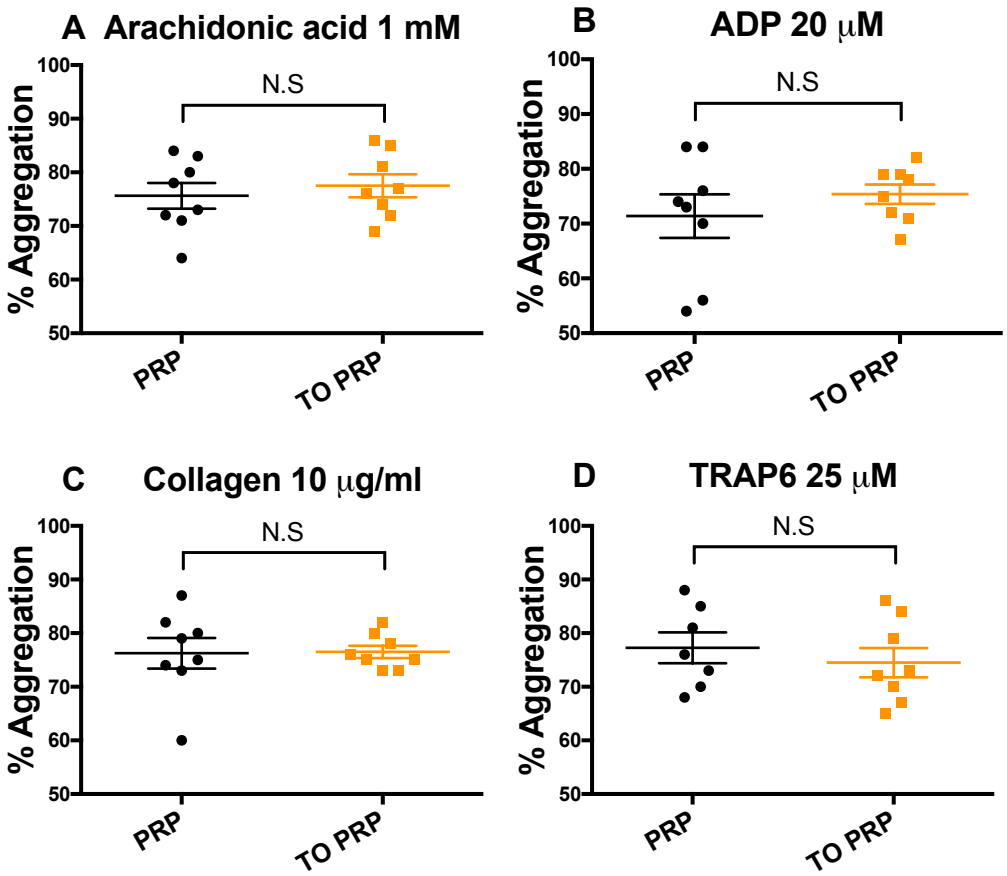

Figure 4.1 LTA data comparing percentage aggregation of PRP treated with either thiazole orange or vehicle

LTA aggregation data presented as final percentage aggregation. Results displayed as individual data points with mean ± SEM (n=8). *p<0.05 by paired t-test.

4.3.2 Assessing the impact of thiazole orange staining on Ct values obtained by qRT-PCR

Thiazole orange is a non-specific nucleic acid stain that freely permeates live cell membranes. 2 mL of PRP was stained with 20 µL of 20 µg/mL thiazole orange before being mixed in the PAP8E-aggregometer for 5 min to decrease non-specific binding of thiazole orange to free nucleotides within platelet granules. qRT-PCR was then utilised to obtain average Ct values as an indication of RNA content for thiazole orange stained PRP versus vehicle-treated PRP. Figure 4.2A shows there was significant difference between vehicle and thiazole orange stained PRP at 30 and 60 min for TUBB1. For all other TUBB1 time points and all time points for ITGA2B and PF4 there was no significant difference. For all proceeding thiazole orange-based experiments the time point of 180 minutes was selected based on the stability of the Ct value, as demonstrated in this figure. Consultation with the flow cytometry facility suggested a sorting time of 180 minutes to obtain sufficient platelets for downstream flow cytometric analyses.

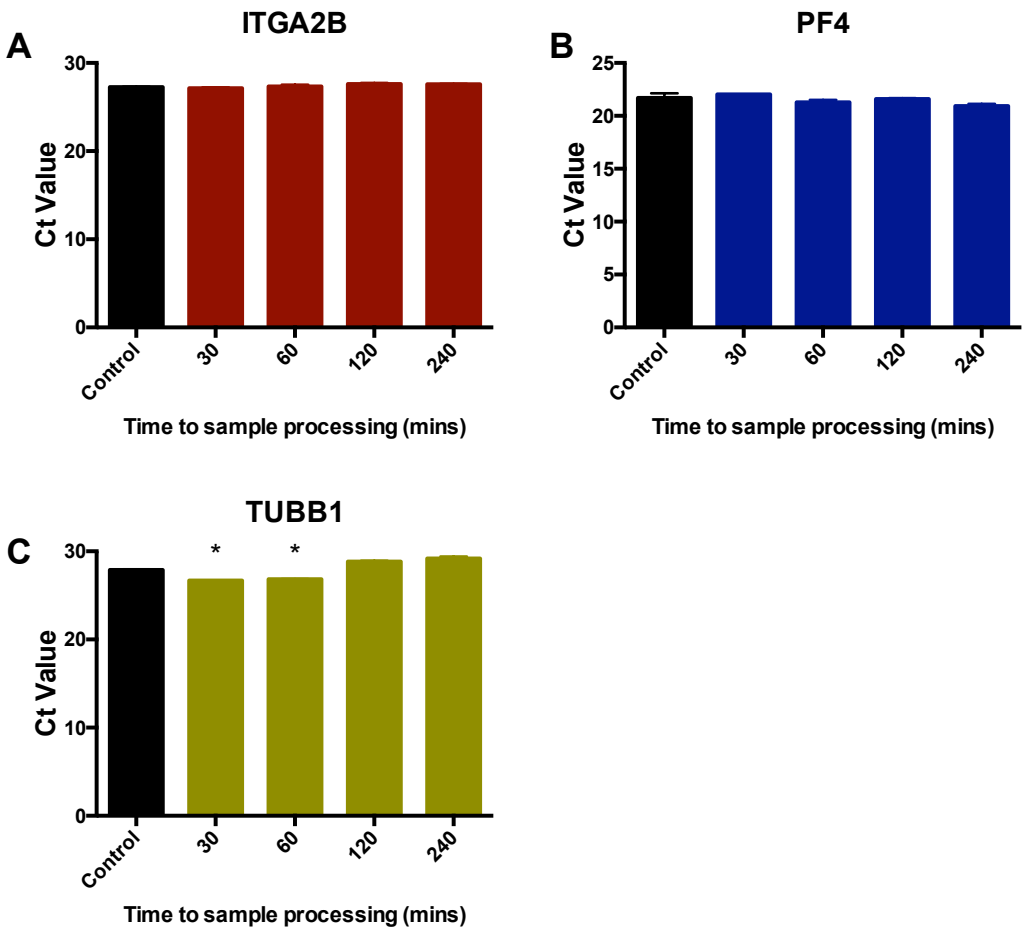

Figure 4.2 The effect of thiazole orange staining and time on the mean expression levels of three abundant platelet genes

qRT-PCR analysis comparing the mean Ct value for three genes which are abundant in platelets; ITGA2B (A), PF4 (B) and TUBB1 (C) in RNA samples extracted from 1 mL PRP at four time points. Each gene was run in triplicate. Results displayed as mean ± SEM (n=3). A one-way ANOVA with a multiple comparisons test comparing each mean to the control mean (PRP incubated with 1% methanol in PBS for 30 min and processed immediately) was used to determine significance ($p<0.05$).

4.3.3 Isolation of reticulated platelets based on thiazole orange intensity using flow cytometry

Flow cytometric cell sorting of thiazole orange stained PRP was achieved using the FACSAria Fusion cell sorter. PRP was incubated with 20 µg/mL thiazole orange at room temperature for 30 min before being diluted 1 in 8 with a modified HEPES buffer plus the platelet inhibitors PGE_1 and apyrase as described in the methods section 4.2.4. The sample was then taken to the cell sorter and based on side scatter and thiazole orange fluorescence intensity three platelet subpopulations were defined as follows; reticulated platelets gated as the top 10% of thiazole orange bright cells, intermediate platelets as the middle 50% of thiazole orange bright cells and non-reticulated platelets as the bottom 30% of thiazole orange bright cells. Figure 4.3 shows the gating parameters for selection of the subpopulations.

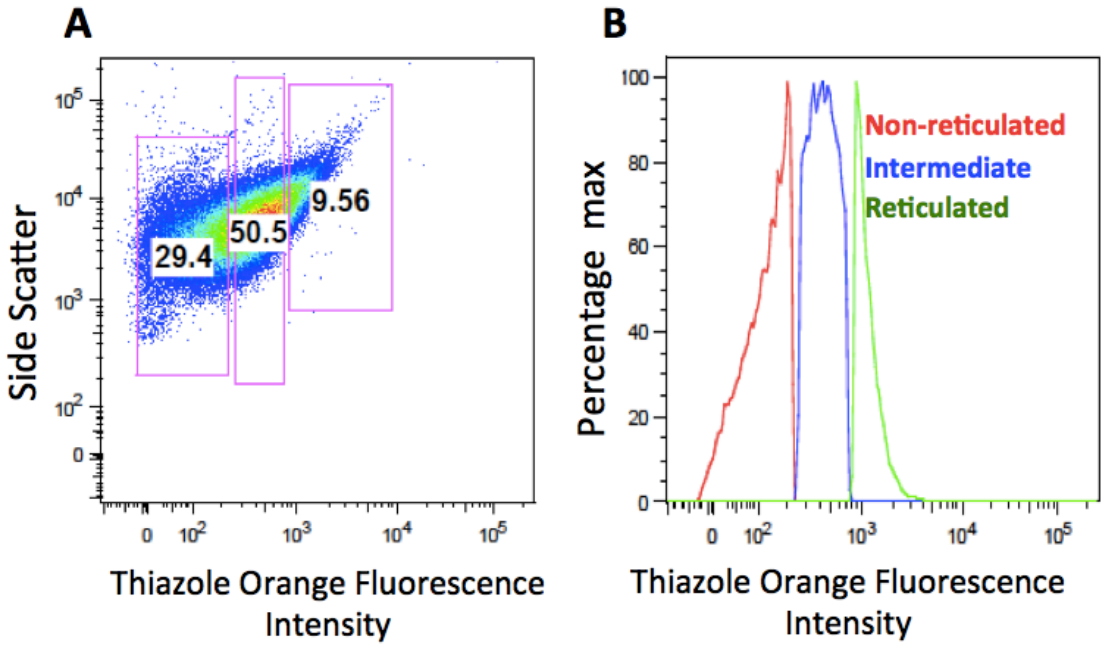

Figure 4.3 Isolation of reticulated platelet subpopulation

Flow cytometry dot–plot of thiazole orange staining of entire platelet rich plasma sample, and gating of three subpopulations for cell sorting (A). B shows the subsequent three populations (red, non-reticulated; blue, intermediate; green, reticulated) expressed as a thiazole orange intensity histogram.

4.3.4 Comparing the mRNA content of the isolated reticulated, intermediate and non-reticulated platelet subpopulations

Reticulated platelets are thought to have acquired their name due to the abundance of RNA and ribosomes within their cytoplasm however robust evidence is lacking. Figure 4.4 shows qRT-PCR data obtained from RNA samples extracted from the three platelet sub-populations cell sorted on the basis of thiazole orange staining. Reticulated platelets have significantly lower mean Ct values for three abundant platelet genes, equating to a higher concentration of mRNA for each gene than either the non-reticulated or intermediate sub-populations. All genes were tested in triplicate.

qRT-PCR analysis was also carried out for functional genes of interest to see if mRNA expression levels in the subpopulations displayed the same characteristic as for the abundant platelet genes. All functional genes, excluding PLA2G4A, showed a significant reduction in mean Ct value in the reticulated sub-population compared to both the intermediate and non-reticulated subpopulations (Figure 4.5)

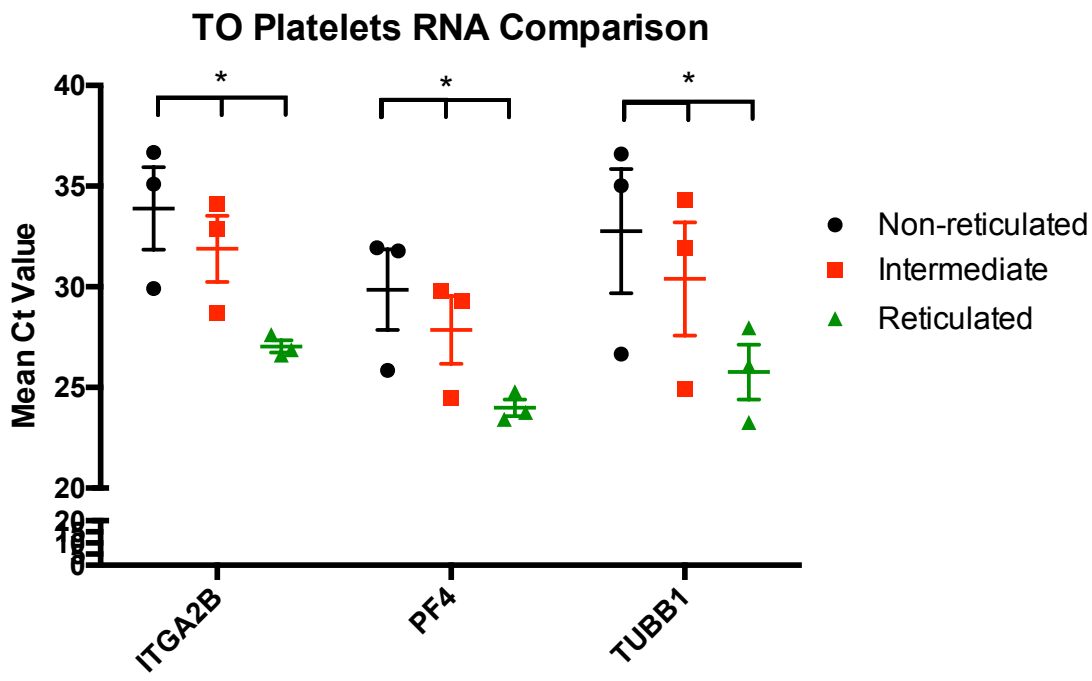

Figure 4.4 Comparison of detection of selected mRNAs for the three isolated platelet subpopulations

qRT-PCR analysis comparing the mean Ct values of the genes ITGA2B, PF4 and TUBB1 in RNA samples isolated from 10,000,000 non-reticulated, intermediate and reticulated platelets sorted from PRP samples using the FACSAria flow cytometer. Results displayed as individual data points with mean ± SEM (n=3). *$p<0.05$ by one-way ANOVA with Tukeys multiple comparisons test.

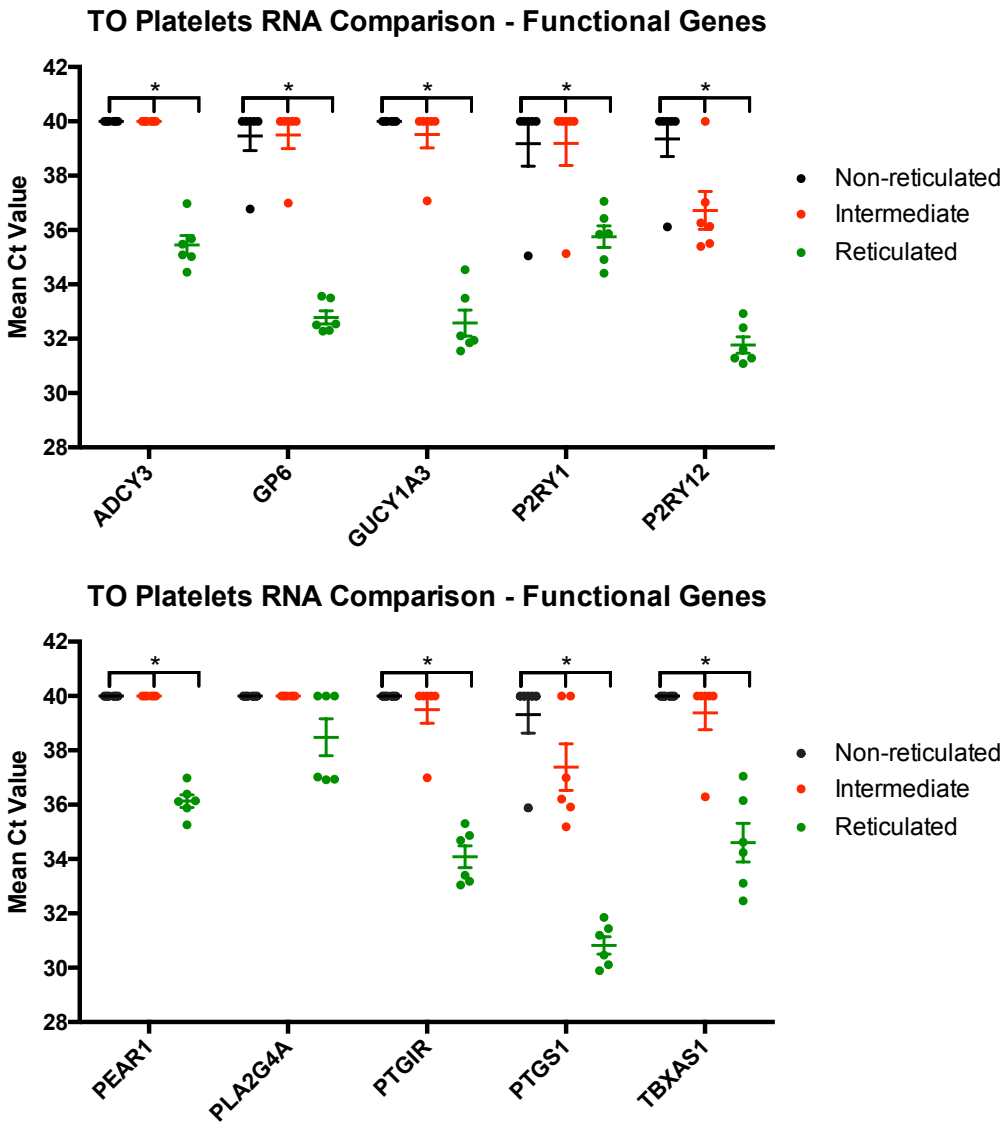

Figure 4.5 Comparison of detection of selected mRNAs for the three isolated platelet subpopulations – functional genes of interest

qRT-PCR analysis comparing the mean Ct values of the genes ADCY3, GP6, GUCY1A3, P2RY12, P2RY1, PEAR1, PLA2G4A, PTGIR, PTGS1 and TBXAS1 in RNA samples isolated from 10,000,000 non-reticulated, intermediate and reticulated platelets sorted from PRP samples using the FACSAria flow cytometer. Results displayed as individual data points with mean ± SEM (n=3). *$p<0.05$ by one-way ANOVA with Tukeys multiple comparisons test.

4.3.5 Assessing platelet activation in the isolated reticulated, intermediate and non-reticulated platelet subpopulations

Platelet surface P-selectin (CD62P) expression in response to either TRAP-6 2.5 µM or 25 µM was measured using flow cytometry. 10 million reticulated, intermediate and non-reticulated platelets were sorted based on thiazole staining intensity as described in section 4.2.4. The cells were then pelleted and resuspended in HEPES-modified Tyrode's buffer as previously detailed, supplemented with glucose (0.1%), bovine serum albumin (0.35%), $CaCl_2$ (2 mM) and fibrinogen (1 mg/mL) before being stimulated with either TRAP-6 or vehicle for 20 min at 25°C. Samples were incubated with CD61-APC as the platelet identifier and with CD62P-PE for P-selectin expression.

Figure 4.6 shows that reticulated platelets have a significantly higher fold increase in surface P-selectin expression than non-reticulated when incubated with TRAP-6 (2.5 µM, 2.6±0.4 fold greater; 25 µM, 2.7±0.4 fold greater $p=<0.05$).

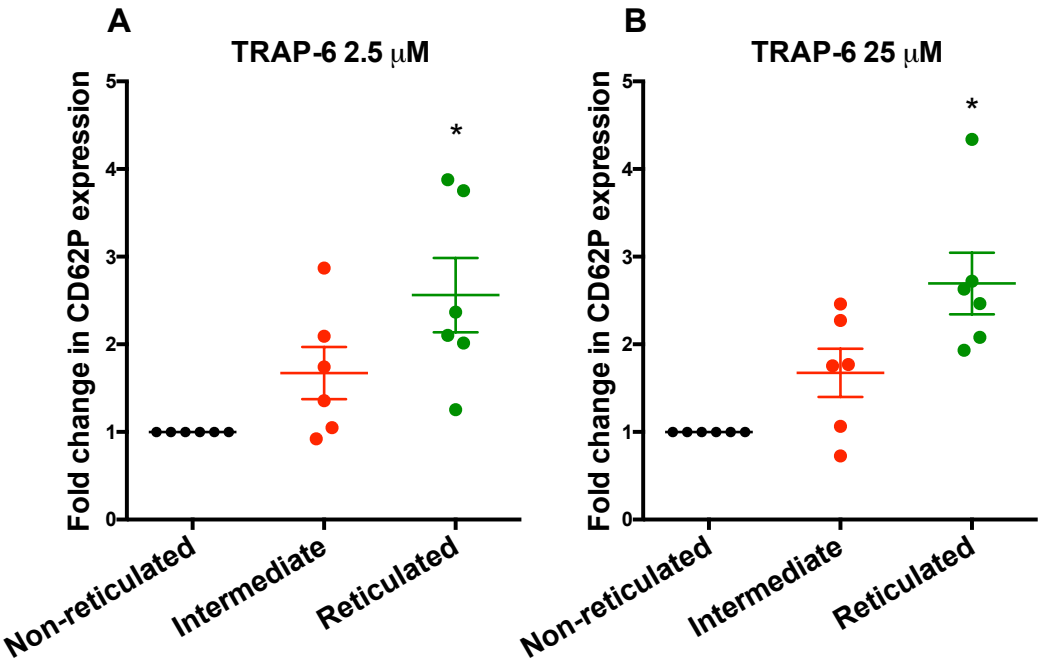

Figure 4.6 Relative P-selectin (CD62P) expression following incubation with TRAP-6 for the reticulated, intermediate and non-reticulated platelet populations

Flow cytometric analysis comparing the relative change in CD62P expression in response to (A) 2.5 μM or (B) 25 μM TRAP-6 amide stimulation of reticulated, intermediate and non-reticulated platelets (which were set at the hypothetical value of one). Results displayed as mean ± SEM. A one-way ANOVA was used to determine significance ($p<0.05$) n=6.

4.3.6 Comparison of ATP release from the isolated reticulated, intermediate and non-reticulated platelet subpopulations following incubation with TRAP-6

2.5 million reticulated, intermediate and non-reticulated platelets were sorted based on thiazole staining intensity as described in section 4.2.4 and stimulated with TRAP-6 25 μM in the wells of a white half area flat bottom 96 well plate before a luminescence assay was used to determine ATP release as described in section 4.2.7. Compared to non-reticulated platelets intermediate platelets demonstrated a 1.8±0.4 fold increase in ATP release and reticulated platelets a 3.0±0.4 fold increase in ATP release (Figure 4.8).

The production of an ATP standard curve (Figure 4.7) enabled quantification of the ATP release for each group. There was no significant effect of the time taken between stimulating the platelets and reading the plate on luminescence value. Using this curve it was determined that the average ATP release (based on raw luminescence values) from the non-reticulated samples was 10.17 pmol, from the intermediate samples was 15.02 pmol and from the reticulated samples was 28.15 pmol as summarised in Table 4.1.

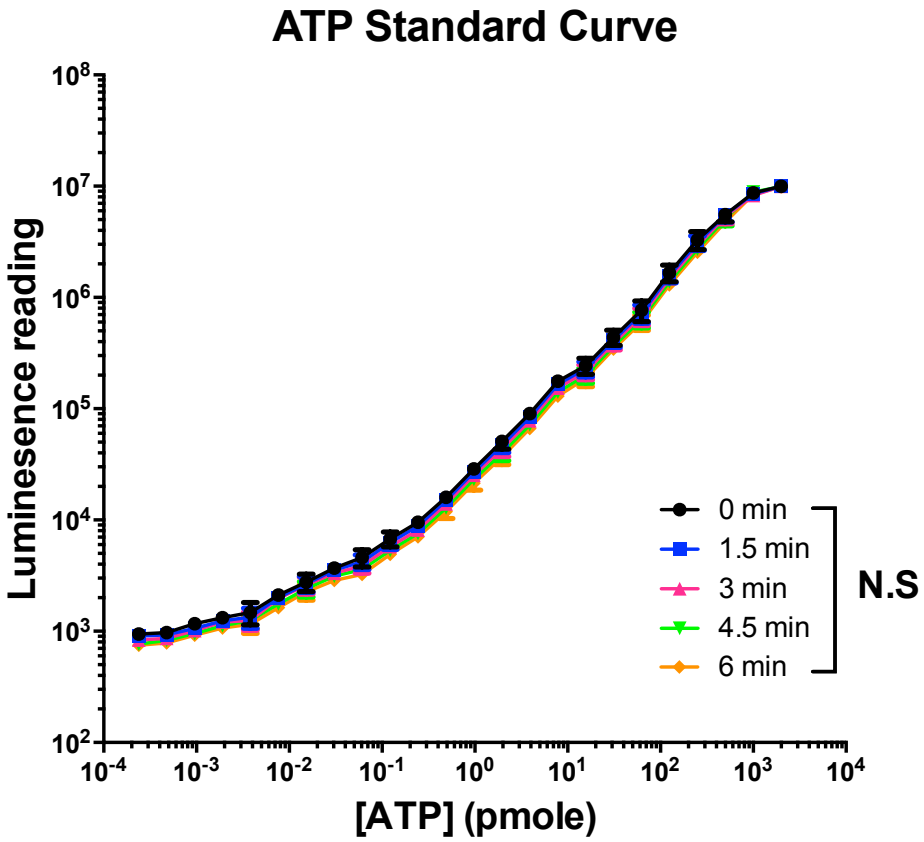

Figure 4.7 ATP standard curves for multiple time points post agonist stimulation

Luminescence readings for 24 serial 1 in 2 dilutions of ATP for six time points (0 min black, 1.5 min blue, 3 min pink, 4.5 min green, 6 min orange) post agonist stimulation. Results displayed as mean ± SEM. A two-way ANOVA with Tukey's multiple comparisons test was used to determine significance ($p<0.05$; $n=3$).

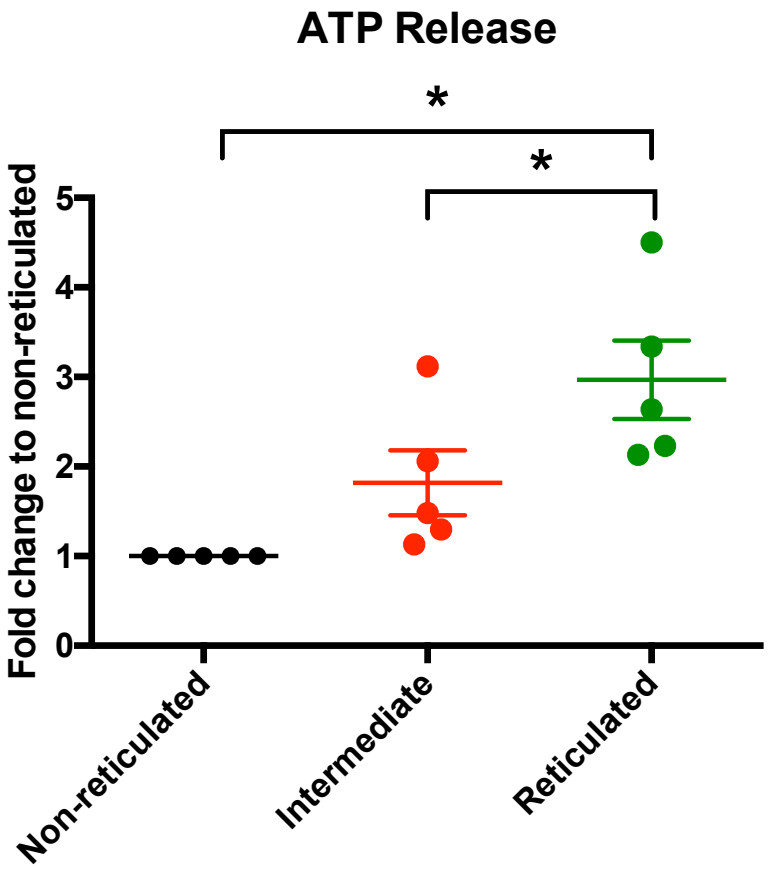

Figure 4.8 Relative ATP release from the reticulated, intermediate and non-reticulated platelet populations in response to TRAP-6

Luminescence based analysis comparing the relative fold change in ATP release in response to TRAP-6 (25 μM) between reticulated and intermediate platelets compared to non-reticulated platelets, which were set at the hypothetical value of one. Results displayed as mean ± SEM. A one-way ANOVA with Holm-Sidak multiple comparisons test was used to determine significance ($p<0.05$) n=5.

Sub-population	Average luminesence value for the group	ATP quantification from standard curve (pmole)
Non-reticulated	181601±89877	10.17
Intermediate	266631±116385	15.02
Reticulated	491733±231093	28.15

Table 4.1 Average ATP release (pmol) for each platelet sub-population

Table summarising the quantification of mean ± SEM ATP release (pmol) from each of the three thiazole orange sorted platelet sub-populations using data from the ATP standard curve (Figure 4.7) and raw luminescence values obtained on the plate reader.

4.3.7 Comparison of eicosanoid production by isolated reticulated, intermediate and non-reticulated platelet subpopulations in response to collagen

10 million reticulated, intermediate and non-reticulated platelets were isolated (section 4.2.4) and incubated with either vehicle or collagen (30 µg/mL) for 30 min at 37°C. Supernatants from these samples were analysed by LC-MS/MS as described in section 4.3.8. Data in Figure 4.9 shows that there was no significant difference in the levels of thromboxane B_2 (Figure 4.9 A), prostaglandin D_2 (Figure 4.9 C), prostaglandin E_2 (Figure 4.9 C), 11-HETE (11-hydroxy-5,8,12,14-eicosatetraenoic acid) (Figure 4.9 D) 12-HETE (12-hydroxy-5,8,12,14-eicosatetraenoic acid) (Figure 4.9 E) or 15-HETE (15-hydroxy-5,8,12,14-eicosatetraenoic acid) (Figure 4.9 F) measured in the supernatants from the three subpopulations.

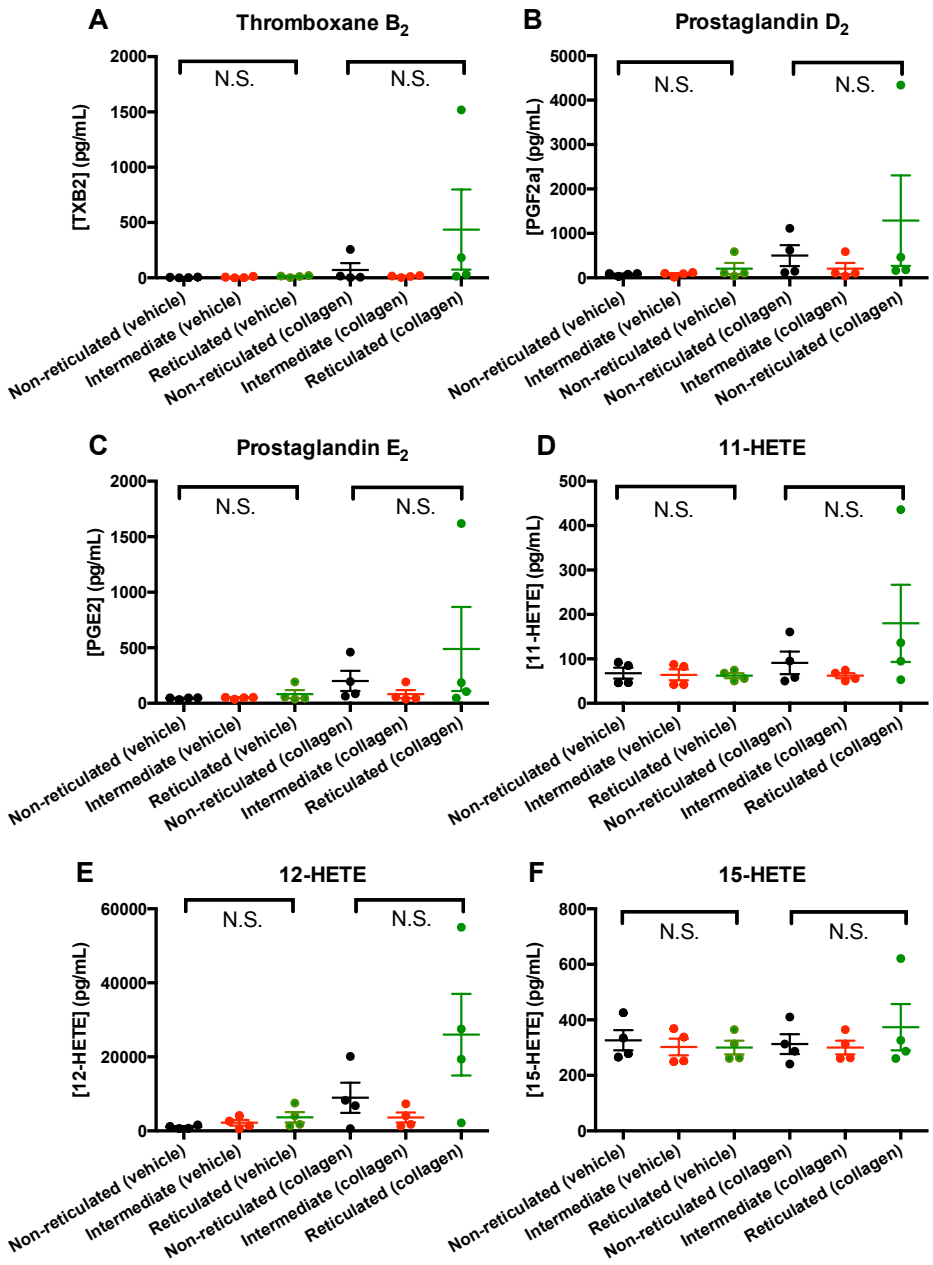

Figure 4.9 LC-MS/MS analysis of selected arachidonic acid metabolites in supernatants of reticulated, intermediate and non-reticulated platelet subpopulations incubated with collagen or vehicle

Data presented as individual data points with mean ± SEM. Significance determined using one-way ANOVA with Tukey multiple comparisons test ($p=<0.05$) n=4.

4.3.8 Comparing the ability of reticulated and non-reticulated platelets to form aggregates

Stimulation of equally mixed populations of platelets (54±2% reticulated vs. 45±2% non-reticulated, $p>0.05$) with TRAP-6 led to the formation of platelet aggregates (Figure 4.10). Of all formed aggregates, reticulated platelets were present in 95±2% and non-reticulated platelets in 42±6% (Figure 4.11 A). Further analysis demonstrated that 57±6% of all aggregates were composed exclusively of reticulated platelets, whereas only 4±2% were composed exclusively of non-reticulated platelets. The remaining 39±7% of aggregates were formed from combinations of the two populations (Figure 4.11 B).

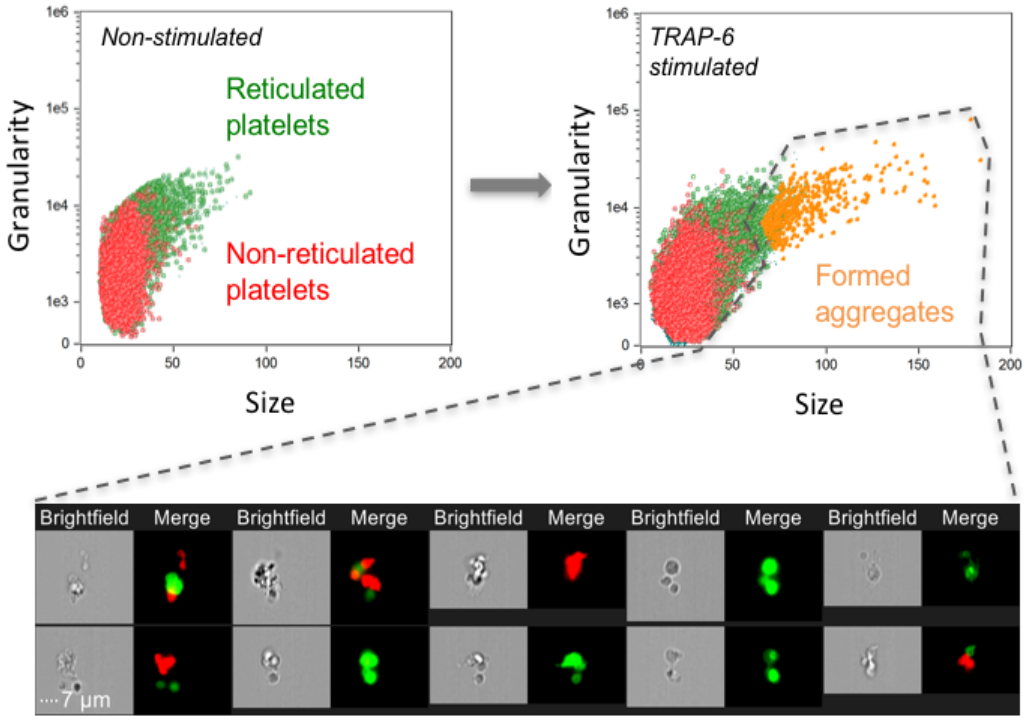

Figure 4.10 Relative reactivity of reticulated and non-reticulated platelets during aggregation

Flow cytometric sorted reticulated (green, CD61-FITC) and non-reticulated (red, CD61-APC) platelets were recombined in equal measures before stimulation with TRAP-6 (25 µM). Representative dot plots from flow cytometric imaging (incorporating x60 magnification) analysis of samples before (left) and after (right) stimulation demonstrated the formation of aggregates (orange).

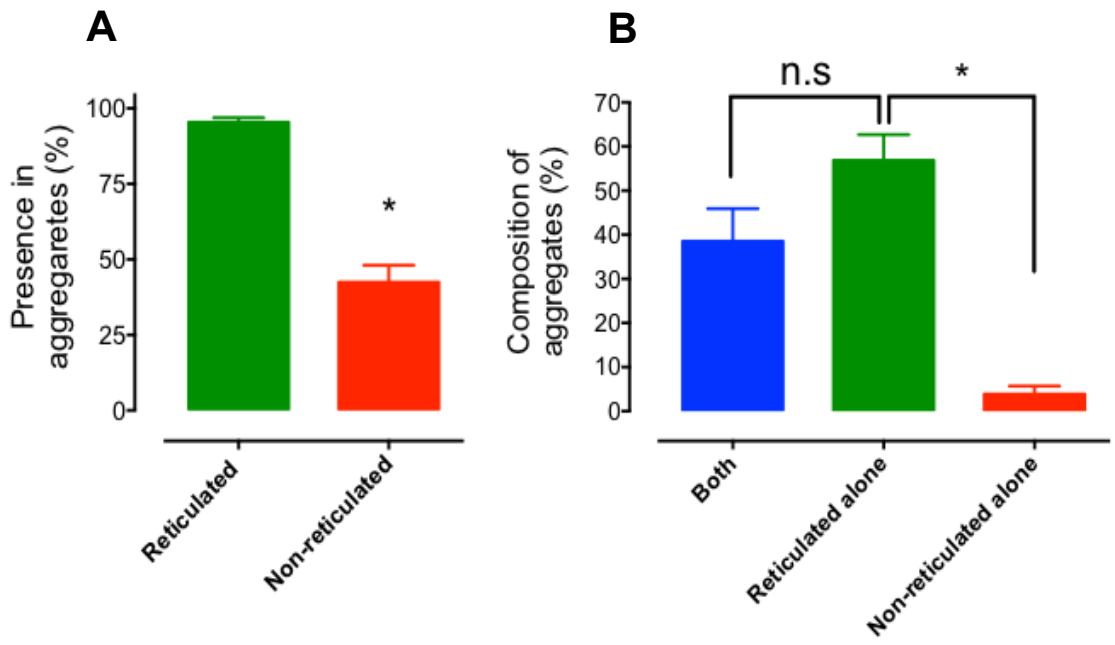

Figure 4.11 Relative reactivity of reticulated and non-reticulated platelets during aggregation – aggregate composition

Images of aggregates formed (Figure 4.10) were scored for the (A) total presence and (B) composition with respect to each sub-population and revealed the involvement of reticulated platelets, either alone or in combination with non-reticulated platelets, in almost all formed aggregates. Scale bars represent 7 μm. Data reported as mean ± SEM (n=3), *$p<0.05$ by paired t test or one-way ANOVA, as appropriate.

4.3.9 Determining the proportional recruitment of reticulated and non-reticulated platelets to aggregate formation

PRP samples from healthy volunteers were stained with thiazole orange as described in section 4.4.2 and stimulated with arachidonic acid 1 mM (Figure 4.13 A), ADP 20 μM (Figure 4.13 B), collagen 1 μg/mL (Figure 4.13 C) or TRAP-6 2.5 μM (Figure 4.13 D) until 40% aggregation had been achieved, samples therefore contained a mix of non-aggregated single platelets and aggregates. The samples were then incubated with CD61 APC to identify platelets and a flow cytometric assay was used to track the change in the proportion of reticulated platelets within the single platelet population in vehicle compared to agonist stimulated samples. Gating strategies for the identification of the reticulated platelet population are outlined in Figure 4.12. Data presented in Figure 4.13 shows a significant decrease in the percentage of reticulated platelets in the single platelet population post agonist stimulation compared to vehicle for all four agonists used. Reticulated platelets are therefore recruited into forming aggregates in a manner that is disproportional to the platelet population as a whole. In addition the formed aggregates were examined using imaging flow cytometry (Figure 4.14) to confirm the presence of reticulated platelets in the majority of aggregates.

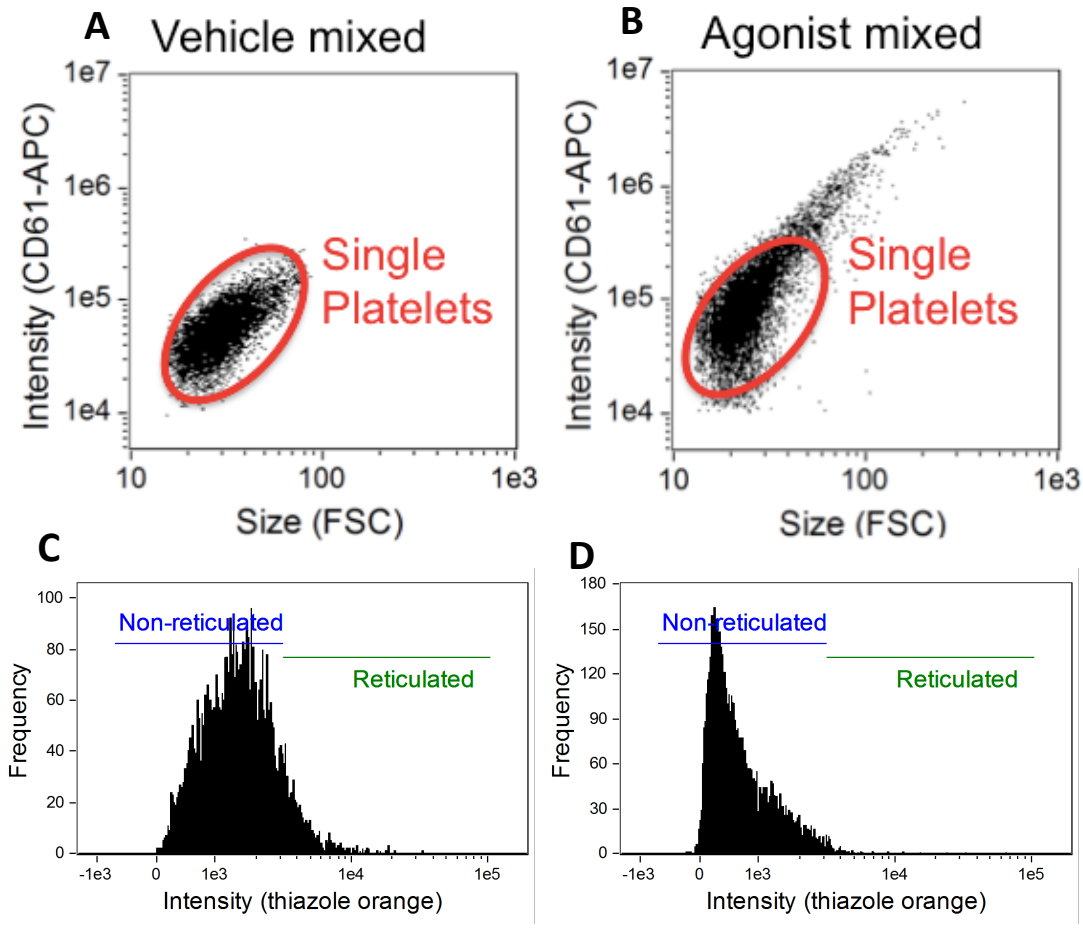

Figure 4.12 Gating strategies for the identification of reticulated platelets in the single platelet population

Representative flow cytometric histograms showing the gates used to identify single platelets based on CD61 expression in PRP treated with either vehicle (A) or TRAP-6 25 μM (B). Reticulated platelets were defined as the top 10% of thiazole orange bright platelet events in vehicle samples (C). The percentage change in this population was measured in response to agonist stimulation (D).

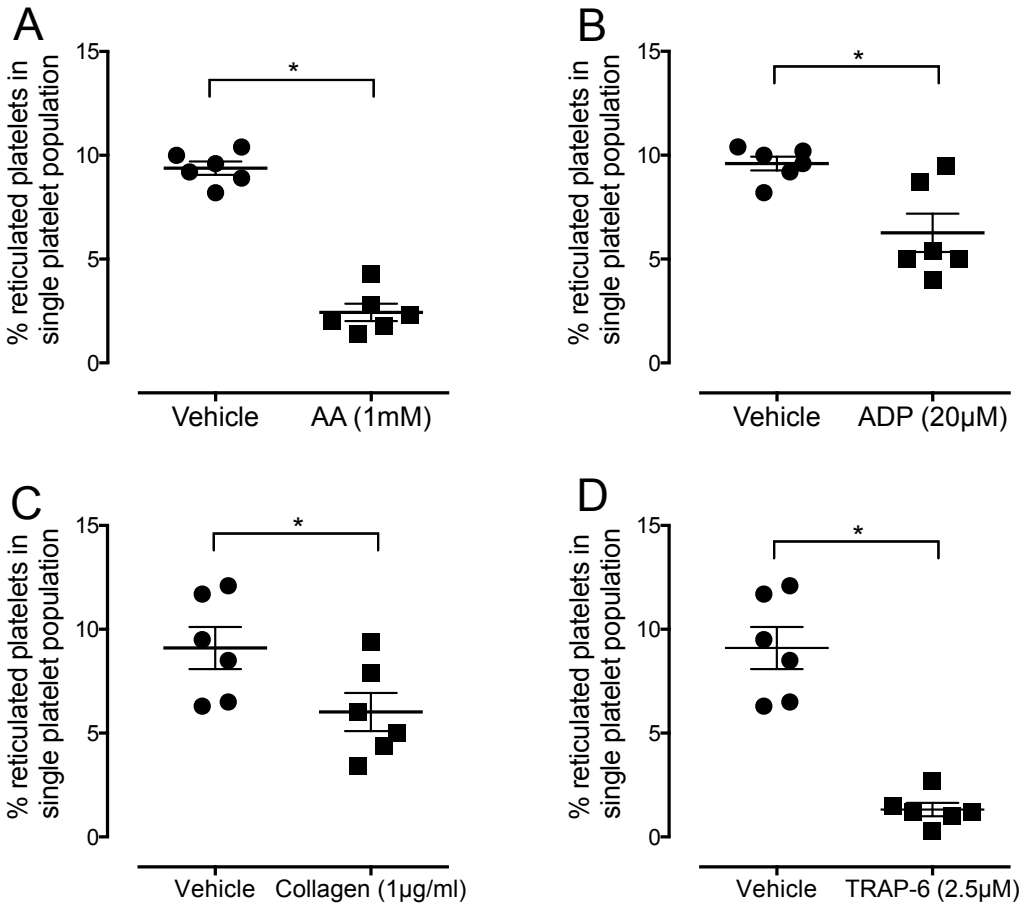

Figure 4.13 Flow cytometric analysis of reticulated and non-reticulated platelet recruitment into forming aggregates

The proportion of reticulated platelets among the non-aggregated single platelet population was assessed by flow cytometry in PRP samples stimulated with arachidonic acid 1 mM (A), ADP 20 μM (B), collagen 1 μg/mL (C) or TRAP-6 2.5 μM (D). Results displayed as individual data points with overlaid mean ± SEM (n=6) and significance determined using a paired t test *$p<0.05$.

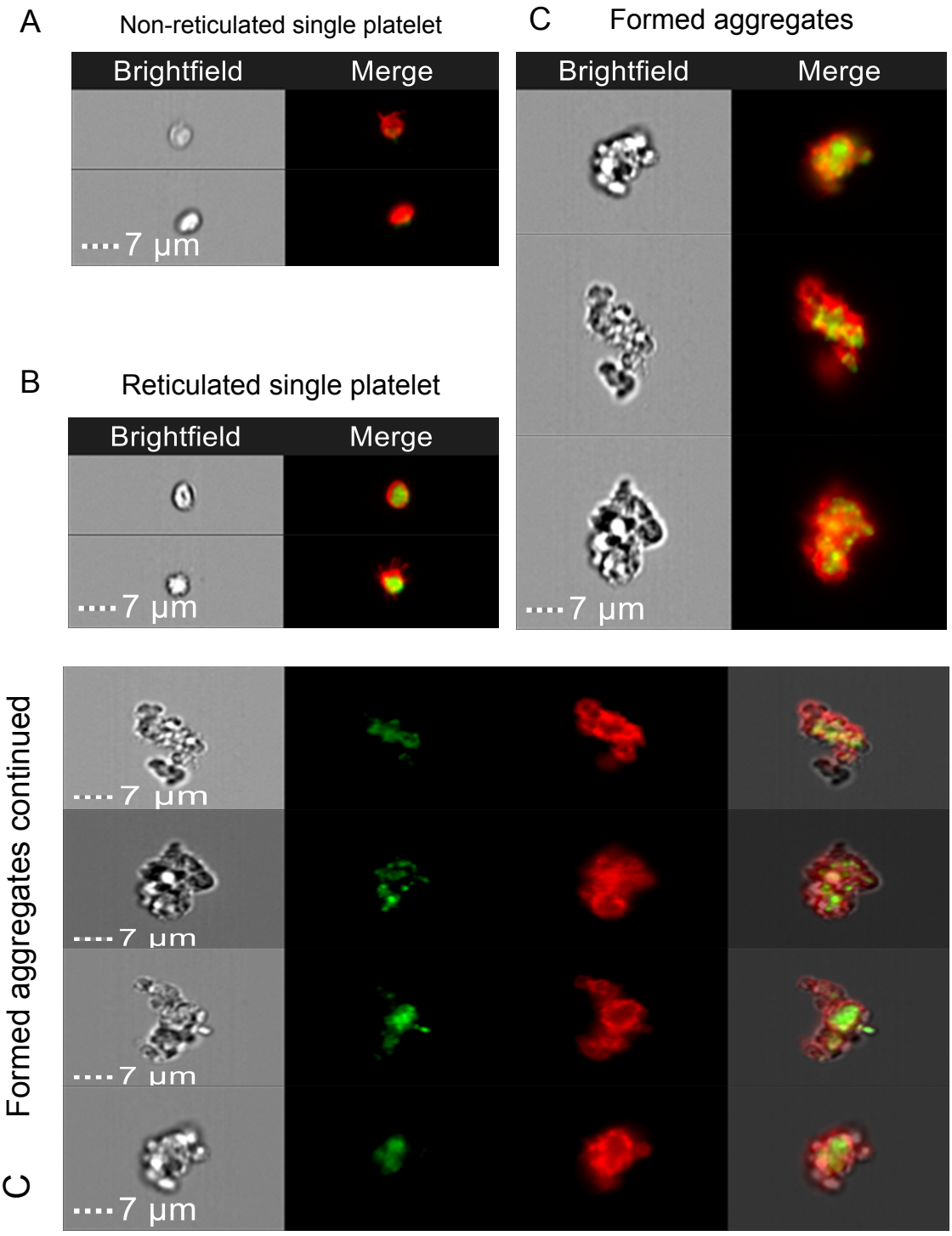

Figure 4.14 Representative Imagestream analysis of forming aggregates

Representative flow cytometric images (Imagestream^X Mark II cytometer) of samples analysed in Figure 4.10 showing non-reticulated single platelets (A) and reticulated (mRNA stain green) single platelets (red) (B), as well as aggregates formed in response to ADP 20 µM (C).

4.4 Discussion

Reticulated platelets are currently of much research interest. Their precise and accurate study is dependent upon obtaining defined platelet populations with preserved function.

Building upon the optimal platelet isolation technique outline in the previous chapter a protocol was developed, based on thiazole orange staining, to extract reticulated platelets from PRP (Figure 4.3) and subsequently to investigate both their mRNA content and function. The use of thiazole orange to identify platelets containing elevated levels of mRNA has previously been questioned on the basis that larger platelets may uptake more dye and that this may skew the analysis [165]. For the first time through careful separation this series of experiments confirms that platelets with stronger thiazole orange staining contain significantly greater amounts of platelet associated mRNA, for both abundant platelet genes ITGA2B, PF4 and TUBB1 (Figure 4.4) and for genes important to platelet function (Figure 4.5). Furthermore this staining was found to have no effect on platelet function as measured using LTA (Figure 4.1) or on the stability of measured Ct values indicating no loss of mRNA over time (Figure 4.2). Although megakaryocyte-derived platelet-specific mRNA declines within platelets as they age it is now understood that platelets take up a wide variety of RNAs released into the circulation by other cell types [82]. As such, total RNA levels within the platelet may be unaffected. My targeted approach for the study of platelet specific mRNA eliminates this potentially confounding observation.

In terms of platelet function, through my approach of platelet staining and testing, I was able to demonstrate definitively that platelets containing higher amounts of mRNA (i.e. the most newly formed, reticulated, platelets) have an exaggerated response to TRAP-6 as determined by the surface expression of CD62P and by ATP release. Indeed the reticulated platelet population was shown to express a 2.6 fold increase in surface CD62P expression (Figure 4.6) and to release 2.8 times more

ATP when stimulated compared to the non-reticulated population (Figure 4.8). Trends in the LC-MS/MS data also support idea that the reticulated platelet population is more reactive showing that this population may release greater amounts of functionally relevant eicosanoids in response to agonist stimulation. It would be interesting to investigate this further to determine whether the increased eicosanoid release can be attributed to an increased ability to metabolise arachidonic acid through the enzymatic pathways as outlined in subsequent chapters. It should be note this idea is based on trends in the data that did not reach statistical significance (Figure 4.9).

The reticulated platelets also showed elevated reactivity during aggregate formation. This was demonstrated by individually staining the reticulated and non-reticulated platelets with different fluorophores, before recombining the populations in equal proportions, and using flow cytometric imaging (Figure 4.10) to demonstrate that reticulated platelets were involved in around 95% of all aggregates compared to 42% for non-reticulated platelets. Furthermore, 57% of aggregates were formed entirely from reticulated platelets (Figure 4.11).

In the more physiologically relevant environment of PRP, reticulated platelets were once again identified based on thiazole orange staining intensity and analysed in situ (Figure 4.12). Just as in the isolated samples, reticulated platelets were recruited in a disproportional manner from the non-stimulated single platelet population into aggregates following exposure to platelet agonists (Figure 4.13). Flow cytometric imaging analysis further showed that the reticulated platelets were present at the centre of aggregates and were therefore most likely recruited first in preference to the non-reticulated platelets.

Despite the fact that reticulated platelets normally comprise only 10% of the total platelet count, the increased reactivity demonstrated here provides evidence that reticulated platelets can be drivers of the thrombotic response. This supports clinical observations associating

increased platelet turnover or immature platelet counts with high platelet reactivity [166,167] and increased incidence of acute coronary syndromes in patients with higher reticulated platelet counts or elevated platelet turnover [95]. The mechanisms underlying this increased reactivity require further research for which the methodology presented could be particularly helpful.

To summarise, reticulated platelets are of great current research interest owing to fact that they contain an abundance of platelet-specific mRNA and increased reactivity. The experiments described here present an optimised approach for reticulated platelet isolation that preserves these properties to permit both genetic and functional downstream analysis. Moreover, using this approach it was established that reticulation status is directly linked to an increased expression of platelet-specific mRNA and, for the first time, that reticulated platelets are more reactive than non-reticulated platelets.

Chapter 5 - Functional and RNA sequencing analysis of platelets obtained from a cytosolic phospholipase $A_{2\alpha}$ ($cPLA_{2\alpha}$) deficient patient

5.1 Introduction

A patient with a homozygous 4 base pair deletion within the PLA2G4A gene resulting in the loss of the C-terminal region of the group IV A cytosolic phospholipase A_2 ($cPLA_2\alpha$) protein [168] was identified at the department of clinical immunology at The Royal London Hospital (Barts Health NHS Trust of London).

As discussed below, $cPLA_2\alpha$ enzyme is central to the production of a wide range of bioactive eicosanoids and phenotypically the patient presented with an extensive life-long history of severe peptic and intestinal ulceration, small intestinal strictures and fibrosis and duodenal stenosis. Collectively these features suggested a diagnosis of cryptogenic multifocal ulcerating stenosis enteritis (CMUSE) [169]. The gastrointestinal lesions of patients with this rare condition often resemble those associated with the chronic use of non-steroidal anti-inflammatory drugs (NSAIDS) such as aspirin [170]. This patient was the first known case of CMUSE linked to a homozygotic mutation within PLA2G4A gene that encodes for the $cPLA_2\alpha$ enzyme leading to its inactivation.

$cPLA_2\alpha$ is one of 19 identified PLA_2 isoforms that are classified into three families (cytosolic calcium dependent $cPLA_2$; cytosolic calcium independent; $iPLA_2$ and secretory; $sPLA_2$) based on enzymatic function, biochemical structure and cellular distribution. $cPLA_2\alpha$ requires submicromolar- concentrations of Ca^{2+} for its activation and translocation from the cytoplasm to the membrane of the cells in which it is present [171–173]. Together these enzymes have a critical role in the production of bioactive lipids through the hydrolysis of arachidonic acid from the cell membrane [174].

Arachidonic acid is the precursor to many other lipid mediators called eicosanoids. Eicosanoid formation from arachidonic acid requires the action of three enzymatic pathways, the cyclooxygenase (COX) -1 and -2 pathway, the 5-, 12- and 15-lipoxygenase (LOX) pathway and the

cytochrome P450 epoxygenase ω-hydroxylase pathway [171,175] (Figure 5.1).

Through the action of COX-1 and 12-LOX platelets produce eicosanoids that regulate platelet, WBC and vascular function [43]. Through the activity of COX-1 platelets produce prostaglandin G_2 (PGG_2) that is reduced to prostaglandin H_2 (PGH_2). PGH_2 is further converted into prostaglandin D_2 (PGD_2), prostaglandin E_2 (PGE_2), prostaglandin $F_{2\alpha}$ ($PGF_{2\alpha}$), prostacyclin (PGI_2) and thromboxane A_2 (TXA_2) via the action of specific synthase enzymes [176,177]. Through the action of 12-LOX platelets produce 12-hydroxyeicosatetraenoic acid (12(S)-HETE) [178].

Previous studies have shown that the loss of $cPLA_2\alpha$ activity significantly alters the ability of platelets both to respond to agonist stimulation and to synthesise various arachidonic acid derived eicosanoids essential to platelet function [179,180]. Figure 5.2 highlights the platelet specific production of eicosanoids and their biological functions.

This chapter aims to test the reactivity of platelets from the $cPLA_2\alpha$ mutated patient by comparing them to data obtained from healthy control samples using multiple platelet function testing assays. In addition RNA sequencing (RNA-Seq) analysis will be carried out in order to determine whether loss of $cPLA_2\alpha$ activity affects the expression of other platelet genes.

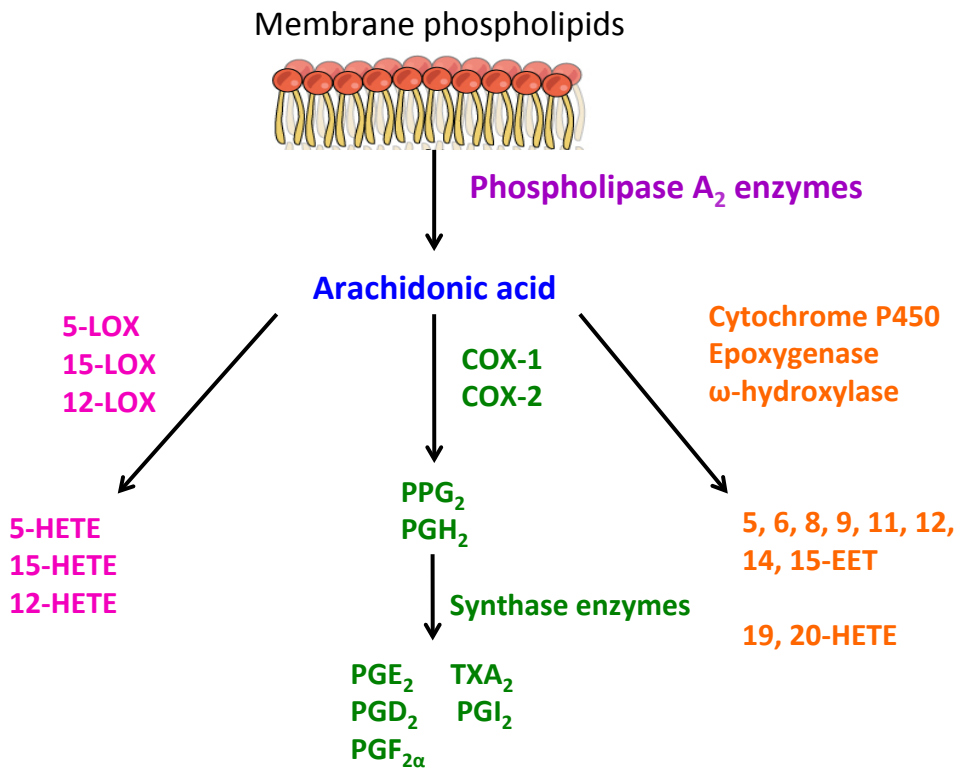

Figure 5.1 General scheme of arachidonic acid derived eicosanoid products

Figure showing the conversion of arachidonic acid into its bioactive eicosanoid products via the lipoxygenase (LOX), cyclooxygenase (COX) and cytochrome P450 pathways. PG = prostaglandin, TX = thromboxane, EET = epoxyeicosatrienoic acid, HETE = hydroxyeicosatetraenoic acid.

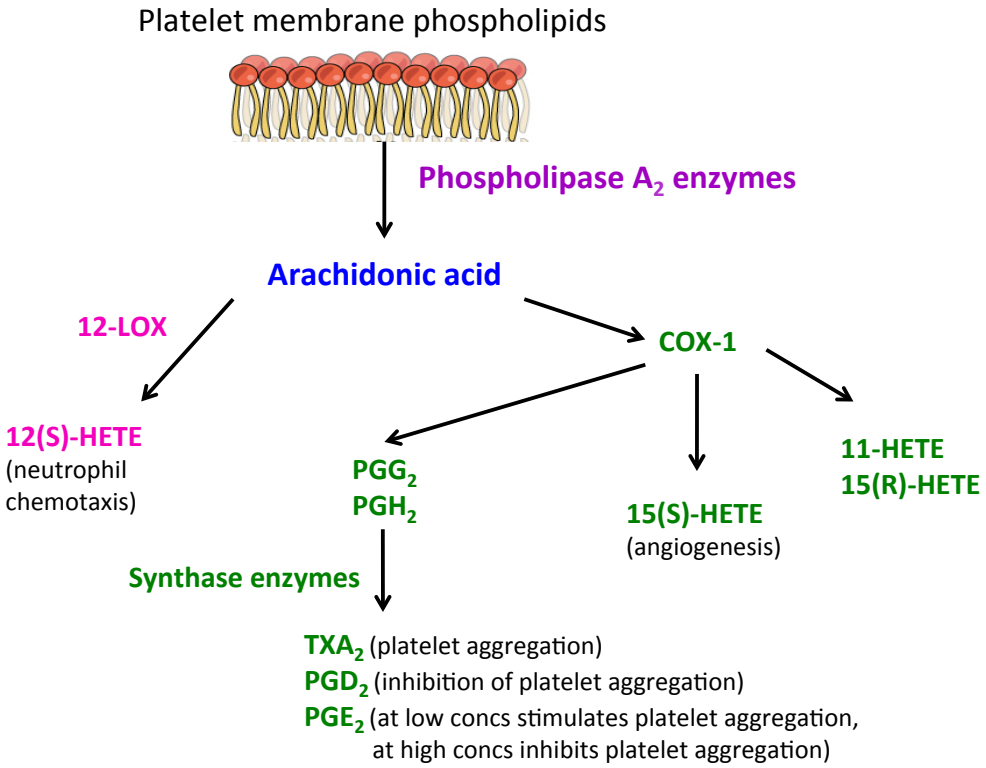

Figure 5.2 Arachidonic acid derived eicosanoid products – platelet specific

Figure showing the conversion of arachidonic acid into its bioactive eicosanoid products via the 12-lipoxygenase (12-LOX) and cyclooxygenase-1 (COX-1) specific to platelets. Eicosanoid effects on platelet function are shown next to the abbreviation. PG = prostaglandin, TX = thromboxane and HETE = hydroxyeicosatetraenoic acid.

5.2 Methodology

5.2.1 Blood collection and preparation of PRP

Blood was obtained from healthy volunteers or the patient of interest and PRP/PPP prepared as outlined previously in section 3.2.1 and 3.2.2. Written informed consent was obtained from the patient. This study was approved by the South East NHS Research Ethics Committee and was performed according to the Declaration of Helsinki Principles. At the time of sampling a proton pump inhibitor was the only medication the patient was prescribed.

5.2.2 Light transmission aggregometry (LTA)

225 µL of PRP was added to each cuvette that was then placed in one of eight channels in a Bio/Data PAP-8E turbidometric aggregometer and stimulated with 25 µL of agonist as described in section 3.2.6. Agonists and their final concentrations used were as follows; ADP 10 µM, epinephrine 10 µM, TRAP-6 25 µM, U46619 3 µM, arachidonic acid 1 mM, ristocetin 1.5 mg/mL and collagen 1 µg/mL or 3 µg/mL.

5.2.3 Optimul plate assay

Optimul plates were prepared according to section 3.2.7. For their use, 40 uL of PRP or PPP was added to the appropriate wells and plates shaken on a Bioshake plate shaker at 1200 rpm, for 5 min at 37°C before the absorbance was read at 595 nm on a Tecan Sunrise plate reader. Agonists used were ADP (0.00540 µM), epinephrine (0.0004-10 µM), TRAP-6 amide (0.03-40 µM), U46619 (0.055-40 µM), arachidonic acid (0.03-40 µM), ristocetin (0.144 mg/mL) and Horm collagen (0.01-40 µg-/mL).

5.2.4 Luminescence (lumi) aggregometry – ATP release

Lumi-aggregometry measures the release of ATP from platelet dense granules as an indication of activation. It is a bioluminescent assay using the luciferin-luciferase system.

200 µL of PPP was added to four flat bottom cuvettes and placed in the four channels of the lumi-aggregometer to set baselines. The trace line was left to settle for 2 min before placing a cuvette containing 200 µL PRP into the sample wells. All PPP and PRP cuvettes contained 20 µL chrono-lume reagent. Samples were continually stirred and kept at 37°C. PRP was left to equilibrate for 2 min before 25 µL of chosen inhibitor was added. 1 min later 5 µL of selected agonist was added and the trace was left to run for a further 5 min after which 5 µL of 2 µM ATP standard was added. Once the trace had settled the experiment was ended. Aggregation and luminescence traces were recorded and analysed using Chart v4.2.

The calculation used to determine maximum ATP release is as follows and its derivation is explained in Figure 5.3:

Max ATP release = ((min ATP - max ATP) / (pre spike – post spike)) / 2

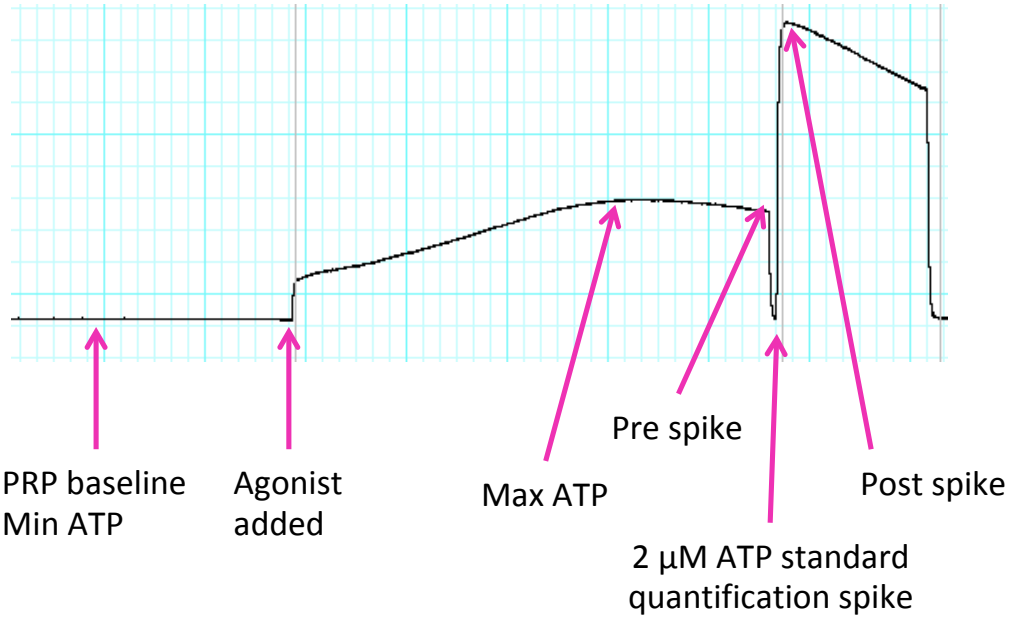

Figure 5.3 Example lumi aggregometry trace

Figure showing an example luminescence trace obtained by lumi aggregometry. The trace is labelled to show how the components of the calculation are derived.

5.2.5 Platelet surface P-selectin expression – whole blood

A flow cytometric assay was used to assess platelet surface P-selectin (CD62P) expression as an indicator of platelet activation in response to agonist stimulation [181]. 45 µL of whole blood was added to wells of a gelatin coated half area plate containing 5 µL of agonist or vehicle to achieve final concentrations of ADP 40 µM, U46619 0.5 µM, or a combination of both. The plate was then shaken at 1200 rpm for 5 min. 160 µL of ACD (2.2 g sodium citrate dehydrate, 0.7 g citric acid, 2.4 g dextrose, 100 mL dH_2O) was then added to each well to terminate reaction and prevent aggregation. 10 µL of the sample was then incubated for 30 min in the dark at 4°C with an equal volume of an antibody mix containing CD61 APC (1:160) as the platelet identifier and CD62P PE (1:80) as the indicator of activation in saline. Samples were fixed using 1% formalin in saline. Flow cytometry was then used to quantify mean fluorescence intensity values for 100,000 CD61 positive events. Data was acquired on a FACSCalibur flow cytometer using CellQuest software.

5.2.6 RNA-Seq

5.2.6.1 Platelet RNA extraction

RNA was extracted from 25-30 mL of PRP obtained from 100 mL of whole blood for each of the six control donors and from three samples taken on separate days from the test patient. RNA was extracted using the RNeasy minikit as described in full in section 3.2.9.

5.2.6.2 Sample quality control

RNA samples were assessed for quantity and integrity using the NanoDrop 8000 spectrophotometer V2.0 and Agilent 2100 Bioanalyser,

respectively. Samples displayed low levels of degradation with RNA integrity numbers (RIN) between 6.7 and 8.4.

5.2.6.3 cDNA synthesis

Full-length cDNA molecules were generated from 1ng of total RNA per sample using the SMARTer kit for cDNA generation. cDNA quantity was measured using the Qubit® 2.0 Fluorometer, and were checked for quality using the Agilent 2200 Tapestation.

5.2.6.4 Library generation and RNA-sequencing

Libraries were prepared using the Illumina Nextera XT Sample Preparation Kit with an input of 150pg of cDNA per sample. 40 million 75bp paired-end reads were generated for each library using the Illumina NextSeq®500 High-output kit.

5.2.7 Statistical analysis

For the platelet function testing assays statistical analyses were conducted used GraphPad Prism v6 and described in each results section. For RNA-Seq analyses FastQ data was quality checked using MultiQC http://multiqc.info/. Data was aligned to the human genome (build hg19) using TopHatv2 implemented in Illumina's BaseSpace cloud resource using the default parameters [182]. BAM files were downloaded and differential expression analysis performed using Genome Suite. Partek v 6.6 was used for the differential gene expression analysis annotating reads with the latest build of the RefSeq database (v83). Analysis of variance was used to calculate list of differentially expressed genes. The Benjamini-Hochberg, false discovery rate (FDR) method was used to control for multiple texting with values reported with an FDR of 0.05 and fold change of 2 or greater.

5.3 Results

5.3.1 Aggregation of platelets from a $cPLA_{2\alpha}$ mutated patient measured using LTA

LTA as described in 5.2.2 was used to assess the function of platelets belonging to a patient with a mutation in the $cPLA_2\alpha$ gene. PRP was stimulated in the aggregometer with arachidonic acid 1mM (Figure 5.4 A), ADP 5 µM (B), ADP 20 µM (C), collagen 0.4 µg/mL (D), collagen 4 µg/mL (E), collagen 10 µg/mL (F), TRAP-6 25 µM (G) or U46619 10 µM (H). There was a significant decrease in aggregation measured between control and patient in response to ADP 20 µM, collagen 0.4 µg/mL and collagen 4 µg/mL.

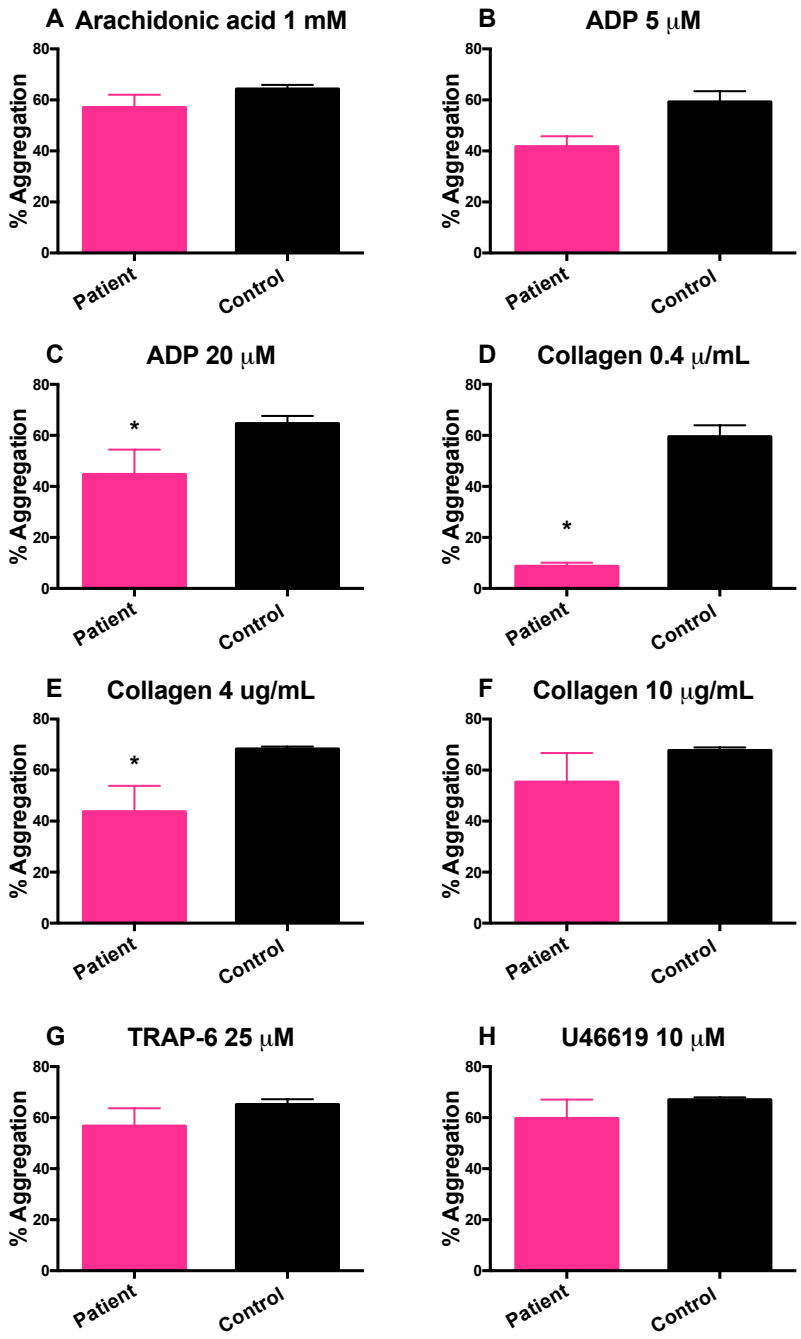

Figure 5.4 LTA data showing percentage aggregation of platelets obtained from a cPLA$_2$α-mutated patient compared to healthy controls

LTA aggregation data presented as final percentage aggregation. Results displayed as mean ± SEM. Two samples were obtained from the test patient on two separate days (n=12 for controls, *p<0.05 by unpaired t test).

5.3.2 Aggregation of platelets from a cPLA$_2$α mutated patient measured using the Optimul assay

Platelet aggregation was investigated using the Optimul plate assay enabling the use of multiple agonists across a concentration range. Agonists used were arachidonic acid (Figure 5.5 A), ADP (B), collagen (C), epinephrine (D), ristocetin (E), TRAP-6 (F) and U46619 (G). Data in Figure 5.3 show that there was a significant decrease in aggregation observed for the patient sample compared to control samples for the agonists collagen (C), epinephrine (D) and U46619 (G).

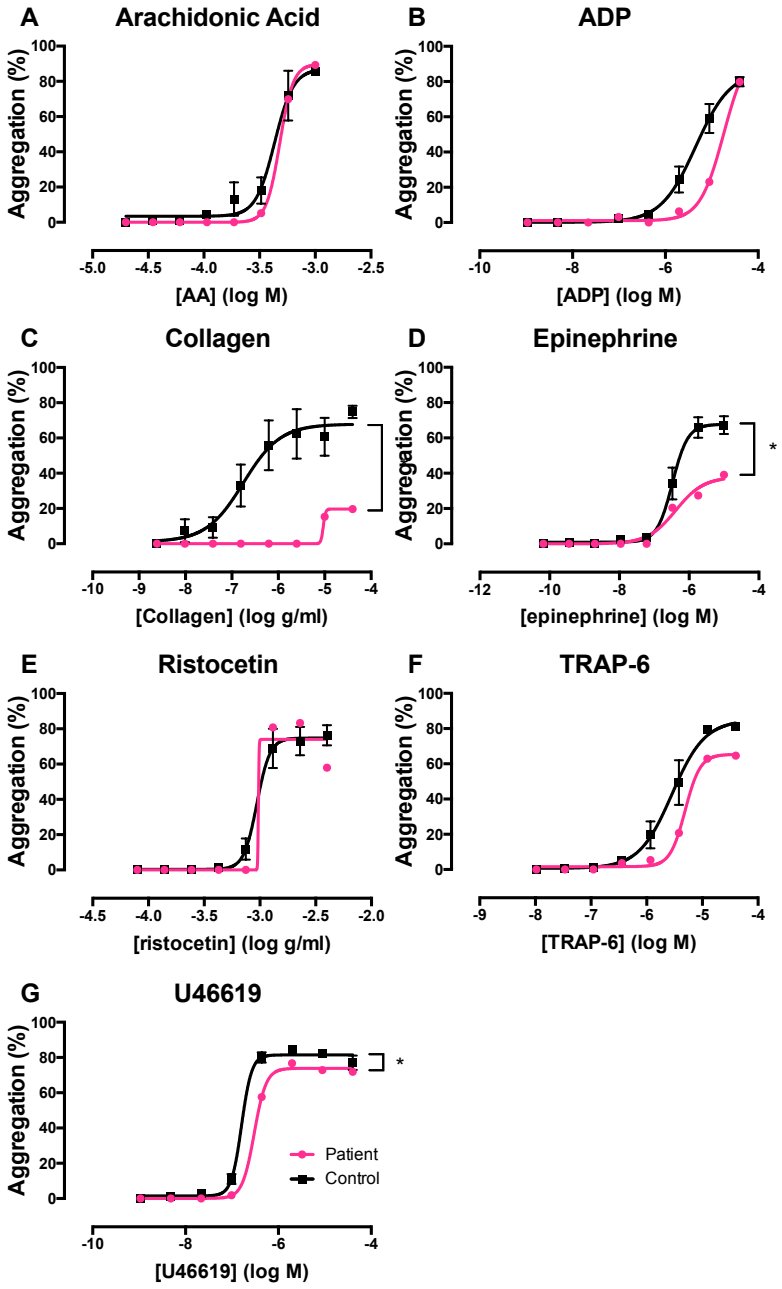

Figure 5.5 Optimul plate data showing percentage aggregation of platelets obtained from a cPLA$_2$α-mutated patient compared to healthy controls

Optimul plate platelet aggregation data presented as percentage aggregation form PRP samples obtained from a cPLA$_2$α mutated patient and 20 healthy controls. Results displayed as mean ± SEM. Significance was assessed using a two-way ANOVA (p=<0.05).

Agonist	Control Log EC50	Control 95% confidence interval of Log EC50	Patient Log EC50	Patient 95% confidence interval of Log EC50
Arachidonic acid	-3.37	-3.448 to -3.282	-3.32	-3.319 to -3.318
ADP	-5.34	-5.565 to -5.124	-4.74	-5.453 to -4.029
Collagen	-6.75	-7.234 to -6.274	-5.03	Not calculated
Epinephrine	-6.48	-6.603 to -6.358	-6.39	-6.957 to -5.813
Rsitocetin	-3.03	-3.102 to -2.953	-2.92	-2.974 to -2.857
TRAP-6	-5.55	-5.718 to -5.374	-5.31	-5.425 to -5.193
U46619	-6.79	-6.940 to -6.646	-6.52	-6.651 to -6.389

Table 5.1 Optimul data log EC50 values and 95% confidence intervals obtained from a cPLA$_2$α-mutated patient compared to healthy control

Log EC50 values and 95% confidence intervals for the non-linear regression curves fitted to the Optimul data comparing percentage aggregation of PRP samples obtained from a cPLA$_2$α mutated patient and 20 healthy controls.

5.3.3 Activation of platelets from a cPLA$_2$α mutated patient - ATP release

PRP obtained from a cPLA$_2$α mutated patient was stimulated with arachidonic acid 1 mM (Figure 5.6 A), ADP 5 μM (B), collagen 4 μg/mL (C) or TRAP-6 25 μM (D) in channels of the luminescence aggregometer. ATP release was measured as an indicator of platelet activation and quantified using an ATP spike as outlined fully in section 5.2.4. There was a significant reduction in collagen-induced ATP release from platelets derived from the test patient compared to those from controls.

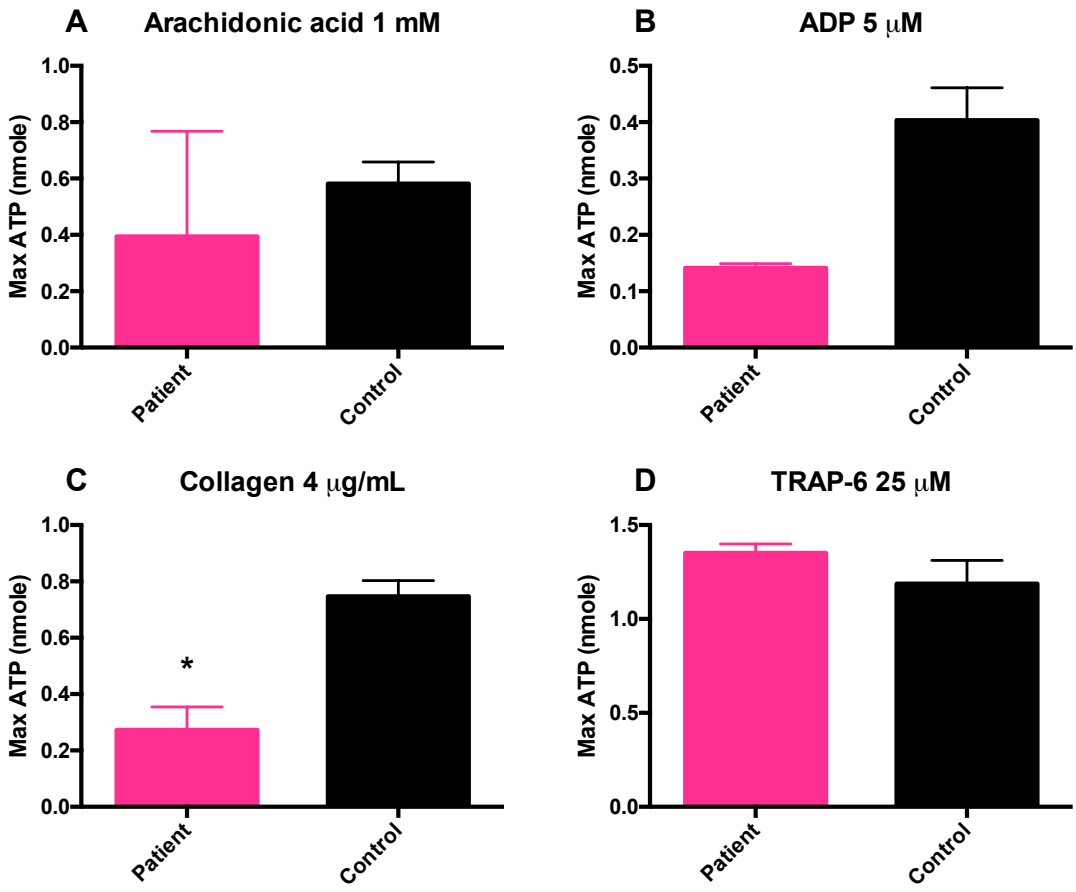

Figure 5.6 Maximum ATP release in response to various agonists of platelets derived from a cPLA$_2$α mutated patient or healthy controls

ATP release from platelets stimulated with arachidonic acid 1 mM (A), ADP 5 μM (B), collagen 4 μg/mL (C) or TRAP-6 25 μM. Results displayed as mean ± SEM. Two samples were obtained from the test patient on two separate days (n=20 for controls) *p<0.05 by unpaired t-test.

5.3.4 Activation of platelets from a cPLA$_2$α mutated patient – surface P-selectin expression

Whole blood was incubated with EDTA vehicle, ADP 40 μM, U46619 0.5 μM or a combination of both in a 96 well plate as described in section 5.2.5 and flow cytometry used to obtain mean fluorescence intensity values of cell surface P-selectin (CD62P). Data presented in Figure 5.7 indicates that the patient sample has an increase in P-selectin expression compared to controls when stimulated with either U46619 alone or in combination with ADP. The n=1 patient sample prohibits the use of appropriate statistical analysis.

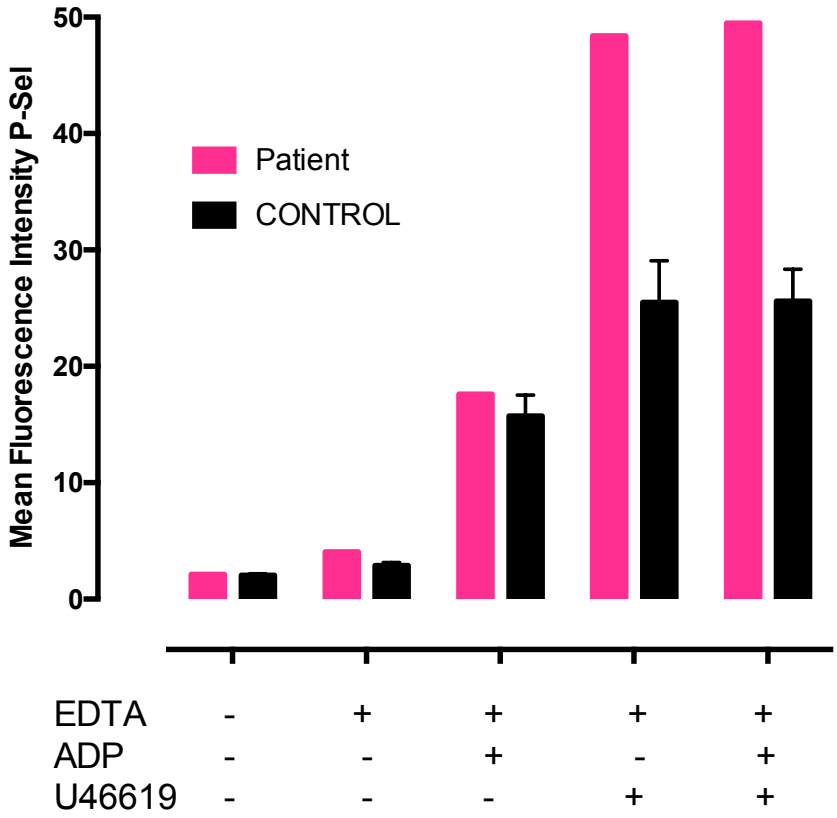

Figure 5.7 Flow cytometric analysis of agonist stimulated P-selectin expression in platelets from a cPLA$_2$α mutated patient compared to healthy controls

Mean florescence intensity values for P-selectin (CD62P) expression per 100,000 CD61 positive platelet events. Results displayed as mean ± SEM for control values n=20 and as absolute values for the n=1 patient data.

5.3.5 Pre- and post-sequencing sample assessment

Pre- and post-sequencing analyses of the RNA input, cDNA libraries and aligned reads required for RNA-Seq are essential to decisions regarding which samples to take forward into differential expression calculations.

RNA quality was assessed using the total RNA pico chips and reagents for the Agilent 2100 Bioanalyser that produces a normalised value, called the RNA integrity number (RIN), allowing direct comparisons between samples. RNA samples are given a RIN between 1-10 with 1 being the most and 10 being the least degraded, as calculated using Agilent patented algorithms available on the Bioanalyser software which takes into account multiple features of the electrophoretic trace. All samples, had an acceptable RIN value of >6.5. Full-length cDNA molecules were generated from 1ng of total RNA per sample using the SMARTer kit that includes a poly-A selection step to enrich samples for protein coding genes, a cDNA amplification step using PCR and an adaptor removal step in order to produce cDNA libraries for each sample. Libraries where then quantified in terms of molarity and average size using the QuBit fluorometer. For RNA-Seq differential expression applications it is preferable that the library molarity is greater than 3 nM (libraries are then diluted to achieve the same molarity for all libraries) and that the library size is 300-500 bp. Column 2 in Table 5.2 shows the library molarity in nmol for each sample and column 3 in Table 5.2 shows the average library size in bp for each sample

Sequencing coverage describes the average number of reads that align to known reference bases, the number of reads required depends upon what sensitivity is required to detect genes expressed at low levels. Owing to the fact that many functionally important platelets genes are expressed at a low level the decision was made to use a depth of coverage of 40 million reads per sample. Column four in table 5.2 shows the total number of reads for each sample, with all samples apart from patient replicate 2 have acceptable values ranging from 28-39 million of

which between 89-91% of those align to the reference genome (column five Table 5.2). For these reasons patient replicate 2 sample highlighted in yellow was removed for the subsequent differential expression analysis (Table 5.2). All samples evenly distributed the number of aligned reads to each of the two DNA strands as indicated by the percentage of aligned reads to each strand being 50%. The decision to perform un-stranded RNA-Seq was made as for differential expression analysis it is not essential to know to which DNA strand the transcript maps.

Sample ID	RNA integrity number (RIN)	Library concentration (ng/uL)	Library average size (bp)	Number of reads	Total reads aligned (%)	Aligned reads on each strand (%)
Control 1	8.4	5.56	394	39,436,367	90.66%	50.10%
Control 2	7.8	1.86	369	29,959,188	90.15%	50.13%
Control 3	6.9	3.80	364	38,417,943	89.85%	50.24%
Control 4	6.7	1.50	335	30,635,690	90.02%	50.24%
Control 5	6.8	1.98	336	32,767,537	90.51%	50.20%
Control 6	7.4	0.61	306	28,818,265	89.95%	50.14%
Patient replicate 1	7.4	1.60	319	34,300,286	90.53%	50.29%
Patient replicate 2	7.2	0.10	237	8,037,788	83.30%	50.00%
Patient replicate 3	N/A	1.43	308	30,133,687	88.48%	50.21%
Patient replicate 4	6.8	2.32	324	29,872,748	90.40%	50.21%

Table 5.2 RNA-Seq sample quality analyses

Parameters commonly measured to ensure sample quality; RNA integrity number, library molarity (nM), library average size (bp), number of reads, percentage of total reads aligned and percentage of aligned reads on each strand.

5.3.6 Comparing RPKM values obtained using RNA-Seq against a previously published data set

Reads per kilo base per million (RPKM) are quantitative approximations of the abundance of all target transcripts. RNA-Seq provides this quantification in the form of raw counts from which RPKM values can be calculated as a way of removing biased estimations of transcript abundance inherent to the sequencing process. For example longer transcripts will have more reads mapped to their region as there are more bases there to begin with, this would bias comparisons of genes of different length. RPKM values are calculated in three steps: 1) count the total reads in a sample and divide by 1,000,000 to give the 'per million' scaling factor; 2) divide the read counts for each gene by the 'per million scaling factor' to give the 'reads per million', this step normalises for difference in sequencing depth; and 3) divide the 'reads per million values' for each gene by the length of the gene in kilobases to derive the RPKM value.

In order to understand how the data compared to other platelet RNA-Seq studies a comparison was made between these current results and results produced by Rowley et al in their 2011 study titled "Genome-wide RNA-seq analysis of human and mouse platelet transcriptomes" [54]. Working from the logged RPKM values from each of the six healthy control data sets an average log-RPKM value for each expressed gene was calculated.

Using the average control values the data was sorted based on log RPKM values ordered highest to lowest. The top 40 expressed genes were taken, ranked 1-40 with rank number 1 being the most abundant (Table 5.3 columns 1 (gene names) and 2 (ranking)) and directly compared to the top 40 expressed genes published in the Rowley study (Table 5.3 columns 3 (gene names), 4 (ranking in my control data set). The average patient top 40 (Table 5.4 column 1) was then compared to both the control top 40 (Table 5.4 column 2) and the Rowley study top 40

(Table 5.4 column 3). Values highlighted in orange indicate a ranking that falls outside of the top 40. Values assigned with '?' indicates a ranking that was not in the published data set. Tables 5.3 and 5.4 shows that there was a good similarity between the control and patient data sets as well as between the current data sets and the historical Rowley study data set.

My control data set top 40	Top 40 ranking	Rowley data set top 40	Position in control data set top 40
TMSB4X	1	MIR1978	?
B2M	2	B2M	2
FTH1	3	MIR1974	?
PPBP	4	FTH1	3
ACTB	5	PF4	7
OST4	6	PPBP	4
PF4	7	NRGN	19
HBB	8	OST4	6
HBA2	9	HIST1H2AC	24
FTL	10	ACTB	5
GNG11	11	GP1BB	25
SH3BGRL3	12	FTL	10
TAGLN2	13	OAZ1	16
TUBB1	14	GPX1	27
SDPR	15	HLA-E	119
OAZ1	16	TUBB1	14
RGS18	17	GNAS	6040
H3F3AP4	18	TAGLN2	13
NRGN	19	CLU	30
SPARC	20	SDPR	15
MYL12A	21	CCL5	31
F13A1	22	SH3BGRL3	12
MYL6	23	SPARC	20
HIST1H2AC	24	F13A1	22
GP1BB	25	HBB	6494
MAP3K7CL	26	PPDPF	174
GPX1	27	FLNA	237
H3F3A	28	MYL6	23
ARPC1B	29	PGRMC1	36
CLU	30	HLA-B	190
CCL5	31	CALM3	95
ITM2B	32	ITGA2B	55
PTMA	33	TLN1	152
SAT1	34	TGFB1	219
LOC101927854	35	MYL9	121
PGRMC1	36	HLA-C	613
PRKAR2B	37	ARPC1B	29
HIST1H3H	38	ITM2B	32
MMD	39	RGS18	17
CA2	40	ITGB3	520

Table 5.3 Comparing the top 40 most highly expressed genes in control versus patient PRP samples – My control data set versus Rowley data set

Log RPKM values were used to rank genes according to their abundance. This ranking was used to compare control data obtained in this current study (blue) to data published in another platelet RNA-Seq study (green).

Patient data set	Position in control data set top 40	Position in Rowley data set top 40
TMSB4X	1	?
B2M	2	2
HBB	8	25
HBA2	9	?
FTH1	3	4
PPBP	4	6
ACTB	5	10
OST4	6	8
FTL	10	12
PF4	7	5
HBA1	48	?
SH3BGRL3	12	22
GNG11	11	?
MYL6	23	28
TUBB1	14	16
OAZ1	16	13
TAGLN2	13	18
RGS18	17	39
GP1BB	25	11
SDPR	15	20
H3F3AP4	18	?
NRGN	19	7
F13A1	22	24
SPARC	20	23
MYL12A	21	?
HIST1H2AC	24	9
ARPC1B	29	37
CCL5	31	21
ITM2B	32	38
CLU	30	19
MAP3K7CL	26	?
GPX1	27	14
FCER1G	58	?
H3F3A	28	?
SAT1	34	?
CA2	40	?
ARHGDIB	44	?
HIST1H3H	38	?
ITGA2B	56	32
MMD	39	?

Table 5.4 Comparing the top 40 most highly expressed genes in control versus patient PRP samples

Log RPKM values were used to rank genes according to their abundance. This ranking was used to compare the top 40 genes expressed in the cPLA$_2$α data set with the top 40 genes expressed in the control data sets generated in this experiment and as published by Rowley et al.

5.3.7 Differential expression analysis

Using the RPKM values for the averaged control data set and the averaged patient data set a one-way ANOVA with p=<0.0001 was used to determine which genes were differential expressed between control and patient. Fold changes were expressed using the log 2 scale.

Table 5.3 shows all statistically different differentially expressed genes, their chromosomal location, P-values, mean ratio (the ratio of the mean values of RPKMs of the two groups, numbers less than 1 indicate down regulation) and fold change (negative numbers indicate down regulation).

Gene symbol	Gene name	Chromosomal location	P-value (Control vs. Patient)	Mean Ratio (Control vs. Patient)	Fold Change (Control vs. Patient)
SLPI	Secretory Leukocyte Peptidase Inhibitor	Chr 2 starting at 45252 KB (- strand)	6.02E-10	0.008	-128.608
TREML4	Triggering Receptor Expressed On Myeloid Cells Like 4	Chr 6 starting at 41228 KB (+ strand)	1.37E-05	0.010	-105.200
TOB2P1	Transducer Of ERBB2, 2 Pseudogene 1	Chr 6 starting at 28183 KB (- strand)	3.28E-05	0.016	-63.452
LPAL2	Lipoprotein (A) Like 2, Pseudogene	Chr 6 starting at 160453 KB (- strand)	6.93E-05	0.023	-44.354
GSG1	Germ Cell Associated 1	Chr 12 starting at 13083 KB (- strand)	7.71E-06	0.024	-41.828
CEACAM3	Carcinoembryonic Antigen Related Cell Adhesion Molecule 3	Chr 19 starting at 41796 KB (+ strand)	2.30E-05	0.028	-35.507
CRISP3	Cysteine Rich Secretory Protein 3	Chr 6 starting at 49727 KB (- strand)	3.75E-05	0.033	-30.547
DSC2	Desmocollin 2	Chr 18 starting at 31058 KB (- strand)	9.87E-09	0.039	-25.420
LINC01296	Long Intergenic Non-Protein Coding RNA 1296	Chr 14 starting at 19156 KB (+ strand)	1.10E-05	0.044	-22.682
APOL4	Apolipoprotein L4	Chr 22 starting at 36190 KB (- strand)	5.25E-05	0.046	-21.603
FCGR3B	Fc Fragment Of IgG Receptor IIIb	Chr 1 starting at 161623 KB (- strand)	3.77E-06	0.051	-19.477
ACSL1	Acyl-CoA Synthetase Long Chain Family Member 1	Chr 4 starting at 184755 KB (- strand)	4.88E-05	0.064	-15.685
ST13P4	ST13, Hsp70 Interacting Protein Pseudogene 4	Chr 13 starting at 50172 KB (+ strand)	8.91E-05	0.071	-14.172

Table 5.3 Continued

Gene symbol	Gene name	Chromosomal location	P-value (Control vs. Patient)	Mean Ratio (Control vs. Patient)	Fold Change (Control vs. Patient)
C19orf81	Chromosome 19 Open Reading Frame 81	Chr 19 starting at 50632 KB (+ strand)	5.95E-05	0.083	-12.099
DCDC2	Doublecortin Domain Containing 2	Chr 6 starting at 24122 KB (- strand)	3.64E-05	0.102	-9.795
KRT23	Keratin 23	Chr 17 starting at 40922 KB (- strand)	6.41E-06	0.108	-9.262
LIN7A	Lin-7 Homolog A, Crumbs Cell Polarity Complex Component	Chr 12 starting at 80792 KB (- strand)	4.44E-05	0.110	-9.085
S100A12	S100 Calcium Binding Protein A12	Chr 1 starting at 153346 KB (- strand)	6.67E-05	0.115	-8.687
HMMR	Hyaluronan Mediated Motility Receptor	Chr 5 starting at 163480 KB (+ strand)	6.41E-05	0.121	-8.298
CSF3R	Colony Stimulating Factor 3 Receptor (Granulocyte)	Chr 1 starting at 36366 KB (- strand)	6.30E-05	0.122	-8.216
LOC643802	U3 Small Nucleolar Ribonucleoprotein Protein MPP10-Like	Chr 16 starting at 53403 KB (- strand)	2.59E-06	0.130	-7.705
POLR2J2	RNA Polymerase II Subunit J2	Chr 7 starting at 102636 KB (- strand)	9.35E-05	0.147	-6.824
QPCT	Glutaminyl-Peptide Cyclotransferase	Chr 2 starting at 37344 KB (+ strand)	5.18E-05	0.189	-5.284
S100A8	S100 Calcium Binding Protein A8	Chr 1 starting at 153357 KB (- strand)	2.81E-07	0.193	-5.176
S100A9	S100 Calcium Binding Protein A9	Chr 1 starting at 153357 KB (+ strand)	2.35E-05	0.298	-3.351
GCA	Grancalcin	Chr 2 starting at 162318 KB (+ strand)	7.51E-05	0.381	-2.624

Table 5.5 Differentially expressed genes: Control versus Patient

The 26 differentially expressed genes in the control samples compared to the patient samples. A one-way ANOVA p=<0.0001 was used to test significance.

Discussion 5.4

Group IV A cytosolic phospholipase A_2 ($cPLA_2\alpha$) is a calcium-activated enzyme that preferentially binds arachidonic acid over other available fatty acids. Phosphorylation of this enzyme by mitogen activated protein kinases following agonist stimulation enables the translocation of $cPLA_2\alpha$ from the cytoplasm to the membrane of cells where it can exert its enzymatic functions [183].

The enzymatic actions of the phospholipase A_2 (PLA_2) family of proteins are critical to the production of important eicosanoids within the cardiovascular system. PLA_2 enzymes catalyse the hydrolysis of membrane phospholipids to release arachidonic acid which is then further broken down into its active eicosanoids via specific enzymatic pathways [172].

In this chapter I obtained blood samples from a patient with a mutation in PLA2G4A gene that causes inactivation of the $cPLA_2\alpha$ enzyme, in order to specifically assess platelet function compared to healthy controls.

Previous investigations carried out on this patient have shown that loss of $cPLA_2\alpha$ activity has significant negative effects on eicosanoid production that subsequently diminishes platelet aggregation and ATP release [168]. In a study focussed on the specific cardiovascular effects of this mutation investigators showed an absolute requirement for $cPLA_2\alpha$ in eicosanoid synthesis. By assessing effects on platelets, leukocytes and endothelial cells it was shown that lack of eicosanoid production caused a consequent loss in platelet activation, reduced antithrombotic prostacyclin and increased inflammatory sensitivity of both endothelial cells and leukocytes [184]. Supportive work using the specific pharmacological inhibitor for the $cPLA_2\alpha$ isoform, pyrrophenone, has demonstrated this enzyme's role in arachidonic acid release and subsequent eicosanoid synthesis using whole blood assays [185,186]. Additionally $cPLA_2\alpha^{-/-}$ mice

display phenotypes, including protection against thromboembolism, prolonged bleeding, protection from asthma and reduced incidences of certain cancers all of which can be explained by the lack of eicosanoid production [187–192]. Studies using these animals further highlight the importance of the $cPLA_2$ enzyme to the production of bioactive lipids [193–195].

In this current investigation I used traditional light transmission aggregometry (LTA) and the Optimul plate assay to assess platelet aggregation in response to the agonists arachidonic acid, ADP, collagen, epinephrine, ristocetin, TRAP-6 and U46619. In the LTA assay there was significant reduction in percentage aggregation recorded in response to ADP 20 μM, collagen 0.4 μg/mL and collagen 4 μg/mL (Figure 5.4). Acting through the cell surface receptors $P2Y_{12}$ and $P2Y_1$, ADP causes platelet aggregation, platelet intracellular calcium mobilisation, platelet shape change and release of granule content [196–198]. ADP activation also stimulates TXA_2 production that then feeds-back on the platelet to further increase the activating response [41]. Thus in this patient there was a decreased response to ADP due to the lack of TXA_2 production from arachidonic acid. Similarly collagen activation of platelets is enhanced by the production of TXA_2 stimulated by a rise in intracellular calcium [199–201]. Hence the significant reduction in aggregation seen for this patient particularly in response to the lower concentrations of collagen used (0.4 and 4 μg/mL).

Likewise ATP release from the patient's platelets was significantly lower for collagen 4 μg/mL stimulated samples in the luminescence aggregometry based assay (Figure 5.6) as collagen is also known to stimulate platelet granule secretion partly through the production of TXA_2 [202].

In addition to this there was significant reduction in percentage aggregation recorded in response to epinephrine and U46619 across the concentration ranges used in the Optimul plate assay (Figure 5.5).

Epinephrine has been shown to increase the release of TXA_2 from platelets [203–205], as the patient cannot produce this eicosanoid the reduction in aggregation is as expected. Although U46619 is a synthetic stable TXA_2 receptor agonist there is still a diminished response to this agonist in platelets from the test patient owing to the lack of secondary TXA_2 release in response to the initial agonist stimulation [206], which can be seen in the midpoint of the agonist response curve.

The increase in platelet activation, as measured by P-selectin expression, in response to U46619 or ADP stimulation was significantly increased in the patient compared to the controls (Figure 5.7). This could potentially hint towards a compensatory mechanism whereby the platelets increase their ability to form platelet-leukocyte aggregates as a response to the loss of TXA_2 mediated platelet-platelet aggregation. Further investigations are required to fully test this hypothesis as it is based on a single observation.

As well as testing the function of platelets obtained from the $cPLA_2\alpha$ mutated patient I compared the platelet mRNA expression profiles between patient and control samples using RNA-Seq in combination with the optimised protocol for platelet isolation as described in chapter 3. The rationale for mRNA sequencing platelets from this patient was to investigate whether the lack of $cPLA_2\alpha$ protein activity and subsequent changes in bioactive eicosanoid production affects platelet mRNA expression. I hypothesised that platelets from this patient could show changes in expression of genes related to the arachidonic acid-eicosanoid pathway of platelet activation such as reductions in synthase enzymes, due to reduced substrate, and decrease in receptors, due to reduced agonists. It is interesting to note that the PLAG4A gene appears at rank number 4763 in my control data set and at rank number 7009 in the patient data set suggesting that lack of $cPLA_{2\alpha}$ protein activity could as a consequence be having a negative feedback on PLAG4A mRNA expression within the platelet.

Using differential expressions analysis I found 26 transcripts that were significantly upregulated in the patient platelet samples compared to control (Table 5.5). Of these 26 transcripts, 4 (S100A8, S100A9, S100A12 and SLP1) had previously been linked to aspects of platelet biology and would thus be interesting targets for further investigation.

S100A8, A9 and A12 are all genes that encode for low molecular weight calcium binding proteins. As a whole the S100 family of proteins function to regulate a variety of intracellular and extracellular processes including proliferation, differentiation, migration, apoptosis, calcium homeostasis, energy metabolism and inflammation. The S100 proteins, of which there are thirteen, all cluster on chromosome 1q21. S100A8, A9 and A12 proteins all have very similar functions and play prominent roles in the regulation of the immune system and in the inflammatory response. As such these proteins help to induce leukocyte chemotaxis, adhesion, degranulation, phagocytosis whilst also possessing pro-inflammatory, antimicrobial, oxidant-scavenging and apoptosis-inducing activities [207–210].

The S100A8, A9 and A10 gene products are referred to by various names in the literature. The S100A9 protein is also known as migration inhibitory factor-related protein-14 (MRP-14) or as calgranulin A, likewise the S100A8 protein is also known as MRP-8 or calgranulin B. Together the S100A9 and S100A8 protein form a heterodimer called calprotectin (MRP-8/14).

MRP-8/14 levels have been linked to numerous inflammatory disease states including many cardiovascular disease processes [211]. In 2006 in a study profiling platelet mRNA from patients with acute ST-segment elevation myocardial infarction (STEMI) or stable coronary artery disease (CAD) investigators reported a significant increase in MRP-14 at the mRNA level and a consequent significant increase in plasma levels of the MRP-8/14 heterodimer in the STEMI patients compared to the stable CAD patients. Following on from this the group then sought to validate the MRP-14 gene target in a group of 28,345 healthy postmenopausal

women in order to assess the risk of future cardiovascular events associated with plasma levels of the MRP-8/14 heterodimer. At the end of the three-year follow up period it was shown that initially healthy women who subsequently developed cardiovascular events during follow-up had higher median MRP-8/14 levels at baseline than women who remained free of disease. After various risk correction analyses it was demonstrated that having an MRP-8/14 level in the top quartile equated to a 4-fold elevation in risk for all cardiovascular events [212].

Two years later another study sought to investigate the risk of cardiovascular death or myocardial infarction associated with MRP-8/14 measured 30 days after an acute coronary syndrome event. What they found was that patients who died as a result of a cardiovascular event or who had had a myocardial infarction after the 30 days had higher levels of MRP-8/14 compared to patients who remained free of recurrent events [213].

Other groups have also linked increased platelet MRP-8/14 protein and serum levels to systemic lupus erythematosus patients who also have cardiovascular disease [214,215].

In an attempt to strengthen the link between MRP-8/14, cardiovascular disease risk and thrombosis, investigators used wild-type mice to show that platelets up-regulate expression of MRP-8/14 and increase secretion of MRP-8/14 during arterial thrombosis and that this can signal through CD63 on other platelets to drive the thrombus formation. They also obtained arterial thrombi from STEMI patients and found that they stained positive for the MRP-14 protein [216]. Further evidence suggests that MRP-8/14 levels, in particular reference to acute coronary syndrome patients, were linked to enhanced TXA_2 dependent platelet activation [217] and that more generally serum MRP-8/14 levels correlate positively with platelet aggregation [218].

To a lesser extent increased expression of S100A12 has also been linked to increased cardiovascular disease risk in the context of determining atherosclerotic plaque rupture risk. However S100A12 was only measured as protein levels in the serum with no evidence to support that this was derived from platelets [219].

Together these studies provide evidence to support the further investigation of MRP-8/14 as a biomarker or therapeutic target for future cardiovascular events linked to thrombosis and reinforces the idea that the platelet transcriptome can be used as a source of disease biomarkers. MRP-8/14 blockers have been developed and are approved for clinical testing [211,220].

It is interesting then that the $cPLA_{2\alpha}$ deficient patient presented in this chapter had significantly up-regulated platelet expression of these three genes. One possible explanation is that this may be a compensatory mechanism for the lack of eicosanoid driven platelet activation. While more evidence is needed to substantiate this idea, the patient's strong aspirin-like phenotype yet lack of bleeding symptoms is supportive. Furthermore there is evidence from groups working on human neutrophils showing that the MRP-8/14 complex binds arachidonic acid and thus provides an intracellular reservoir of arachidonic acid for the cell [221]. When combining this knowledge with the fact that endothelial cells have the ability to utilise exogenous arachidonic acid for trans-cellular production of thromboxane [222] it could be speculated that platelets could also take up arachidonic acid from other cell type for its metabolism into functionally important eicosanoids. This would be particularly relevant in the case of the $cPLA_{2\alpha}$ deficient patient whose platelets lack the ability to liberate arachidonic acid from the cell membrane but retain the ability to metabolise arachidonic acid.

The SLPI (secretory leukocyte protease inhibitor) transcript, which was up-regulated in the patient samples, has also been shown to modulate platelet function. Rap-1 (Ras-related protein-1) plays a key role in platelet activation as shown previously by multiple groups [223–225]. In platelets Rap-1 activity is regulated by the GTPase activating protein Rap1GAP2 [226]. SLPI is a binding partner for Rap1GAP2 and has been shown to inhibit dense granule release in human platelets [227]. The test patient did indeed show a reduced dense granule ATP release response that could be partially explained by the increase in SLPI expression. However further experiments would be needed to separate out the effects of SLPI over-expression and lack of TXA_2 signalling which could both be contributing to the diminished platelet release response. Located at chromosome position 20q13.12 SLPI's most well documented function is in the immune system where is protects mucosal epithelial surfaces from serine proteases [228].

An obvious progression of the differential expression data would have been to perform pathway analysis of the significantly up/down regulated transcripts. Unfortunately due to there being only 26 such transcripts in my data set there was not enough statistical power to provide meaningful results. However performing a basic enrichment analysis search using the Gene Ontology Consortium online tool produced a list of over-represented functional classes within those 26 gene with the top five being immune system process, immune response, exocytosis, secretion by cell and secretion. As already described SLPI has a clear link to the to secretion terms whereas the roles of S100A8, A9 and A10 have quite obvious links to an immune system process, namely inflammation.

In conclusion lack of $cPLA_2$ enzymatic activity results in the loss of eicosanoid production from arachidonic acid. This in turn has significant effects upon various aspects of platelet function including aggregation and granule release. In addition RNA-Seq of platelets obtained from this patient revealed a number of differentially expressed transcripts when compared to control sample four of which (S100A8, S100A9, S100A12

and SLPI) have previously been linked to the regulation of platelet function, thrombosis and cardiovascular disease risk making them interesting targets for future investigations.

Chapter 6 - Assessment of platelet function in patients with bleeding disorders featuring a case study of a patient with a PTGS1 mutation

6.1 Introduction

Bleeding and platelet disorders (BPD) are a group of diseases caused by defects to the coagulation system, platelets or vessel walls often presenting as abnormal bleeding. The heterogeneous nature and rarity of these conditions makes clinical diagnosis and management difficult. Current clinical diagnostic tools can pinpoint the cause of a BPD in around 40-60% of cases and only a fraction of these receive a genetic diagnosis owing to the fact that the genetic basis of BPDs are mostly unknown.

As part of the larger BRIDGE-BPD consortium this chapter aims to investigate the use of in depth platelet function testing for patients with bleeding disorders of unknown aetiology or with confirmed mutations predicted to alter platelet function in order to provide better phenotypic information, enabling more accurate diagnoses. The BRIDGE-BPD study is an observational multicentre study that aims to identify causal gene mutations in patients with BPDs by using next generation sequencing technologies. The study inclusion criteria are as follows; platelet count of less than 100 x 10(9)/L or greater than 400 x 10(9)/L, or mean platelet volume less than 6 fL or greater than 12 fL, or reproducible abnormal platelet function tests, or abnormal platelet morphology by light or electron microscopy, or pathological bleeding of unknown aetiology, and considered by referring clinician to be of genetic aetiology. The study exclusion criteria are as follows; acquired bleeding or platelet disorder including any of the following: use of any medication known to affect platelet function, immune thrombocytopenia, HIV infection, malignancies, bone marrow aplasia, thrombotic thrombocytopenic purpura / haemolytic-uremic syndrome, acute viral infection, splenomegaly and uraemia or hepatic failure.

In particular this chapter focuses on a family consisting of an index case with a homozygous mutation in the PTGS1 gene encoding for the cyclooxygenase-1 enzyme (COX-1) and their reportedly asymptomatic

parents. The index patient was identified at The Royal London Hospital (Barts Health NHS Trust) presenting with cystic fibrosis with recurrent respiratory infections, complement component-6 deficiency, recurrent miscarriages, haemoptysis, epistaxis, peri-operative bleeding and a tendency to bruise easily. As a consequence the index patient is treated with desmopressin, tranexamic acid and antibiotics when required. The parents are consanguineous and present with no current or historical symptoms of bleeding. They take no medications known to alter platelet function.

The PTGS1 gene encodes for the cyclooxygenase-1 protein (COX-1) also known as prostaglandin G/H synthase-1. The enzyme itself consists of two catalytic sites the cyclooxygenase site to which arachidonic acid binds and the peroxidase site to which prostaglandin G_2 binds. Figure 6.1 outlines the conversion of arachidonic acid, through the activity of platelet COX-1, into various eicosanoids. The COX-1 enzyme works downstream of the PLA_2 enzymes, as discussed in the previous chapter, to produce biologically active eicosanoids that are essential to platelet function, through the metabolism of arachidonic acid [177]. The mutation identified in the index case was a homozygous missense mutation G>C found on chromosome 9 resulting in a tryptophan to serine amino acid change within exon 8. A representation of the location of this mutation can be seen in Figure 6.2. This figure, created using the UCSC genome browser and mapped to the Human February 2009 (GRCh37/hg19) assembly, shows the location of the PTGS1 gene to be on the long arm of chromosome 9 with the patient's mutation occurring at position 125132069. Based on the H3K4Me1 and H3K27Ac signals overlaid on Figure 6.2 in blue/pink the mutation does not appear to be within these chromatin domains that are highly associated with activation and repression of gene translation. Thus the mutation is unlikely to affect transcription of the PTGS1 gene These observation fall in line with the fact that the mutation is an exonic variant which is expected to have a direct effect on the protein rather then its regulation. It should be noted that the variant is in a highly conserved area. Thus indicating that this

mutation will likely have a functional effect upon the cycol-oxygenase-1 protein.

This chapter will investigate the functional consequences to the platelet of this specific mutation by comparing the patient data to both the unaffected parents and to a data set of twenty healthy controls.

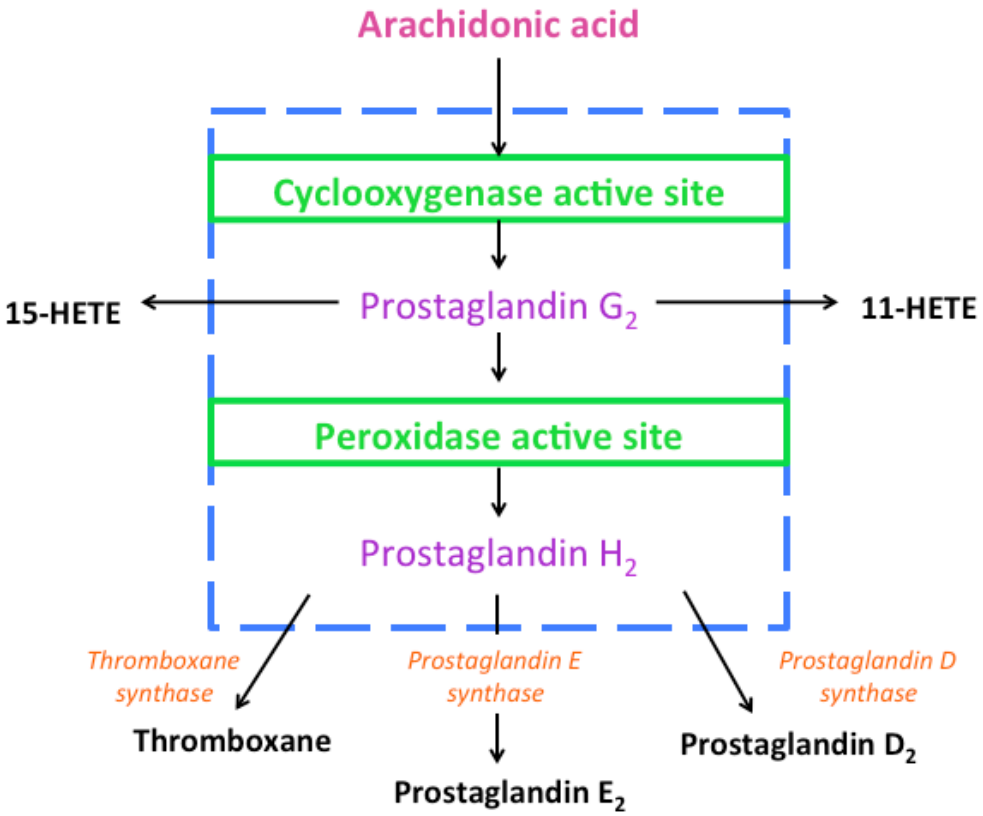

Figure 6.1 Outline of COX-1 catalytic sites

Schematic showing the conversion of arachidonic acid to biologically active eicosanoids through the activity of the platelet COX-1 enzyme.

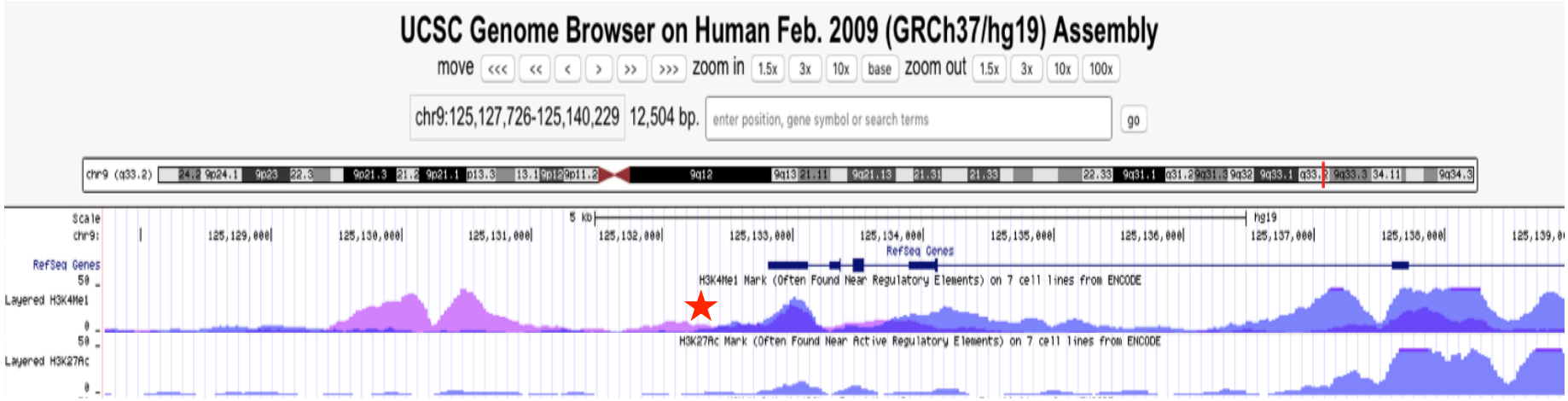

Figure 6.2 Representation of patient mutation within the PTGS1 gene

Representation of the human chromosome 9 showing the location of the PTGS1 gene indicated on the chromosome itself by a red line. Beneath this the histone trimethylation signals H3K4Me1 and H3K27Ac are displayed in blue and pink; peaks indicate high expression of these signals at that particular location. The PTGS1 mutated patient variant is occurs at position 125132069 and is indicated with a red star.

6.2 Methodology

6.2.1 Blood collection, preparation of PRP and BRIDGE-BPD study

Blood was obtained from healthy volunteers or patients of interest and PRP/PPP prepared as outlined previously in sections 3.2.1 and 3.2.2. Bleeding disorder patients were recruited as part of the BRIDGE-BPD study approved by a UK Research Ethics Committee (Cambridgeshire 1 Research Ethics Committee 10/H0304/66). All study procedures were performed after the participants provided informed written consent and were in accordance with the Declaration of Helsinki.

6.2.2 Light transmission aggregometry (LTA) agonist stimulation of PRP

225 µL of PRP was added to add to each test cuvette, placed into the PAP8-E aggregometer and stimulated with 25 µL of agonist as described in section 3.2.6 to achieve final concentrations of arachidonic acid 1 mM, ADP 10 µM, collagen 1 µg/mL, collagen 3 µg/mL, TRAP-6 25 µM, U46618 3 µM, epinephrine 10 µM or ristocetin 1.5 mg/mL.

6.2.3 Optimul plate assay

Optimul plates were prepared according to section 3.2.7. Upon use of the plate, 40 uL of PRP or PPP are added to the appropriate wells, the plate is shaken on a Bioshake plate shaker at 1200 rpm, for 5 min and 37°c and the absorbance is read at 595 nm on a Tecan Sunrise plate reader. Agonists used were ADP (0.005-40 µM), epinephrine (0.0004-10 µM), TRAP-6 amide (0.03-40 µM), U46619 (0.055-40 µM), arachidonic acid (0.03-40 µM), ristocetin (0.14-4 mg/mL) and Horm collagen (0.01-40 µg/mL).

6.2.4 Luminescence (lumi) aggregometry – ATP release

225 µL of PRP was added to add to each test cuvette, placed into the lumi aggregometer and stimulated with 25 µL of agonist as described in section 5.2.4 to achieve final concentrations of arachidonic acid 1 mM, ADP 10 µM, collagen 3 µg/mL or TRAP-6 25 µM. Maximum ATP release was recorded and calculated as outlined in Figure 5.3.

6.2.5 Platelet surface P-selectin expression – whole blood

A flow cytometric assay was used to assess platelet surface P-selectin (CD62P) expression in whole blood samples as an indicator of platelet activation in response to ADP (40 µM) or U46619 (0.5 µM) stimulation as described in 5.2.5.

6.2.6 Quantifying COX-1 protein expression using confocal imaging

2 mL of PRP was fixed in 1 mL of 8% paraformaldehyde in PBS (PFA-PBS) for 15 min at room temperature. Platelets were then pelleted at 900 x g for 10 min and the supernatant removed. The platelet pellet was then resuspended in 2 mL of acid citrate dextrose PBS buffer (ACD-PBS) at pH 6.1 and centrifuged again at 900 x g for 10 min. The pellet was resuspended again in ACD-PBS and centrifuged again at 900 x g for 10 min. The supernatant was removed and the pellet resuspended in 1 mL of 1% BSA in PBS. The platelets were then pipetted onto glass cover slips and incubated at 37°C for 90 min. Cover slips were then rinsed three times with PBS and blocked with a solution containing 0.2% Triton, 2% donkey serum and 1% BSA for 1 hour. A primary antibody mix containing rabbit anti-COX-1 (1:100) and mouse anti-tubulin (1:100) diluted in 0.2% Triton, 2% donkey serum and 1% BSA was pipetted onto the coverslips and left to incubate overnight at room temperature. Coverslips were washed in the morning three times with PBS and incubated with Alexa647 anti-rabbit (1:500) and Alexa488

anti-mouse (1:500) secondary antibodies for 1 hour at room temperature. The coverslips were then washed again three times in PBS and then fixed with 4% PFA-PBS for 5 min and washed again three times in PBS. The coverslips were then mounted onto glass slides using ProLong Diamond anti-fade mountant and left to dry for 1 hour at room temperature before storing at 4°C until imaging.

Confocal fluorescence microscopy images were obtained with oil immersion objectives (CFI Plan Apochromat 100 X, N.A.1.4, working distance 0.17 mm) using the LSM 710 confocal microscope. The microscope is equipped with 4 lasers: diode laser 405 nm 30 mW, multi-line argon lase 458/488/514 nm 25 mW, HeMe 543 nm 1 mW and HeNe 633 nm 5 mW. Acquisition and image processing were performed using the ZEN 2009 software.

6 images were analysed taken using the x100 oil immersion lens with a 2.5 zoom. For each image 10 platelets were randomly selected for analysis. Using ZEN software enabled quantification of the brightness of both the tubulin (green) and COX-1 (red) stains. These values were averaged to produce a single value for all six control images versus all six patient (386Q) images. There was no significant difference between COX-1 staining intensity between patient and control (Figure 6.14) indicating that the mutation is unlikely to cause a loss of protein expression. A t-test was used to determine significance ($p=0.05$).

6.2.7 Liquid chromatography tandem mass spectrometry (LC-MS/MS) analysis of agonist stimulated whole blood

Whole blood was stimulated with collagen 30 µg/ml or vehicle in the PAP8E aggregometer for 30 min at 37°C whilst being continually stirred. 30 µL of diclofenac/heparin solution (31.8 mg diclofenac sodium salt, 8.8 mL phosphate buffered solution, 200 uL heparin) was then added to each cuvette to stop the reaction. The contents of the cuvettes were

transferred into 1.5 mL Eppendorf tubes and centrifuged at 1000 x g. Supernatants (200 µL) were removed and stored at -80°C until required.

Samples were sent to Matthew Edin at The National Institutes of Health, National Institute of Environmental Health Science, North Carolina, USA for liquid chromatography tandem mass spectrometry analysis as described fully in 4.2.8.

6.2.8 Statistical analysis

All statistical analyses were conducted used GraphPad Prism v6 and are described in each results section.

6.3 Results

6.3.1 Determining control ranges for LTA measured platelet aggregation in response to various agonists

LTA as described in 5.2.2 was used to determine aggregation responses for twenty healthy control samples in order to produce reference percentiles to compare the bleeding disorder patient samples. PRP was stimulated in the aggregometer and percentile ranges produced for aggregation in response to arachidonic acid 1mM (Figure 6.3 A, Figure 6.4 A), ADP 10 µM (Figure 6.3 B, Figure 6.4 B), collagen 1 µg/mL (Figure 6.3 C, Figure 6.4 C), collagen 3 µg/mL (Figure 6.3 D, Figure 6.4 D), TRAP-6 25 µM (Figure 6.3 E, Figure 6.4 E), U46619 3 µM (Figure 6.3 F, Figure 6.4 F), epinephrine 10 µM (Figure 6.3 G, Figure 6.4 G) and ristocetin 1.5 mg/mL (Figure 6.3 H, Figure 6.4 H).

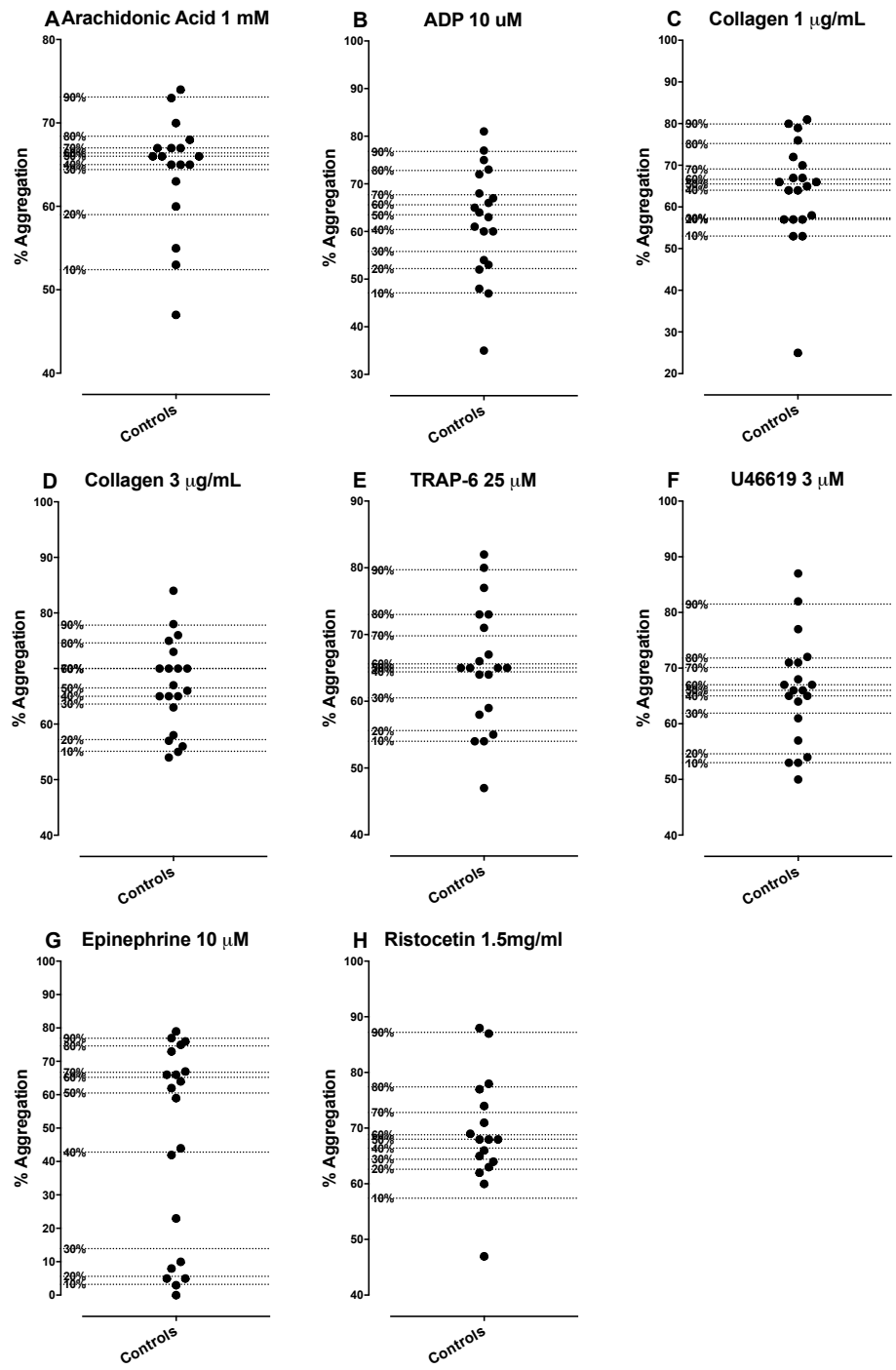

Figure 6.3 LTA aggregation responses for twenty healthy controls

Percentage final aggregation responses measured using LTA in response to arachidonic acid (A), ADP (B), collagen (C and D), TRAP-6 (E), U46619 (F), epinephrine (G) and ristocetin (H). Results displayed as individual data points for each control with overlaid percentile indicators (dotted lines).

A

Arachidonic acid 1 mM	
Percentile	**Percentage aggregation (%)**
90th percentile	≤ 73.1
80th percentile	≤ 68.4
70th percentile	≤ 67.0
60th percentile	≤ 66.4
50th percentile	≤ 66.0
40th percentile	≤ 65.0
30th percentile	≤ 64.4
20th percentile	≤ 59.0
10th percentile	≤ 52.4

B

ADP 10 µM	
Percentile	**Percentage aggregation (%)**
90th percentile	≤ 76.8
80th percentile	≤ 72.8
70th percentile	≤ 67.7
60th percentile	≤ 65.6
50th percentile	≤ 63.5
40th percentile	≤ 60.4
30th percentile	≤ 55.8
20th percentile	≤ 52.7
10th percentile	≤ 47.1

C

Collagen 1 µg/mL	
Percentile	**Percentage aggregation (%)**
90th percentile	≤ 79.9
80th percentile	≤ 75.2
70th percentile	≤ 69.1
60th percentile	≤ 66.6
50th percentile	≤ 65.5
40th percentile	≤ 64.0
30th percentile	≤ 57.3
20th percentile	≤ 57.0
10th percentile	≤ 53.0

D

Collagen 3 µg/mL	
Percentile	**Percentage aggregation (%)**
90th percentile	≤ 77.8
80th percentile	≤ 74.6
70th percentile	≤ 70.0
60th percentile	≤ 70.0
50th percentile	≤ 66.5
40th percentile	≤ 65.0
30th percentile	≤ 63.6
20th percentile	≤ 57.2
10th percentile	≤ 55.1

E

TRAP-6 25 µM	
Percentile	**Percentage aggregation (%)**
90th percentile	≤ 79.7
80th percentile	≤ 73.0
70th percentile	≤ 69.8
60th percentile	≤ 65.6
50th percentile	≤ 65.0
40th percentile	≤ 64.4
30th percentile	≤ 60.5
20th percentile	≤ 55.6
10th percentile	≤ 54.0

F

U46619 3 µM	
Percentile	**Percentage aggregation (%)**
90th percentile	≤ 81.5
80th percentile	≤ 71.8
70th percentile	≤ 70.1
60th percentile	≤ 67.0
50th percentile	≤ 66.0
40th percentile	≤ 65.0
30th percentile	≤ 61.9
20th percentile	≤ 54.6
10th percentile	≤ 53.0

G

Epinephrine 10 µM	
Percentile	**Percentage aggregation (%)**
90th percentile	≤ 76.9
80th percentile	≤ 74.6
70th percentile	≤ 66.7
60th percentile	≤ 65.2
50th percentile	≤ 60.5
40th percentile	≤ 42.8
30th percentile	≤ 13.9
20th percentile	≤ 5.60
10th percentile	≤ 3.20

H

Ristocetin 1.5 mg/mL	
Percentile	**Percentage aggregation (%)**
90th percentile	≤ 87.2
80th percentile	≤ 77.4
70th percentile	≤ 72.8
60th percentile	≤ 68.8
50th percentile	≤ 68.0
40th percentile	≤ 66.4
30th percentile	≤ 64.4
20th percentile	≤ 62.6
10th percentile	≤ 57.4

Figure 6.4 LTA aggregation responses for twenty healthy controls: percentile tables

Percentage final aggregation responses measured using LTA in response to arachidonic acid (A), ADP (B), collagen (C and D), TRAP-6 (E), U46619 (F), epinephrine (G) and ristocetin (H). Results for PRP prepared from twenty healthy control subjects.

6.3.2 Determining control curves for Optimul plate measured platelet aggregation in response to various agonists

The Optimul plate assay, as described in 3.2.7, was used to determine aggregation responses for twenty healthy control samples in order to produce reference percentiles to compare the bleeding disorder patient samples. PRP was stimulated in the pre-prepared 96 well plates and percentile ranges produced for aggregation in response to multiple concentrations of arachidonic acid 0.03-40 μM (Figure 6.5 A), ADP 0.005-40 μM (Figure 6.5 B), collagen 0.01-40 μg/mL (Figure 6.5 C), epinephrine 0.0004-10 μM (Figure 6.5 D), ristocetin 0.14-4 mg/mL (Figure 6.5 E), TRAP-6 0.03-40 μM (Figure 6.5 F) and U46619 0.055-40 μM (Figure 6.5 G).

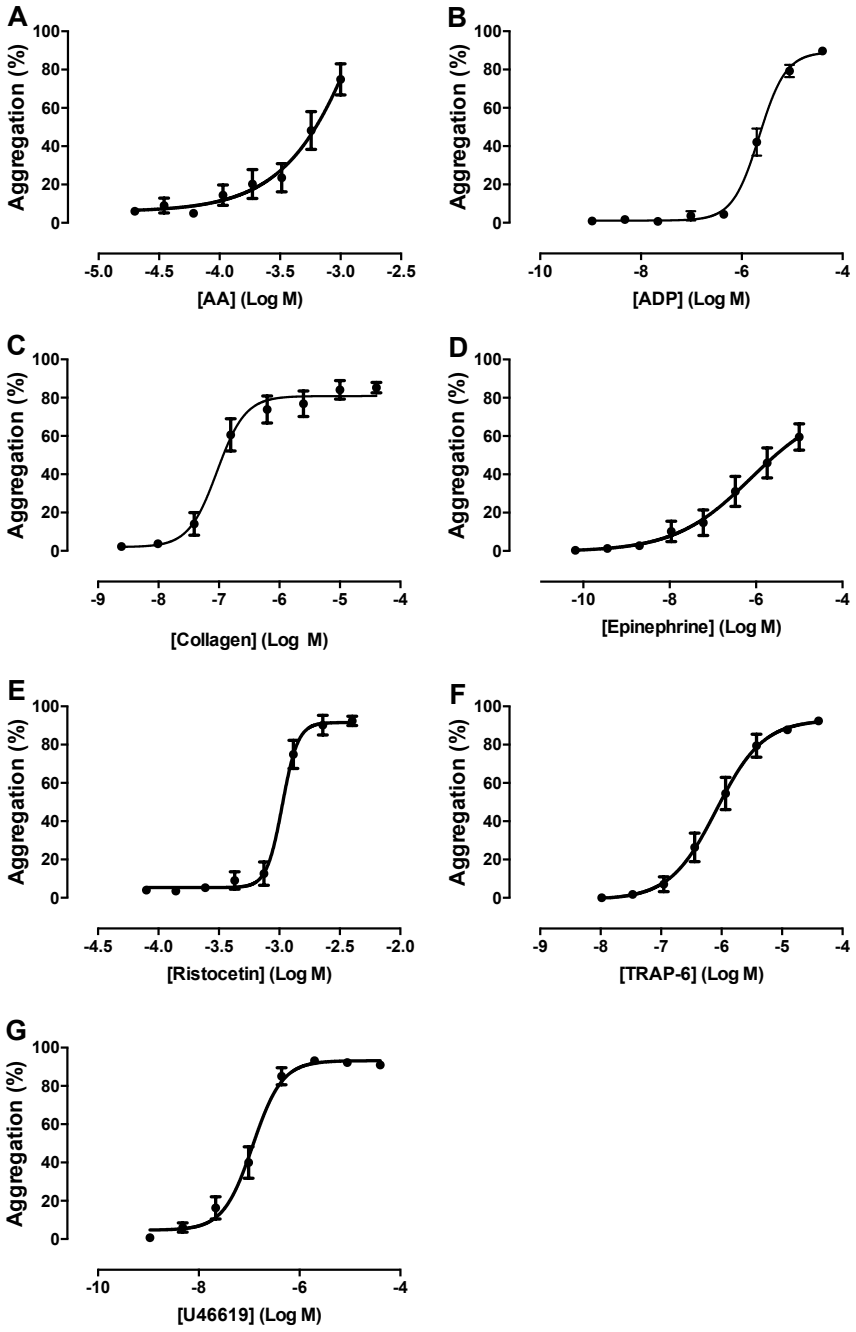

Figure 6.5 Optimul plate aggregation response curves for twenty healthy controls

Percentage final aggregation responses measured using the Optimul plate assay in response to concentration ranges of arachidonic acid (A), ADP (B), collagen (C), epinephrine (D), ristocetin (E) TRAP-6 (F) and U46619 (G) Results for PRP prepared from twenty healthy control subjects.

6.3.3 Determining control ranges for ATP release measured in response to various agonists

A luminescence aggregometry assay, as described in 5.2.4, was used to determine maximum ATP release values in order to generate reference percentiles to compare bleeding disorder patient samples. Percentile ranges were produced for ATP release in response to arachidonic acid 1 mM (Figure 6.6 A, Figure 6.7 A), ADP 10 µM (Figure 6.6 B, Figure 6.7 B), collagen 3 µg/mL (Figure 6.6 C, Figure 6.7 C) and TRAP-6 25 µM (Figure 6.6 D, Figure 6.7 D).

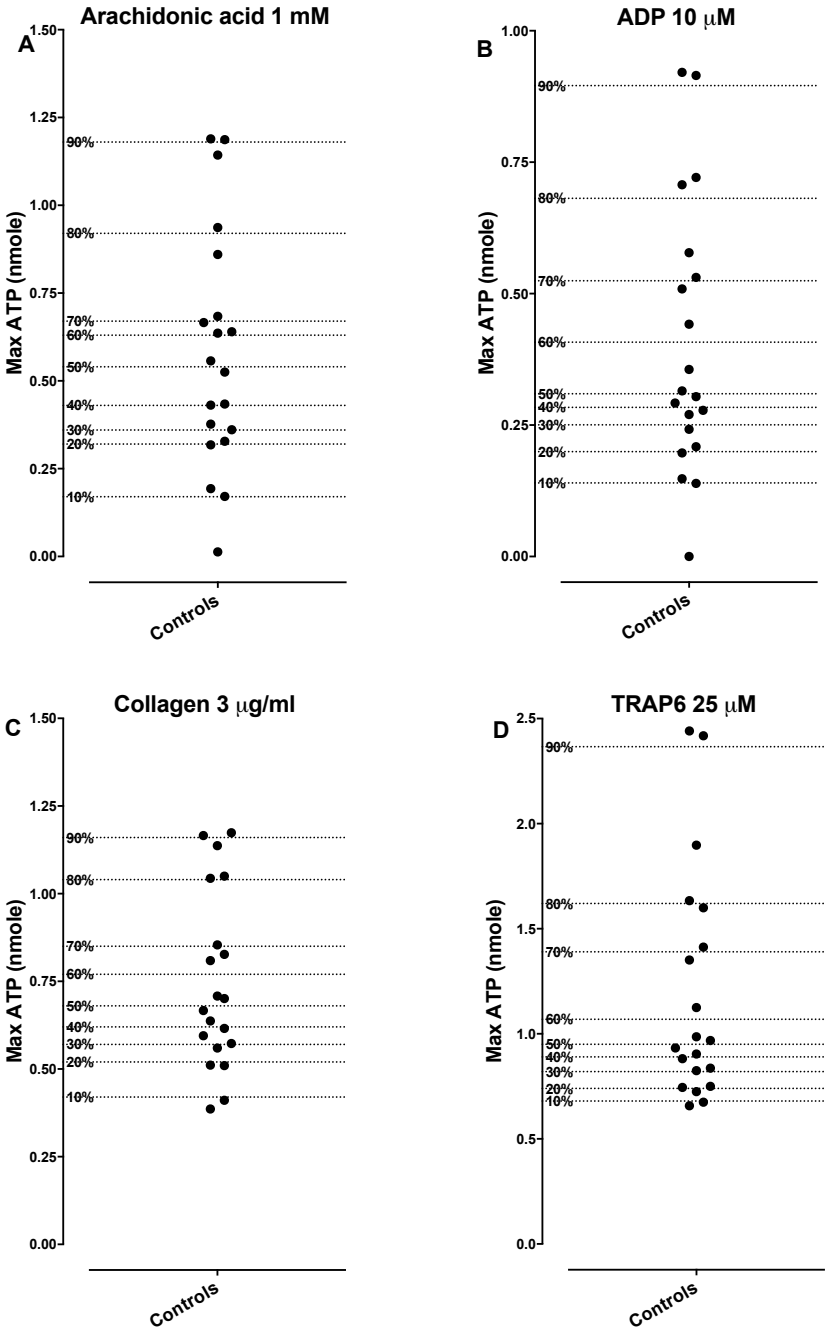

Figure 6.6 Agonist stimulated ATP release for twenty healthy controls

Max ATP release (nmol) in response to arachidonic acid (A), ADP (B), collagen (C) and TRAP-6 (D). Results displayed as individual data points for each control with overlaid percentile indicators (dotted lines).

A

Arachidonic acid 1 mM	
Percentile	**Max ATP release (nmoles)**
90th percentile	≤ 1.18
80th percentile	≤ 0.92
70th percentile	≤ 0.67
60th percentile	≤ 0.638
50th percentile	≤ 0.54
40th percentile	≤ 0.43
30th percentile	≤ 0.36
20th percentile	≤ 0.32
10th percentile	≤ 0.17

B

ADP 10 µM	
Percentile	**Max ATP release (nmoles)**
90th percentile	≤ 0.90
80th percentile	≤ 0.68
70th percentile	≤ 0.52
60th percentile	≤ 0.41
50th percentile	≤ 0.31
40th percentile	≤ 0.28
30th percentile	≤ 0.25
20th percentile	≤ 0.20
10th percentile	≤ 0.14

C

Collagen 3 µg/mL	
Percentile	**Max ATP release (nmoles)**
90th percentile	≤ 1.16
80th percentile	≤ 1.04
70th percentile	≤ 0.85
60th percentile	≤ 0.77
50th percentile	≤ 0.68
40th percentile	≤ 0.62
30th percentile	≤ 0.57
20th percentile	≤ 0.52
10th percentile	≤ 0.42

D

TRAP-6 25 µM	
Percentile	**Max ATP release (nmoles)**
90th percentile	≤ 2.37
80th percentile	≤ 1.62
70th percentile	≤ 1.39
60th percentile	≤ 1.07
50th percentile	≤ 0.95
40th percentile	≤ 0.89
30th percentile	≤ 0.82
20th percentile	≤ 0.74
10th percentile	≤ 0.68

Figure 6.7 Agonist stimulated ATP release for twenty healthy controls: percentile tables

Max ATP release (nmol) measured using a lumi aggregometer in response to arachidonic acid (A), ADP (B), collagen (C) and TRAP-6 (D). Results for PRP prepared from twenty healthy control subjects.

6.3.4 Determining control ranges for whole blood P-selectin expression measured in response to various agonists

A whole blood flow cytometric assay for the determination of platelet surface P-selectin (CD62P) expression, as described in 5.2.5, was used to determine mean florescence intensity values for P-selectin in order to produce reference percentiles against which to compare the bleeding disorder patient samples. Whole blood was stimulated in the wells of a 96 well plate containing the agonist and percentile ranges were produced for P-selectin expression in response to vehicle (Figure 6.8 A, Figure 6.9 A), ADP 40 μM (Figure 6.8 B, Figure 6.9 B), U46619 0.5 μM (Figure 6.8 C, Figure 6.9 C) or ADP 40 μM + U46619 0.5 μM (Figure 6.8 D, Figure 6.9 D).

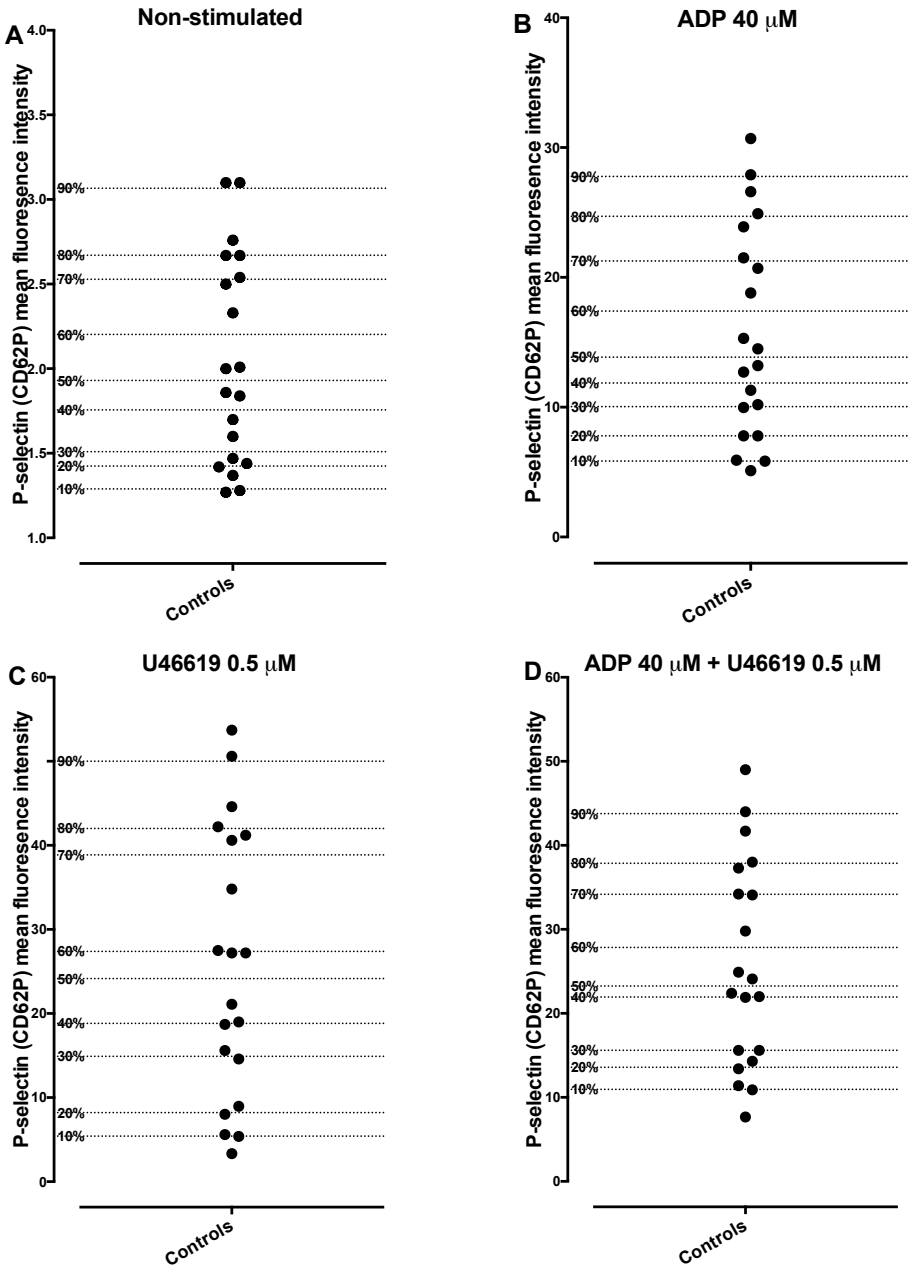

Figure 6.8 Agonist stimulated surface P-selectin expression for twenty healthy controls

Mean fluorescence intensity values of platelet surface P-selectin expression in samples treated with vehicle (non-stimulated, A), ADP (B), U46619 (C) or ADP+U46619 (D) measured using a flow cytometric assay. Results displayed as individual data points for each control with overlaid percentile indicators (dotted lines).

A

Non Stimulated	
Percentile	**Mean fluoresence intensity**
90th percentile	≤ 3.07
80th percentile	≤ 2.67
70th percentile	≤ 2.53
60th percentile	≤ 2.20
50th percentile	≤ 1.93
40th percentile	≤ 1.76
30th percentile	≤ 1.51
20th percentile	≤ 1.42
10th percentile	≤ 1.29

B

ADP 40 µM	
Percentile	**Mean fluoresence intensity**
90th percentile	≤ 27.77
80th percentile	≤ 24.70
70th percentile	≤ 21.26
60th percentile	≤ 17.40
50th percentile	≤ 13.85
40th percentile	≤ 11.86
30th percentile	≤ 10.04
20th percentile	≤ 7.79
10th percentile	≤ 5.85

C

U46619 0.5 µM	
Percentile	**Mean fluoresence intensity**
90th percentile	≤ 50.00
80th percentile	≤ 42.00
70th percentile	≤ 38.86
60th percentile	≤ 27.38
50th percentile	≤ 24.15
40th percentile	≤ 18.82
30th percentile	≤ 14.90
20th percentile	≤ 8.21
10th percentile	≤ 5.41

D

ADP + U46619	
Percentile	**Mean fluoresence intensity**
90th percentile	≤ 43.77
80th percentile	≤ 37.86
70th percentile	≤ 34.17
60th percentile	≤ 27.84
50th percentile	≤ 23.25
40th percentile	≤ 21.94
30th percentile	≤ 15.60
20th percentile	≤ 13.58
10th percentile	≤ 10.95

Figure 6.9 Agonist stimulated surface P-selectin expression for twenty healthy controls: percentile tables

Mean fluorescence intensity values of platelet surface P-selectin expression in non-stimulated samples (A) or samples stimulated with ADP (B), U46619 (C) or ADP+U46619 (D) measured using a flow cytometric assay. Results for PRP prepared from twenty healthy control subjects.

6.3.5 LTA measured platelet aggregation – COX-1 mutated family + healthy control percentiles

LTA as described in 5.2.2 was used to determine aggregation responses for the COX-1 mutated index case (386Q; green) and the two parents (394Q; pink and 395O; blue). Each individual was tested in duplicate, by collection of two blood samples on two separate days, and compared to the control percentiles defined in section 6.3.1 (Figure 6.10).

In response to arachidonic acid index 386Q and parent 394Q had final percentage aggregation values that fell below the 10^{th} percentile of healthy control responses, parent 395O fell below the 50^{th} percentile (Figure 6.10 A). In response to ADP index 386Q fell below the 10^{th} percentile, parent 394Q fell below the 20^{th} percentile and parent 395O fell below the 50^{th} percentile (Figure 6.10 B). In response to low concentration collagen index 386Q and parent 394Q fell below the 10^{th} percentile whereas parent 395O fell below the 20^{th} percentile (Figure 6.10 C). In response to the higher concentration of collagen index 386Q and parent 394Q still fell below the 10^{th} percentile whereas parent 395O fell below the 60^{th} percentile (Figure 6.10 D). In response to TRAP-6 index 386Q fell below the 40^{th} percentile and both parents 394Q and 395O fell below the 80^{th} percentile (Figure 6.10 E). In response to U46619 index 386Q and parent 394Q fell below the 40^{th} percentile whereas parent 395O fell below the 70^{th} percentile (Figure 6.10 F). In response to epinephrine index 396Q fell below the 10^{th} percentile and both parents fell below the 30^{th} percentile (Figure 6.10 G). In response to ristocetin index 386Q fell below the 10^{th} percentile, parent 394Q fell below the 50^{th} percentile and parent 395O fell below the 80^{th} percentile (Figure 6.10 H).

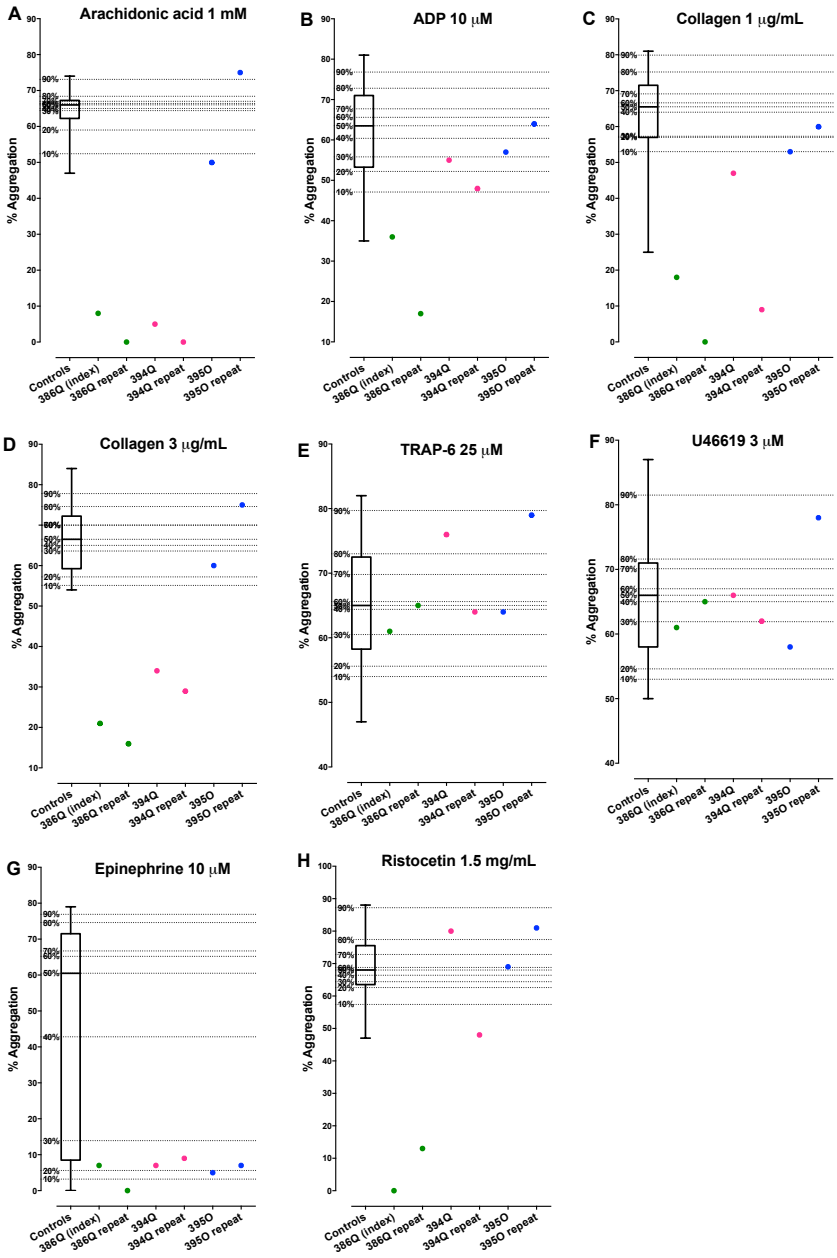

Figure 6.10 LTA aggregation responses – COX-1 mutated family + healthy control percentile

Percentage final aggregation responses measured using LTA in response to arachidonic acid (A), ADP (B), collagen (C and D), TRAP-6 (E), U46619 (F), epinephrine (G) and ristocetin (H). Results displayed as a box and whisker plot with overlaid percentile indicators (dotted lines) or as duplicates for each patient, index 386Q (green), parent 394Q (pink) and parent 395O (blue).

6.3.6 Optimul plate measured platelet aggregation – COX-1 mutated family + healthy controls

As each family member was only tested one using this assay, it is not possible to statistically compare the compare the curves and so the Log EC50 values are displayed in a separate table (Table 6.1). However descriptions of the curves are as follows; in response to arachidonic acid index 386Q and parent 394Q had reduced aggregation responses to the highest four concentrations of agonist used (Figure 6.11 A). In response to ADP index 386Q had a reduced response to the highest concentration of agonist used (Figure 6.11 B). In response to collagen index 386Q and parent 394Q showed rightward and downward shifts in their aggregation curves indicating that higher concentrations of agonist were required to reach a lower percentage aggregation compared to control, parent 3950 however did reach a comparable maximum aggregation to controls but required a much higher concentration of agonist to achieve this (Figure 6.11 C). In response to epinephrine index 386Q had no response and both parents 394Q and 395O showed reduced responses to the top four concentrations of agonist tested (Figure 6.11 D). All three patients had normal responses to ristocetin (Figure 6.11 E). In response to TRAP-6 both index 386Q and parent 395O displayed normal agonist response curves whereas parent 394Q showed a reduction in percentage aggregation for the top six concentrations of agonist used. All three patients had a reduced response to U46619, indicated by the rightward shift of each curve compared to control. Non-linear regression curves were fitted using GraphPad Prism software for each agonist using the following constraints; bottom ≥ 0 and top ≤ 100.

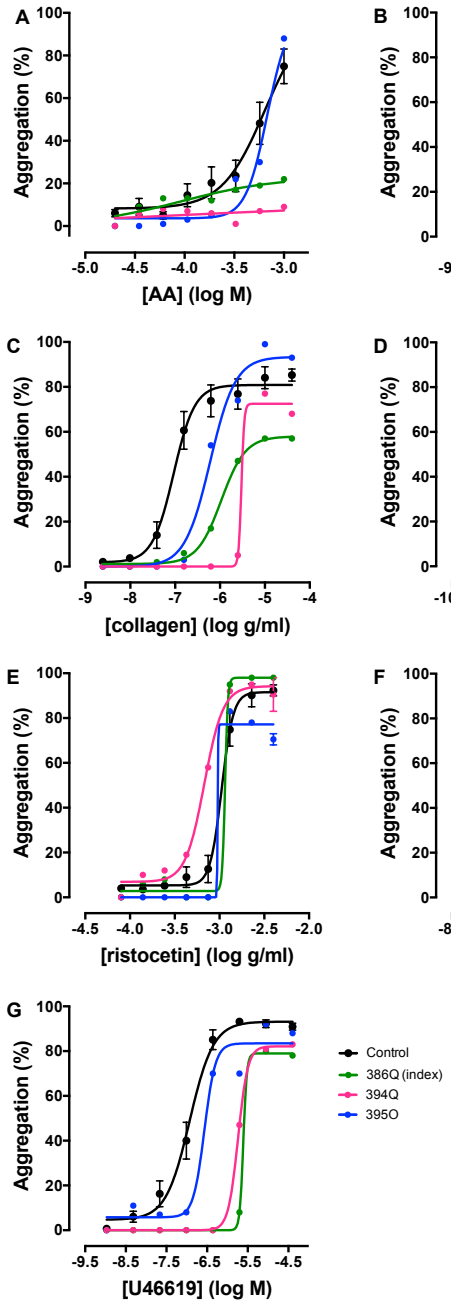

Figure 6.11 Optimul plate aggregation response curves – COX-1 mutated family + healthy control percentile

Percentage final aggregation responses measured using the Optimul plate assay in response to arachidonic acid (A), ADP (B), collagen (C), epinephrine (D), ristocetin (E) TRAP-6 (F) and U46619 (G). Results displayed as individual mean ± SEM for control (black, n=20), index 386Q (green, n=1), parent 394Q (pink, n=1) and parent 395O (blue, n=1).

Agonist	Control Log EC50	Control 95% confidence interval of Log EC50	386Q Log EC50	386Q 95% confidence interval of Log EC50	394Q Log EC50	394Q 95% confidence interval of Log EC50	395O Log EC50	395O 95% confidence interval of Log EC50
Arachidonic acid	-3.19	-3.723 to -2.663	-4.04	-6.250 to -1.830	-4.04	-37.63 to 29.54	-3.17	-3.654 to -2.683
ADP	-5.66	-5.739 to -5.572	-5.58	-5.594 to -5.569	-5.41	-5.410 to -5.405	-5.38	-5.408 to -5.360
Collagen	-7.03	-7.213 to -6.854	-5.97	-6.075 to -5.867	-5.52	Not calculated	-6.22	-6.504 to -5.937
Epinephrine	0.22	-6.733 to -5.497	N/C	Not calculated	N/C	Not calculated	0.50	-8.261 to -5.458
Ristocetin	-2.98	-3.008 to -2.943	-2.94	Not calculated	-3.17	-3.245 to -3.095	-3.02	Not calculated
TRAP-6	-6.08	-6.128 to -6.025	-5.23	-5.231 to -5.229	-5.83	-5.870 to -5.790	-6.12	-6.434 to -5.802
U46619	-6.93	-7.092 to -6.766	-5.61	Not calculated	-5.74	-5.766 to -5.713	-6.57	-7.087 to -6.047

Table 6.1 Optimul data EC50 values and 95% confidence intervals obtained from COX-1 mutated family and healthy controls

EC50 values and 95% confidence intervals for the non-linear regression curves fitted to the Optimul data comparing percentage aggregation of PRP samples obtained from the COX-1 mutated family members (386Q, 394Q, 395O) and 20 healthy controls.

6.3.7 Measuring ATP release – COX-1 mutated family + healthy controls

In response to arachidonic acid stimulation index 386Q and parent 395O showed maximum ATP releases that fell below the 10th percentile of healthy control responses whereas parent 394Q had an average response falling below the 50th percentile (Figure 6.12 A). In response to ADP index 386Q falls below the 30th percentile whereas both parents 395Q and 395O fall below the 10th percentile (Figure 6.12 B). In response to collagen index 386Q and parent 394Q fall below the 10th percentile whereas on average parent 395O falls below the 60th percentile (Figure 6.12 C). In response to TRAP-6 agonist stimulation index 386Q falls below the 30th percentile, parent 394Q falls below the 40th percentile and parent 395O falls below the 10th percentile (Figure 6.12 D).

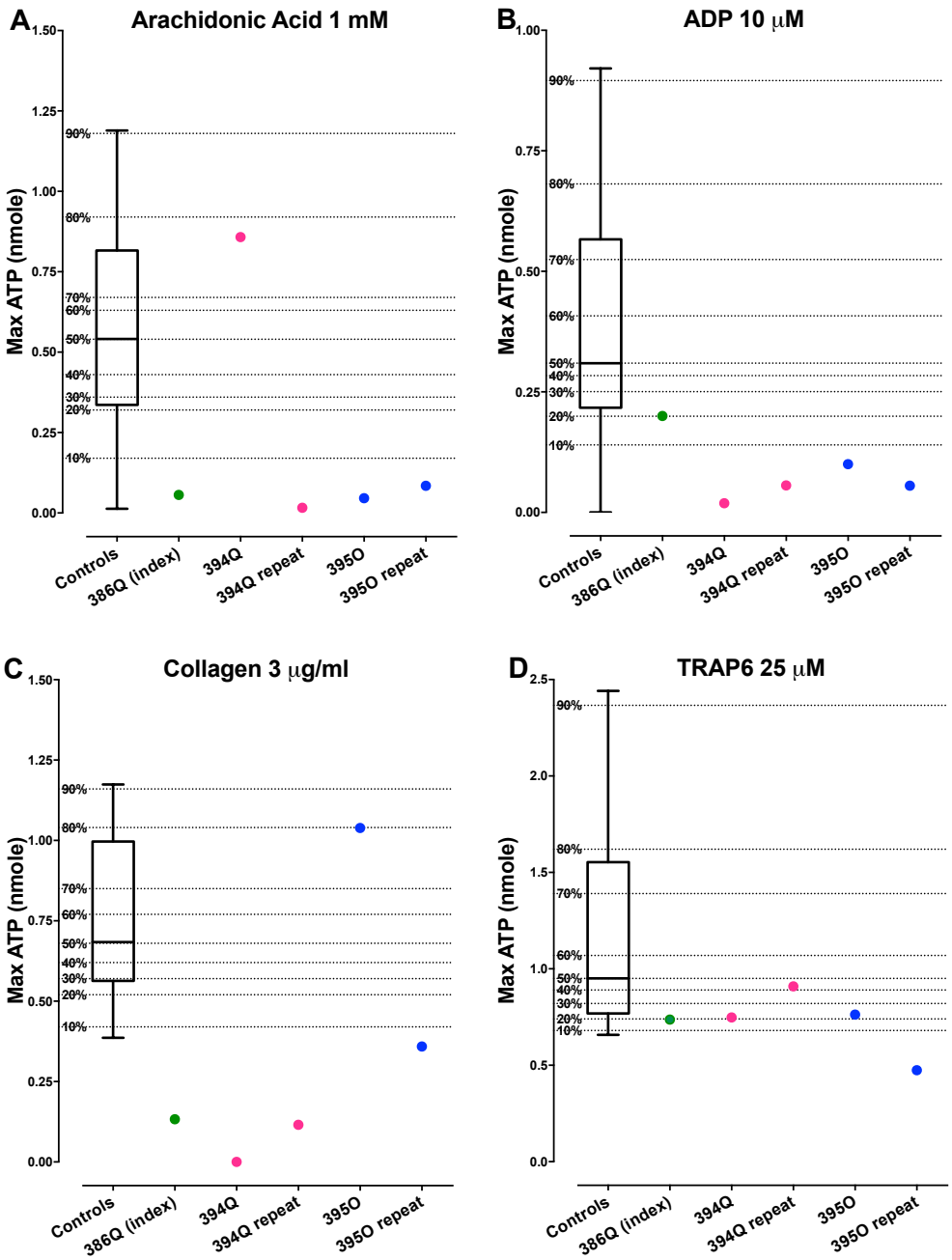

Figure 6.12 Agonist stimulated ATP release – COX-1 mutated family + healthy controls

Max ATP release (nmol) measured using a lumi aggregometer in response to arachidonic acid (A), ADP (B), collagen (C) and TRAP-6 (D). Results displayed as a box and whisker plot for each control with overlaid percentile indicators (dotted lines). Index case in duplicate (green), parent 394Q in duplicate (pink) and parent 395O in duplicate (blue).

6.3.8 Flow cytometric measurement of P-selectin expression – COX-1 mutated family + healthy controls

Basal P-selectin expression varied between samples taken from the same patient on different days. If averaged samples from all three patients produced P-selectin mean fluorescence intensity values that fell above the 60th percentile and below the 80th percentile (Figure 6.13 A). In response to stimulation with ADP index 386Q and parent 395O fell below the 70th percentile whilst parent 389Q fell below the 80th percentile (Figure 6.13 B). In response to U46619 index 386Q fell below the 30th percentile whilst both parents fell below the 60th percentile (Figure 6.13 C). In response to ADP + U46619 386Q index fell below the 70th whilst both parents fell below the 60th percentiles for P-selectin mean fluorescence intensity (Figure 6.13 D).

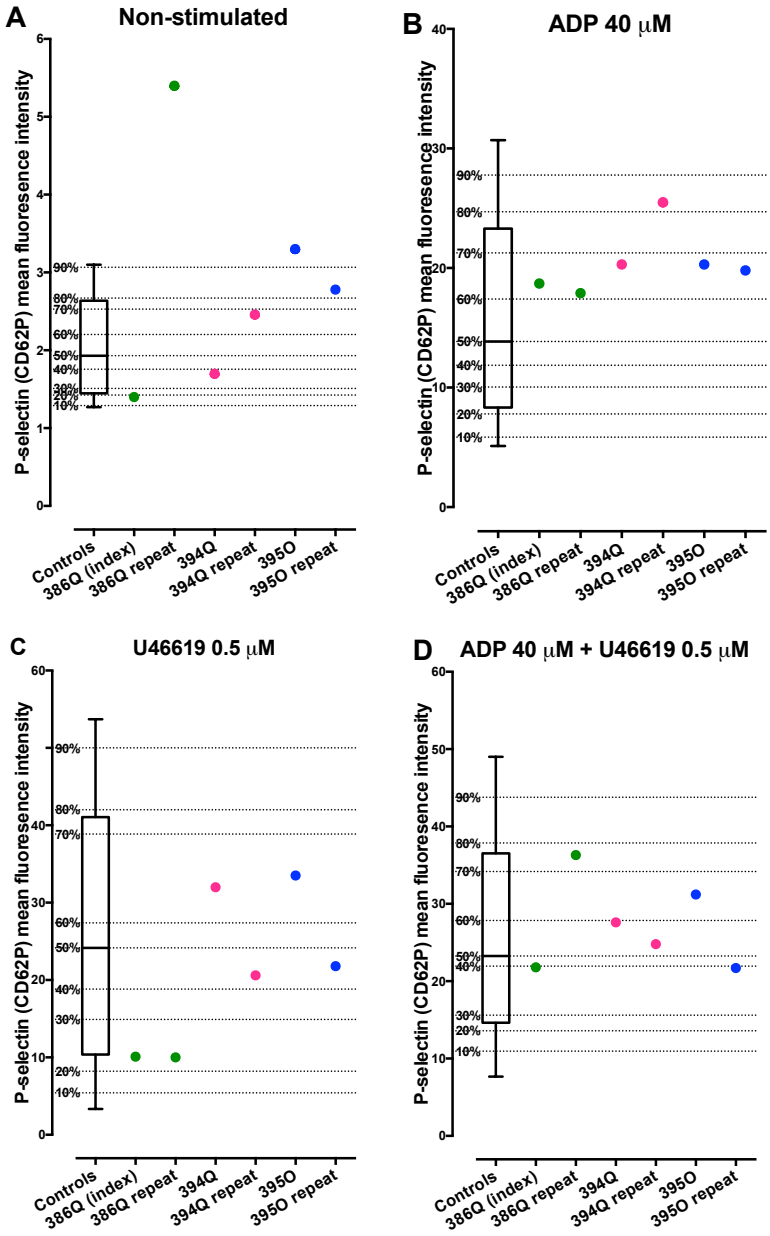

Figure 6.13 Agonist stimulated surface P-selectin expression – COX-1 mutated family + healthy controls

Mean fluorescence intensity values of platelet surface P-selectin expression in samples treated with vehicle (A), ADP (B), U46619 (C) or ADP+U46619 (D) measured using a flow cytometric assay. Results displayed as a box and whisker plot for control with overlaid percentile indicators (dotted lines) and as duplicate values for index case 386Q (green), parent 394Q (pink) and parent 395O (blue).

6.3.9 Comparing agonist stimulated arachidonic acid metabolite release from the COX-1 mutated index case compared to healthy controls

Marked decreases in the production of thromboxane B_2 (Figure 6.14 A), prostaglandin D_2 (Figure 6.14 B), prostaglandin E_2 (Figure 6.14 C), 11-HETE (11-hydroxy-5,8,12,14-eicosatetraenoic acid) (Figure 6.14 D) and 15-HETE (15-hydroxy-5,8,12,14-eicosatetraenoic acid) (Figure 6.14 F) in response to collagen (30 µg/mL) or TRAP-6 (25 µM) were detected between samples from the COX-1 mutated patient and controls. There was no difference seen in the production of 12-HETE (Figure 6.14 E) (12-hydroxy-5,8,12,14-eicosatetraenoic acid) between patient and controls.

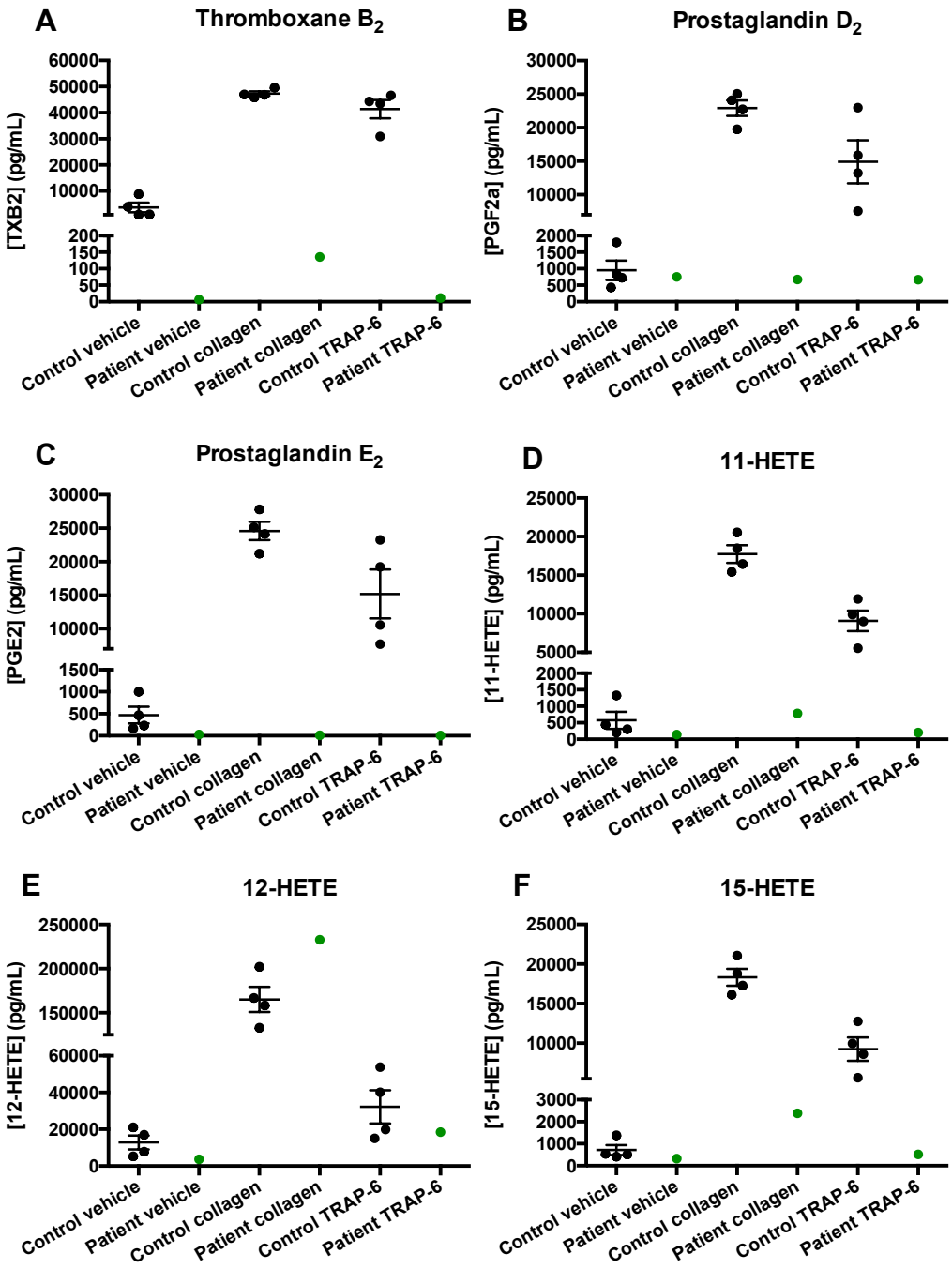

Figure 6.14 LC-MS/MS analysis of select arachidonic acid metabolite release from agonist stimulated whole blood

Data presented as mean ± SEM n=4 for control, n=1 for index patient.

6.3.10 Confocal microscopy imaging of COX-1 protein expression

There was no significant difference seen between COX-1 staining intensity between patient and control samples (Figure 6.15). The mean fluorescence intensity value of COX-1 staining for control platelets was 24.71±1.30 and for patient platelets 23.99±1.53. A t-test was used to determine significance (p=0.05).

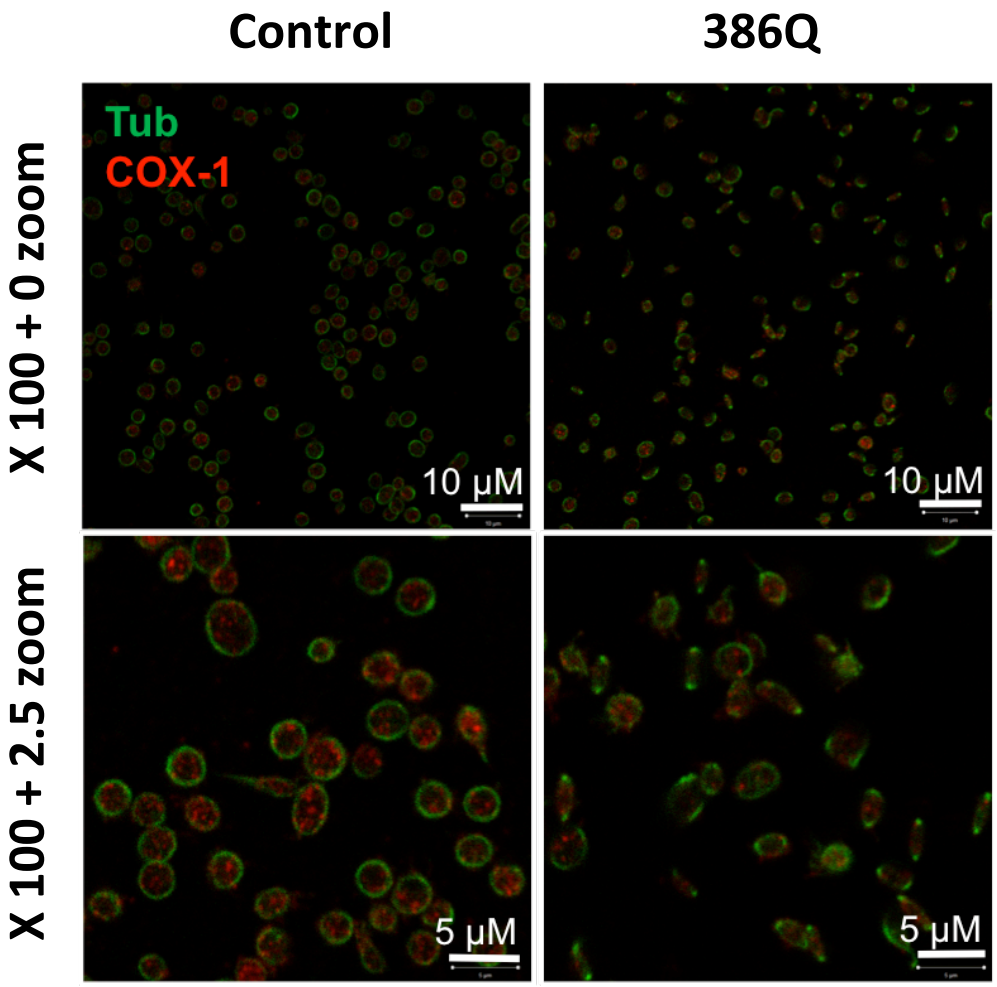

Figure 6.15 Representative confocal images for COX-1 expression in platelets from index patient and a healthy control subject

Representative images from confocal microscopy of platelet tubulin (green) and COX-1 (red) protein expression in platelets obtained from a healthy control (left panels) and from the COX-1 mutated patient (386Q) (right panels) using a x100 oil immersion lens alone (top panels) and a 2.5 zoom (bottom panels). Scale bars = 10 or 5 µM.

6.4 Discussion

In the UK rare diseases affect roughly 1 in 17 people at some point in their lives, and if left undiagnosed 30% of individuals with a rare disease will die before their fifth birthday. In an effort to tackle this The National Institute for Health Research (NIHR) set up the NIHR BioResource which aims to establish a comprehensive BioResource of participants with rare diseases, and their relatives, in order to identify the cause of disease and to improve the rate of diagnosis [229]. The BRIDGE-BPD consortium feeds in to the NIHR BioResource and features a network of clinicians and researchers who are specifically working towards understanding better the causes of rare bleeding and platelet disorders by using next generation sequencing technologies in combination with tailored in-depth phenotyping (Figure 6.16).

As part of the BRIDGE-BPD consortia I obtained patient samples in order to specifically test whether their bleeding disorders could be in part explained by abnormalities in platelet function. In order to test multiple aspects of platelet function I used the following platelet assays; traditional light transmission aggregometry using agonist concentrations reflective of those used by the Genotyping and Phenotyping of Platelets (GAPP) study [230,231] to assess platelet aggregation, the Optimul plate assay to assess platelet aggregation across full concentration ranges of standard platelet agonists, luciferin-luciferase based luminescence aggregometry to assess platelet ATP release, and flow cytometric measurement of surface P-selectin expression to assess platelet activation. If the patient sample reponses appeared abnormal after these experiments further liquid chromatography tandem mass spectrometry to assess platelet arachidonic acid derived lipid content and confocal microscopy imaging to assess protein expression was performed.

For all of these assays it was necessary to produce control data sets of samples from healthy volunteers to provide a reference range against which to compare the patient results. Owing to the fact that each patient

was an individual n=1 it was not possible to determine statistically the difference between the patient values and the control set. Consequently the most appropriate way to express the data was to present the control data set in terms of percentiles of the mean and to then assign a percentile value to each patient data point. This provided a means by which each patient could be compared to the control data set.

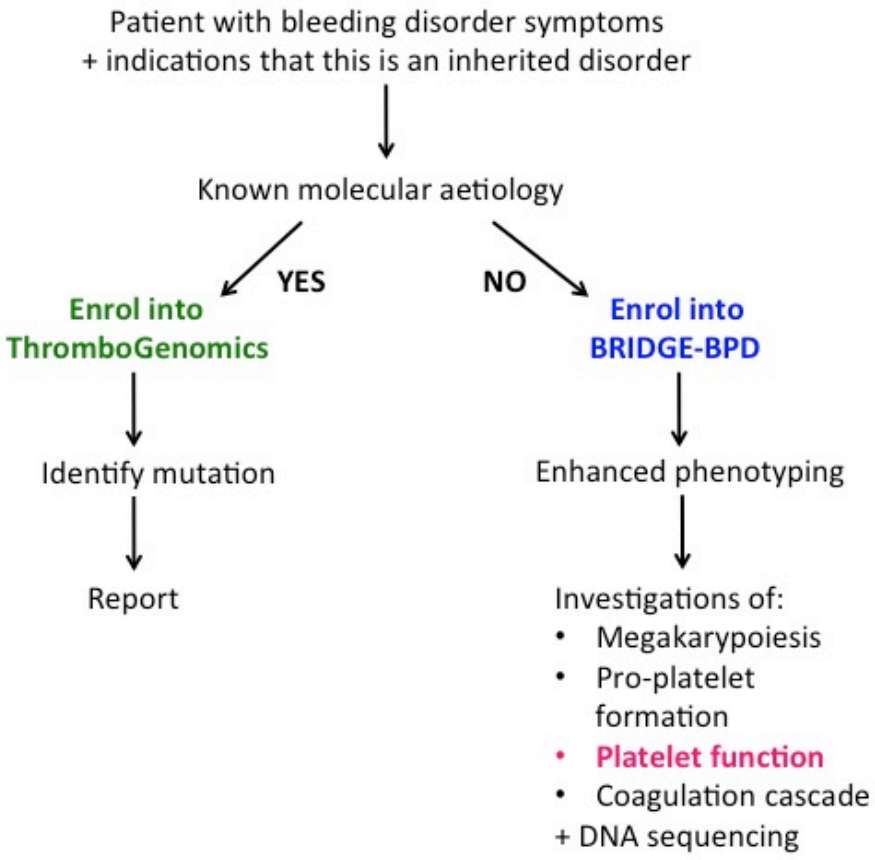

Figure 6.16 Diagram outlining BRIDGE-BPD study investigations

Participants are recruited into the BRIDGE-BPD study (see inclusion/exclusion criteria in section 6.1) for extensive phenotyping and DNA sequencing.

In total I provided in depth platelet phenotyping for 55 individuals of which only two families had a bleeding disorder that appeared to be of platelet origin according to our panel of analyses. This is not surprising as in the UK it is estimated that less than 15% of bleeding disorders are attributable to factors outside of the coagulation cascade. One case, on initial platelet phenotyping, presented with aspirin like LTA traces which were supported by reductions in response to agonists as assessed by the Optimul assay. These results were also seen in parent 394Q but not for parent 395O. When reporting these finding to the consortium we were made aware that the DNA sequencing, performed by the BRIDGE-BPD group in Cambridge, had revealed a homozygous mutation within the PTGS1 gene in the index case and in parent 394Q. Parent 395O was heterozygous for the same mutation.

The PTGS1 gene encodes for the prostaglandin G/H synthase-1 also known as cyclooxygenase-1 (COX-1) enzyme. Once liberated from membrane phospholipids by phospholipase enzymes (see chapter 5), free arachidonic acid becomes the substrate for the COX enzymes of which there are two isoforms; COX-1 and COX-2 [176]. This current investigation is only concerned with the platelet specific action of the COX-1 enzyme. COX-1 is a constitutively expressed enzyme that produces prostanoids mainly involved in normal homeostasis. Through two catalytic steps (Figure 6.1) the enzyme converts arachidonic acid into biologically active prostanoids [177,232]. In the platelet these include TXA_2 functioning to promote platelet aggregation, PGE_2 functioning to promote platelet aggregation at low concentration and to inhibit platelet aggregation at high concentrations and PGD_2 functioning to inhibit platelet aggregation.

The PTGS1 mutation identified in the index case and parent 394Q was a homozygous missense mutation G>C found on chromosome 9 resulting in a tryptophan to serine amino acid change within exon 8. The in-depth platelet function testing I carried out on these patient samples revealed multiple deviations from normal platelet function that appeared in part

similar to results produced by pharmacological inhibition of the COX-1 enzyme by aspirin [233–237].

Light transmission aggregometry results revealed percentage aggregation values that fell below the 10th percentile of the normal range in response to stimulation with arachidonic acid, collagen and epinephrine (Figure 6.10) consistent with the loss of thromboxane A_2 release from the platelet due to COX-1 inhibition. Thromboxane A_2 release is essential to sustain and amplify platelet-activating responses following stimulation by other agonists [206,238].

These results were supported by the Optimul assay with curves showing downwards and/or rightwards shifts for percentage aggregation recorded in response to arachidonic acid, collagen, epinephrine, TRAP-6 and U46619 (Figure 6.11). In addition, there were marked reductions in aggregation in response to ADP in both assays suggesting that this patient may have another form of platelet dysfunction acting in combination with the confirmed aspirin-like defect.

Further support also came from measurements of ATP release, used as an indicator of platelet activation, where the responses of platelets from the index patient were below the 20th percentile of the control range for each agonist (Figure 6.12). Lipid release profiles indicate a reduction in all five major platelet COX-1 products measured supportive of a COX-1 inhibition as documented my by group previously. Levels of 12-HETE remained unchanged between the patient and control groups as this eicosanoid is not a platelet COX-1 product (Figure 6.14) [239]. In order to test statistically the significance of these results more patient samples need to be tested.

The mutation had no observable effect on COX-1 protein expression as determined by confocal microscopy (Figure 6.15) indicating that the changes to platelet function observed cannot be attributed to decreased protein levels. However this data is in opposition to western blot analyses

carried by BRIDGE-BPD consortium partners in Leuven who show almost total absence of the COX-1 protein. Replicates are needed for both assays in order to definitively determine the effects the mutation has on COX-1 protein expression. Furthermore qRT-PCR quantification of COX-1 mRNA expression needs to be carried out in order to assess the impact the mutation may be having at an mRNA level. In addition it would be interesting to collect urine samples from each family member and to use an ELISA kit to look for various eicosanoid metabolites such as the thromboxane B_2 – the stable metabolite of thromboxane A_2 cleared in urine. Such kits are commercially available, easy to use and would help to clarify the contradicting protein expression data. Alternatively LC-MS/MS could be used on the urine samples to identify all potential eicosanoid metabolites present in the sample [240].

Interestingly the index case also fell below the 10th percentile for percentage aggregation in response to ristocetin on the LTA assay (Figure 6.10 H) and the Optimul curve for ristocetin displayed a downward shift (Figure 6.11 E). This could indicate that as well as having an aspirin-like defect the index patient might also have a mild form of von Willebrand's disease (vWD). vWD usually results from a deficiency and/or abnormality of von Willebrand Factor (vWF) and is the most frequently diagnosed bleeding disorder [241–243]. The main role of vWF is to promote the adhesion of platelets to the subendothelium via the platelet glycoprotein Ib receptor and to facilitate platelet-platelet interactions via the platelet glycoprotein IIb/IIIa receptor. These events lead to the formation of a stable platelet plug functioning to stop bleeding at the site of injury [244,245]. Absent or defective vWF would therefore produce bleeding symptoms. Reduced measures of ristocetin induced platelet agglutination are used clinically to diagnose vWD and to distinguish from other defects of platelet aggregation [242,246]. The idea that the index patient may have a mild form of vWD in addition to the COX-1 mutation is supported by her history of bleeding symptoms (haemoptysis, epistaxis, peri-operative bleeding and a tendency to bruise easily) that would not be accounted for by an aspirin-like defect in isolation. Within the platelet

research community there is growing support for the idea that in order to produce the clinical symptoms of a bleeding disorder there must be simultaneous defects affecting both the platelets and the coagulation system. This ‘double hit’ theory implies that a COX-1 mutation alone would be insufficient to cause this particular patient phenotype. Further investigations focussing on the coagulation system need to be undertaken for this patient.

In conclusion, in depth platelet function testing tailored to individual cases with comparisons to robust control data sets are essential for the diagnosis of platelet bleeding disorders and for guiding DNA/RNA sequencing investigations for the identification of causal mutations. Using this approach I phenotyped 55 individuals who reported bleeding symptoms with unknown molecular aetiology. Following on from this I focussed particularly upon one family who had a confirmed mutation to the PTGS1 gene encoding for the COX-1 enzyme and found significant impairments in platelet function closely resembling an aspirin-like defect for the index case which were also reflected in the parent 394Q data. In addition to this the index case also has indications of a mild vWD that could also be contributing to her bleeding tendency. This chapter clearly shows the benefit of combining deep phenotyping with next generation sequencing to understand the causation of bleeding disorders.

Chapter 7 - General Discussion

Platelets play an active part in a diverse range of biological processes and are associated with multiple disease states [247]. The striking observations that less than one 20th of the total platelet population is required to prevent bleeding [248], that platelet granules contain a diverse range of mediators [249] and that platelet surface receptors exist with no obvious link to haemostasis have led many researchers to investigate platelet functions beyond haemostasis [250,251]. As such more attention is being given to the role of less appreciated features of platelet biology, such as platelet RNA species, in an attempt to better define mechanisms determining platelet function. Consequentially, and with the advent of powerful next generation sequencing technologies, both human and mouse platelet transcriptomes data sets were published in their entirety and made publically available resources back in 2011 [54]. Since then there have been multiple studies providing evidence to support the idea that platelet mRNA expression profiles are altered in human disease [77,252,253]. In light of these studies, further investigations focussing on platelet mRNA have the potential to provide new sights into platelet function and so aid the discovery of novel biomarkers of disease.

The importance and clinical utility of studying platelet RNA has been made evident with the launch of Illumina's new daughter company GRAIL [254]. GRAIL is a life science company that aims to detect cancer before a patient is symptomatic through deep sequencing of circulating tumour DNA/RNA found within blood plasma [255]. With financial backing from the likes of Bill Gates and Jeff Bezos and with clinical trails underway there is a lot of excitement surrounding Illumina's new venture. It is relevant to highlight that prior to the development of GRAIL the research group of Thomas Wurdinger at VU University in Amsterdam had published extensively on the ability of platelets to take up RNA species from other cell types and subsequently then on the use of platelet RNA signatures for the detection of cancer [88,256,257]. In turn Thomas Wurdinger formed a company called ThromboDX which was later purchased by Illumina for €70 million in 2017 with the aim of integrating the company's

platelet-powered technology into the deep sequencing platforms being developed at GRAIL.

The study of platelet RNA relies fundamentally on the ability to isolate platelets from whole blood. For platelet RNA analysis it is essential that contamination of samples by other nucleated cell types with very much larger quantities of RNA, such as white blood cells, is kept to a minimum. It is also important that the isolation technique causes minimal activation to avoid, for instance, losing certain sub-populations in the process. Platelet researchers have described many methods for blood collection and platelet isolation but there is no consensus as to which is best. This wide variation in techniques is probably the major reason why there is so much variability in reports of platelet function testing between different laboratories [258,259]. Thus, comparing the variable aspects of the blood collection methods, in this case anticoagulant selection and choice of blood taking receptacle, was a logic beginning to this thesis. In addition, it was also essential to identify the optimal technique for obtaining a pure platelet population before proceeding onto any experiments requiring the isolation of platelet RNAs and the platelet sub-populations rich in them. Through systematic comparisons using LTA and Optimul plate assays as indicators of platelet function I found that there was no significant difference between any of the anticoagulants or blood receptacles used. Selection of a blood taking method should therefore be guided by the specific assay endpoint, for example sodium citrate may alter in vitro platelet reactivity as it is a calcium chelator, as well as by the phlebotomist's personal preference. Following on from this I showed that simple single step centrifugation of whole blood to obtain PRP produces a large reduction in contaminating white blood cell number and RNA content as measured using flow cytometry and qRT-PCR. This reduction equates to roughly a 500-fold decrease that is only further enriched around 11-fold through the use of additional syringe filtering or MACS sorting techniques. This extra enrichment is negated by the potential for platelet activation caused by these more involved protocols. Importantly the simple production of PRP requires much less labour and expense

than more involved techniques making it a suitable method for use in larger population based studies or when testing multiple family members.

The optimisation of a protocol for platelet isolation then allowed me to investigate a platelet sub-population assumed to be both rich in RNA and to be more reactive [260]. These so called newly formed reticulated platelets can be identified from the general platelet population using the nucleic acid binding dye thiazole orange with the idea being that reticulated platelets will stain brighter for thiazole orange than other platelet sub-populations because they contain greater amounts of RNA [104]. The non-specific nature of thiazole orange however means that all RNA species, not just mRNA, and free nucleotides in platelet granules will all be stained. This factor has led to some disagreement within the field prompting investigators to question whether thiazole orange based analyses may be skewed by the potential for larger and more granular platelets to take up more dye [261]. This concern can in part be overcome by stimulating platelets to release their granule content, but this technique is not suitable if one wants to preserve platelet function for testing in other assays. In order to address these concerns, I conducted qRT-PCR experiments on flow cytometric cell sorted reticulated, intermediate and non-reticulated platelet subpopulations and showed definitively for the first time that reticulated platelets express significantly more platelet specific mRNA than their non-reticulated counterparts. In addition, other preliminary studies from our group, not documented in this thesis, indicate that there is no significant difference in size between platelets present in reticulated and non-reticulated sub-populations. The production of newer dyes with the ability to bind mRNA species exclusively, perhaps by targeting the poly-A tail, or those that possess the ability to only fluoresce when a certain concentration of RNA is bound would be of great utility to the field.

Establishing a protocol that isolated reticulated platelets whilst preserving their function allowed me then to investigate the reactive potential of this subpopulation in attempt to elucidate some of the mechanisms which

may underpin the link between increased reticulated platelet counts and the occurrence of acute coronary syndrome. Using various platelet function assays modified to work for low concentrations of cell sorted platelets I demonstrate that the reticulated platelet sub-population express higher amounts of surface CD62P and release larger concentrations of ATP in response to agonist stimulation. Additionally, my data indicates that this sub-population shows elevated reactivity during aggregate formation shown through the disproportional recruitment of reticulated platelets into the centre of forming aggregates; a phenomenon that I observed in both cell-sorted samples and in PRP. Despite comprising only 10% of the total platelet count the increased reactivity of reticulated platelets demonstrated in these investigations provide evidence that this sub-population may be a driver of the thrombotic response.

This data supports clinical observations linking increased reticulated platelet counts, not only to the incidence of acute coronary syndrome [262,263], but also to the increased risk of cardiovascular disease in patient populations, such as those with diabetes and chronic kidney disease [100,264,265], whom are known to have increased platelet turnovers and consequentially a greater proportion of reticulated platelets. Understanding the reactive potential of reticulated platelets is also pertinent to the study of antiplatelet therapy regimens especially in patient groups that display high on treatment platelet reactivity. In a paper from our group this year we showed, using samples from patients receiving the most commonly prescribed antiplatelet regimen of aspirin plus the $P2Y_{12}$ inhibitor clopidogrel, that reticulated platelets act as seeds for the formation of aggregates even in the presence of antiplatelet therapies [98]. This observation was directly linked to the emergence of newly formed reticulated platelet sub-population that was not previously exposed to the pharmacological inhibitors owing to the drugs' short pharmacokinetic half-lives. Strikingly this phenomenon was not seen in patients receiving aspirin plus the newer $P2Y_{12}$ inhibitor ticagrelor which is a circulating inhibitor [266]. This study provides a mechanism by which reticulated

platelets may reduce the efficacy of permanently acting but pharmacokinetically short-lasting antiplatelet therapies, notably aspirin plus clopidogrel. The ability of drugs to target reticulated platelets is clearly an important consideration for future antiplatelet therapies and at the level of personalised therapy could be tracked by assays particularly designed to distinguish newly formed reticulated platelets from older non-reticulated platelets. Identifying characteristics more tractable to assay development than RNA content would be a very good way to begin this new phase of anti-platelet prophylaxis.

An interesting future investigation to understand better the mRNA content of reticulated platelets would be to run RNA-Seq experiments comparing transcript expression profiles between reticulated and non-reticulated platelets. This would help to answer the question as to whether reticulated platelets contain more RNA in general or whether they are enriched in specific genes and whether or not those genes are important to pathways involved in platelet activation. The low RNA concentration within individual platelets, it is postulated that older platelets may contain no RNA at all, combined with lengthy cell sorting process limits the application of RNA-Seq for these platelet sub-populations. In the future, improvements in single-cell sequencing technologies that permit sequencing of small cells with low amounts of starting material could solve this problem.

Studies of the reticulated versus non-reticulated platelet proteomes using techniques such as LC-MS/MS would also be beneficial and could help to determine whether an increase in mRNA content equates to increases in protein expression. In addition, the use of newer non-radioactive assays, such as the Click-iT AHA L-azidohomoalanine kit from ThermoFisher, for the evaluation of protein synthesis in vitro could be used to assess the ability of reticulated platelets to translate mRNA into protein. Unfortunately for platelet researchers, a lot of starting material is needed for these types of analyses and these assays require amounts of platelets that would take a considerable time to sort and separate.

Another interesting continuation of the reticulated platelet work would be to use animal models of thrombosis in combination with in vivo labelling of the reticulated and non-reticulated platelet subpopulations. A mechanical/chemical injury promoting thrombus formation could then be applied upon a vessel wall and the resulting thrombus extracted. Microscopy could then be used to ascertain the relative contributions of both reticulated and non-reticulated platelets to the formation of the thrombus. If our in vitro experiments are correct, one would expect to see a greater number of reticulated platelets present in the thrombus and for those reticulated platelets to be forming aggregate cores. Indeed these investigations would compliment work previously published by platelet research groups in Swansea [267–269], Sydney [270,271] and Maastricht [272–275] who have been combining traditional platelet function assays with advanced rheological analyses to understand better the role of platelets in thrombus formation and composition. Together these groups have provided evidence to suggest that thrombus formation occurs in distinct but complimentary stages involving biomechanical processes followed by soluble-agonist dependent mechanisms. They also emphasise the idea that a thrombus contains different subpopulations of platelets that play distinct roles in the processes leading up the formation of a stable blood clot. My in vitro imagestream data contributes to this growing body of evidence showing that aggregates are composed of a heterogeneous mix of platelets whilst helping to further the discussion by suggesting that thrombi may be composed of multiple layers of platelets each with distinct functional capabilities and/or different responsiveness to antiplatelet therapies.

I also would like to have conducted in-depth imaging studies comparing the two subpopulations in order to help identify some of the physical characteristics that may support the differences in reactivity observed. For example, quantification of granule number, content and size as well as quantification of mitochondrial number would have been informative.

A platelets ability to adhere to an injured vessel wall is another essential feature of platelet function, as such assays using fluorescently labelled platelets in whole blood which is then pumped through a microfluidics chamber coated with adhesive proteins such as collagen and fibrinogen can be used to assess the adhesive properties of different platelet samples [276–279]. Although I made many attempts at optimising protocols for comparing the adhesive properties of the reticulated platelet subpopulations I was unable to get the sorted platelets to stick to the adherent surface. More work is needed to develop this method further as it could be used to give more precise detail as to how the different subpopulations behave in the formation of more physiologically relevant aggregates in whole blood.

Following on from the characterisation of RNA rich subpopulations and the optimisation of protocols for platelet isolation and RNA extraction I sought to investigate the relationships between genomic DNA, platelet specific mRNA and platelet function. I was able to achieve this by obtaining blood samples from a patient known to have a homozygous mutation in the PLA2G4A gene causing inactivation of $cPLA_{2\alpha}$ enzymatic activity and using these to carry out both platelet function and RNA-Seq investigations. Using LTA and Optimul plate assay I demonstrate significant reductions in percentage aggregation recorded in response to the platelet agonists ADP, collagen, epinephrine and U46619 as well as reduced ATP release in response to collagen in platelet samples from this patient. These results can be explained by the loss of arachidonic acid derived eicosanoid production, in particular thromboxane A_2, due to non-existent $cPLA_{2\alpha}$ enzymatic function. It is interesting to note that this patient reports no associated symptoms of bleeding despite having a clear platelet dysfunction; this is in contrast to the PTGS1 mutated patient I also reported on who had an extensive history of bleeding symptoms in spite of having a similar platelet phenotype to the PLA2G4A case. This further supports my supposition that the PTGS1 case has an additional mutation, perhaps affecting an aspect of the coagulation cascade, to thus account for her clinical presentation.

Owing to the fact that platelets from the PLA2G4A mutated patient were unable to produce eicosanoids central to platelet function I hypothesised that there may be differences in the selective sorting of mRNAs into platelets by megakaryocytes and so a change in the platelet transcriptome. I anticipated there being a decrease in mRNA transcripts that encode for proteins playing essential roles in eicosanoid driven pathways of platelet activation. To assess this, I defined the platelet transcriptomes of both healthy control platelet samples and PLA2G4A mutated patient platelet samples using RNA-Seq and compared the expression of transcripts detected using differential expression analysis. My results correlated well with other published RNA-Seq experiments. As more studies are conducted data can be pooled to create a more robust data set representative of the 'healthy' platelet transcriptome from which to make comparisons to. Although I found no significant difference in the levels of expression for any transcripts explicitly linked to eicosanoid activity I did find twenty-six other transcripts that were significantly up regulated in the patient samples compared to controls. Of these twenty-six, four (S100A8, S100A9, S100A12 and SLP1) had previously been reported to be associated with aspects of platelet function and/or cardiovascular disease making them interesting candidates for the establishment of novel biomarkers for disease. Future experiments should seek to ascertain whether these up-regulated transcripts translate into increased protein expression. Increasing the sample size in both the control and patient groups would strengthen the analyses however there is some debate as to whether taking multiple samples from the same patients does in reality just equate to a n=1 group size. The use of RNA-Seq in combination with platelet function testing enabled me to assess the impact of genomic mutations on both platelet mRNA content and platelet reactivity, giving a more complete view of the platelet specific consequences caused by loss of $cPLA_{2\alpha}$ activity.

As well as being an informative basic science tool, next generation sequencing techniques can play a major role in the clinic. Indeed, earlier

this year in her annual report entitled ‘Generation Genome’, England’s chief medical officer, Dame Sally Davies, called for NHS services to routinely perform whole genome sequencing on patient blood samples and biopsies. Resources are currently focussed on patients with cancer but will be shared to other areas of medicine once centralised genomic services are established. The report stresses particularly the urgent need for whole genome sequencing for patients with infectious or rare diseases [280,281].

This news bodes well for studies, such BRIDGE-BPD, which have been designed specially to meet the unmet diagnostic needs of those living with rare bleeding disorders. By providing patients with diagnoses for such rare bleeding disorders clinicians will be better equipped to monitor, manage or treat the patients’ symptoms whilst basic scientists will gain novel insights into molecular pathways underling haemostasis, thrombosis and bleeding. The clinical success of such studies relies critically on the ability to combine the sequencing data with in-depth sample phenotyping [282–285]. As such within this thesis I developed a protocol for the phenotyping of platelets from patients with unknown bleeding disorders. This protocol involved multiple platelet function assays which could be scaled according to how many patient samples were collected per day. Importantly I selected assays that could interrogate different aspects of platelet function and that could be modified in response to any clinically relevant information received. Using this individualised approach, I was able to provide in depth platelet phenotyping data that could be paired with the DNA sequencing data to highlight the functional consequences of any mutations found. I demonstrate this process by presenting a case study of a family with a mutation within the PTGS1 gene encoding for the COX-1 enzyme - a protein known to play an essential role in platelet reactivity. My initial phenotyping results using the LTA and Optimul assays revealed a clear aspirin like defect defined by reduced responses to the platelet agonists arachidonic acid, collagen and epinephrine for both the index case and parent 394Q but not for parent 395O. Further investigations revealed

reductions in markers of platelet activation including P-selectin expression and ATP release. Eicosanoid production in response to agonist stimulation was also diminished for the index patient. These findings are consistent with the loss of COX-1 function. DNA sequencing results validated these phenotypic findings, showing that the index case and parent 394Q were both homozygous for the specific PTGS1 mutation. This may also suggest that this mutation may be more prevalent in the Iranian population. To investigate these possibilities the index cases' extended family will also be recruited into the BRIDGE-BPD study for DNA sequencing and platelet function testing.

In addition to the aspirin-like defect I also found reduced aggregation responses to ristocetin indicative of a vWD like defect in the index case. In order to confirm this quantification of vWF levels in the blood using a von Willebrand factor antigen test should be carried out. It will also be important to go back through the DNA sequencing data and to look for any additional mutations that may be occurring within genes known to be associated to vWD. The idea of needing two separate mutations occurring in different genes to produce a clinical bleeding disorder is not a new theory [286] however rigorous supportive in vivo evidence is lacking. The severity of the patients bleeding symptoms also lends support to the idea that a platelet disorder alone would not be enough to cause their particular bleeding defect. Further support for this hypothesis is given by the lack of bleeding phenotype reported for parent 394Q despite them having a clinical aspirin-like phenotype and the same homozygotic mutation. This particular case study clearly illustrates the benefit of combining deep phenotyping with next generation sequencing to understand the causation of bleeding disorders and to provide molecular diagnoses for patients living with unknown bleeding and platelet disorders.

Together the investigations carried out within this thesis highlight the importance of understanding genomic influences that have the potential to impact upon platelet function and to thus provide fresh insights into the

molecular pathways determining platelet reactivity. This thesis provides the tools for conducting such experiments by establishing robust protocols for the isolation of RNA rich platelet sub-populations and for the extraction of mRNA species. Using such protocols will ensure that all platelet sub-populations are represented in downstream investigations of the platelet transcriptome. This thesis also demonstrates the ability of genomic DNA mutations to alter the platelet transcriptome, demonstrated using the PLA2G4A case study, and to have significant effects upon platelet function. The clinical usefulness of such observations will only become evident by combining genomic data with in-depth, clinically tailored, ex vivo platelet phenotyping as highlighted by the PTGS1 case study. This puts us a step further along the path of personalised medicine both for patients with bleeding disorders and for patients requiring safe and effective anti-platelet prophylaxis.

Bibliography

1. Moran JF. The Cardiovascular System at a Glance. Wiley-Blackwell; 2000.
2. Richard E Klabunde. Cardiovascular Physiology Concepts. Wolters Kluwer; 2011.
3. Gale AJ. Current understanding of hemostasis. *Toxicol. Pathol.* 2011;39(1):273–80.
4. Boon GD. An Overview of Hemostasis. *Toxicol. Pathol.* 1993;21(2):170–179.
5. WHO 2014. WHO | The top 10 causes of death. *Fact sheet N°310 (Updated May 2014)*. 2014;
6. Lozano R, Naghavi M, Foreman K, et al. Global and regional mortality from 235 causes of death for 20 age groups in 1990 and 2010: a systematic analysis for the Global Burden of Disease Study 2010. *Lancet (London, England)*. 2012;380(9859):2095–128.
7. British Heart Foundation. CVD Statistics - BHF UK Factsheet. 2015;(Cvd):
8. Brewer DB. Max Schultze (1865), G. Bizzozero (1882) and the discovery of the platelet. *Br. J. Haematol.* 2006;133(3):251–258.
9. Stone MJ. William Osler's legacy and his contribution to haematology. *Br. J. Haematol.* 2003;123(1):3–18.
10. Cooper B. Osler's role in defining the third corpuscle, or "blood plates". *Proc. (Bayl. Univ. Med. Cent).* 2005;18(4):376–8.
11. Mazzarello P, Calligaro AL, Calligaro A. Giulio Bizzozero: a pioneer of cell biology. *Nat. Rev. Mol. Cell Biol.* 2001;2(10):776–784.
12. Ribatti D, Crivellato E. Giulio Bizzozero and the discovery of platelets. *Leuk. Res.* 2007;31(10):1339–1341.
13. Coller BS. Historical perspective and future directions in platelet research. *J. Thromb. Haemost.* 2011;9 Suppl 1(Suppl 1):374–95.
14. Louis DN, Young RH (Robert H, Massachusetts General Hospital. Keen minds to explore the dark continents of disease : a history of

the pathology services at the Massachusetts General Hospital. Massachusetts General Hospital and Havard Medical School; 2011.

15. Machlus KR, Italiano JE. The incredible journey: From megakaryocyte development to platelet formation. *J. Cell Biol.* 2013;201(6):785–796.
16. Thon JN, Montalvo A, Patel-Hett S, et al. Cytoskeletal mechanics of proplatelet maturation and platelet release. *J. Cell Biol.* 2010;191(4):861–74.
17. Tablin F, Castro M, Leven RM. Blood platelet formation in vitro. The role of the cytoskeleton in megakaryocyte fragmentation. *J. Cell Sci.* 1990;97 (Pt 1):59–70.
18. Junt T, Schulze H, Chen Z, et al. Dynamic Visualization of Thrombopoiesis Within Bone Marrow. *Science (80-.).* 2007;317(5845):1767–1770.
19. Thon JN, Italiano JE. Platelet Formation. *Semin. Hematol.* 2010;47(3):220–226.
20. Italiano JE, Lecine P, Shivdasani RA, Hartwig JH, Hartwig JH. Blood platelets are assembled principally at the ends of proplatelet processes produced by differentiated megakaryocytes. *J. Cell Biol.* 1999;147(6):1299–312.
21. Daly ME. Determinants of platelet count in humans. *Haematologica*. 2011;96(1):10–3.
22. Youle RJ, Strasser A. The BCL-2 protein family: opposing activities that mediate cell death. *Nat. Rev. Mol. Cell Biol.* 2008;9(1):47–59.
23. Mason KD, Carpinelli MR, Fletcher JI, et al. Programmed Anuclear Cell Death Delimits Platelet Life Span. *Cell*. 2007;128(6):1173–1186.
24. Sys J, Provan D, Schauwvlieghe A, Vanderschueren S, Dierickx D. The role of splenectomy in autoimmune hematological disorders: Outdated or still worth considering? *Blood Rev.* 2017;31(3):159–172.
25. White JG. Interaction of membrane systems in blood platelets. *Am. J. Pathol.* 1972;66(2):295–312.
26. Ebbeling L, Robertson C, McNicol a, Gerrard JM. Rapid

ultrastructural changes in the dense tubular system following platelet activation. *Blood*. 1992;80(3):718–723.

27. Cerecedo D. Platelet cytoskeleton and its hemostatic role. *Blood Coagul. fibrinolysis*. 2013;24(8):798–808.
28. Michelson AD. Platelets. Elsevier Inc.; 2013.
29. Bergmeier W, Piffath CL, Goerge T, et al. The role of platelet adhesion receptor GPIbalpha far exceeds that of its main ligand, von Willebrand factor, in arterial thrombosis. *Proc. Natl. Acad. Sci. U. S. A.* 2006;103(45):16900–16905.
30. Sangkuhl K, Shuldiner AR, Klein TE, Altman RB. Platelet aggregation pathway. *Pharmacogenet. Genomics*. 2011;21(8):516–21.
31. Clemetson KJ, Clemetson JM. Platelet collagen receptors. *Thromb. Haemost.* 2001;86(1):189–197.
32. Watson SP. Collagen receptor signaling in platelets and megakaryocytes. *Thromb. Haemost.* 1999;82(2):365–76.
33. Lefkovits, Jeffrey; Plow, Edward F.; Topol EJ. Platelet Glycoprotein IIb/IIIa Receptors in Cardiovascular Medicine. *N. Engl. J. Med.* 1995;332(23):1553–1559.
34. Gibbins JM. Platelet adhesion signalling and the regulation of thrombus formation. *J. Cell Sci.* 2004;117(16):3415–3425.
35. Kroeze WK, Sheffler DJ, Roth BL. G-protein-coupled receptors at a glance. *J. Cell Sci.* 2003;116(24):.
36. Dale MM, Ritter JM, Flower RJ, Henderson G, Rang HP. Rang & Dale's Pharmacology. Churchill Livingstone; 2007.
37. Coughlin SR. Thrombin signalling and protease-activated receptors. *Nature*. 2000;407(6801):258–264.
38. Holinstat M, Voss B, Bilodeau ML, et al. PAR4, but not PAR1, signals human platelet aggregation via Ca2+ mobilization and synergistic P2Y12 receptor activation. *J. Biol. Chem.* 2006;281(36):26665–74.
39. Woulfe D, Yang J, Brass L. ADP and platelets: the end of the beginning. *J. Clin. Invest.* 2001;107(12):1503–5.
40. Kunapuli SP, P. S. P2 receptors and platelet activation.

ScientificWorldJournal. 2002;2:424–33.

41. Jin J. Adenosine diphosphate (ADP)-induced thromboxane A2 generation in human platelets requires coordinated signaling through integrin alpha IIbbeta 3 and ADP receptors. *Blood*. 2002;99(1):193–198.
42. Stalker TJ, Newman DK, Ma P, Wannemacher KM, Brass LF. Platelet signaling. *Handb. Exp. Pharmacol.* 2012;210:59–85.
43. Ricciotti E, Fitzgerald GA. Prostaglandins and inflammation. *Arterioscler. Thromb. Vasc. Biol.* 2011;31(5):986–1000.
44. Breyer RM, Bagdassarian CK, Myers SA, Breyer MD. P ROSTANOIDR ECEPTORS: Subtypes and Signaling 1. *Annu. Rev. Pharmacol. Toxicol.* 2001;41(1):661–690.
45. Morinelli TA, Niewiarowski S, Daniel JL, Smith JB. Receptor-mediated effects of a PGH2 analogue (U 46619) on human platelets. *Am J Physiol Hear. Circ Physiol*. 1987;253(U 46619):H1035–H1043.
46. Moncada S, Vane JR. Prostacyclin: its biosynthesis, actions and clinical potential. *Philos. Trans. R. Soc. Lond. B. Biol. Sci.* 1981;294(1072):305–329.
47. Woodward DF, Jones RL, Narumiya S. International Union of Basic and Clinical Pharmacology . LXXXIII : Classification of Prostanoid Receptors , Updating 15 Years of Progress. 2011;63(3):471–538.
48. Levin G, Duffin KL, Obukowicz MG, et al. Differential metabolism of dihomo-gamma-linolenic acid and arachidonic acid by cyclo-oxygenase-1 and cyclo-oxygenase-2: implications for cellular synthesis of prostaglandin E1 and prostaglandin E2. *Biochem. J.* 2002;365(Pt 2):489–96.
49. Kreutz RP, Nystrom P, Kreutz Y, et al. Inhibition of platelet aggregation by prostaglandin E1 (PGE1) in diabetic patients during therapy with clopidogrel and aspirin. *Platelets*. 2013;24(2):145–50.
50. Smith TM, Hicks-Berger CA, Kim S, Kirley TL. Cloning, expression, and characterization of a soluble calcium-activated nucleotidase, a human enzyme belonging to a new family of extracellular nucleotidases. *Arch. Biochem. Biophys.* 2002;406(1):105–15.

51. Patrono C, Andreotti F, Arnesen H, et al. Antiplatelet agents for the treatment and prevention of atherothrombosis. *Eur. Heart J.* 2011;32(23):2922–32.
52. Cecchetti L, Tolley ND, Michetti N, et al. Megakaryocytes differentially sort mRNAs for matrix metalloproteinases and their inhibitors into platelets: a mechanism for regulating synthetic events. *Blood*. 2011;118(7):1903–11.
53. Platelets, 3rd Edition | Alan Michelson | ISBN 9780123878373.
54. Rowley JW, Oler AJ, Tolley ND, et al. Genome-wide RNA-seq analysis of human and mouse platelet transcriptomes. *Blood*. 2011;118(14):e101-11.
55. McRedmond JP, Park SD, Reilly DF, et al. Integration of proteomics and genomics in platelets: a profile of platelet proteins and platelet-specific genes. *Mol. Cell. Proteomics*. 2004;3(2):133–44.
56. Schubert S, Weyrich AS, Rowley JW. A tour through the transcriptional landscape of platelets. *Blood*. 2014;
57. Lindemann S, Tolley ND, Eyre JR, et al. Integrins Regulate the Intracellular Distribution of Eukaryotic Initiation Factor 4E in Platelets: A CHECKPOINT FOR TRANSLATIONAL CONTROL. *J. Biol. Chem.* 2001;276(36):33947–33951.
58. Weyrich AS, Lindemann S, Tolley ND, et al. Change in protein phenotype without a nucleus: translational control in platelets. *Semin. Thromb. Hemost.* 2004;30(4):491–8.
59. Matera AG, Wang Z. A day in the life of the spliceosome. *Nat. Rev. Mol. Cell Biol.* 2014;15(2):108–121.
60. Denis MM, Tolley ND, Bunting M, et al. Escaping the nuclear confines: signal-dependent pre-mRNA splicing in anucleate platelets. *Cell*. 2005;122(3):379–91.
61. Warshaw AL, Laster L, Shulman NR. The stimulation by thrombin of glucose oxidation in human platelets. *J. Clin. Invest.* 1966;45(12):1923–1934.
62. Ts'ao C-H. Rough Endoplasmic Reticulum and Ribosomes in Blood Platelets. *Scand. J. Haematol.* 1971;8(2):134–140.

63. Kieffer N, Guichard J, Farcet JP, Vainchenker W, Breton-Gorius J. Biosynthesis of major platelet proteins in human blood platelets. *Eur. J. Biochem.* 1987;164(1):189–95.
64. Weyrich AS, Dixon DA, Pabla R, et al. Signal-dependent translation of a regulatory protein, Bcl-3, in activated human platelets. *Proc Natl Acad Sci U S A*. 1998;95(10):5556–5561.
65. Lindemann S, Tolley ND, Dixon DA, et al. Activated platelets mediate inflammatory signaling by regulated interleukin 1beta synthesis. *J. Cell Biol.* 2001;154(3):485–90.
66. Schubert P, Culibrk B, Karwal S, Goodrich RP, Devine D V. Protein translation occurs in platelet concentrates despite riboflavin/UV light pathogen inactivation treatment. *Proteomics - Clin. Appl.* 2016;10(8):839–850.
67. Angénieux C, Maitre B, Eckly A, et al. Time-dependent decay of mRNA and ribosomal RNA during platelet aging and its correlation with translation activity. *PLoS One*. 2016;11(1):e0148064.
68. Mills EW, Green R, Ingolia NT. Slowed decay of mRNAs enhances platelet specific translation. *Blood*. 2017;129(17):e38–e48.
69. Jonas S, Izaurralde E. Towards a molecular understanding of microRNA-mediated gene silencing. *Nat. Rev. Genet.* 2015;16(7):421–433.
70. Selbach M, Schwanhäusser B, Thierfelder N, et al. Widespread changes in protein synthesis induced by microRNAs. *Nature*. 2008;455(7209):58–63.
71. Bray PF, McKenzie SE, Edelstein LC, et al. The complex transcriptional landscape of the anucleate human platelet. *BMC Genomics*. 2013;14(1):1.
72. Sunderland N, Skroblin P, Barwari T, et al. MicroRNA Biomarkers and Platelet Reactivity. *Circ. Res.* 2017;120(2):418–435.
73. Landry P, Plante I, Ouellet DL, et al. Existence of a microRNA pathway in anucleate platelets. *Nat. Struct. Mol. Biol.* 2009;16(9):961–6.
74. Shi R, Ge L, Zhou X, et al. Decreased platelet miR-223 expression is associated with high on-clopidogrel platelet reactivity. *Thromb.*

Res. 2013;131(6):508–513.

75. Zhang Y-Y, Zhou X, Ji W-J, et al. Decreased circulating microRNA-223 level predicts high on-treatment platelet reactivity in patients with troponin-negative non-ST elevation acute coronary syndrome. *J. Thromb. Thrombolysis*. 2014;38(1):65–72.
76. Mutz K-O, Heilkenbrinker A, Lönne M, Walter J-G, Stahl F. Transcriptome analysis using next-generation sequencing. *Curr. Opin. Biotechnol.* 2013;24(1):22–30.
77. Eicher JD, Wakabayashi Y, Vitseva O, et al. Characterization of the platelet transcriptome by RNA sequencing in patients with acute myocardial infarction. *Platelets*. 2015;1–10.
78. Lood C, Amisten S, Gullstrand B, et al. Platelet transcriptional profile and protein expression in patients with systemic lupus erythematosus: Up-regulation of the type I interferon system is strongly associated with vascular disease. *Blood*. 2010;116(11):1951–1957.
79. Raghavachari N, Xu X, Harris A, et al. Amplified Expression Profiling of Platelet Transcriptome Reveals Changes in Arginine Metabolic Pathways in Patients With Sickle Cell Disease. *Circulation*. 2007;115(12):1551–1562.
80. Risitano A, Beaulieu LM, Vitseva O, Freedman JE. Platelets and platelet-like particles mediate intercellular RNA transfer. *Blood*. 2012;119(26):6288–6295.
81. Clancy L, Freedman JE. Blood-Derived Extracellular RNA and Platelet Pathobiology: Adding Pieces to a Complex Circulating Puzzle. *Circ. Res.* 2016;118(3):374–6.
82. Clancy L, Beaulieu LM, Tanriverdi K, Freedman JE. The role of RNA uptake in platelet heterogeneity. *Thromb. Haemost.* 2017;117(5):948–961.
83. Kirschbaum M, Karimian G, Adelmeijer J, et al. Horizontal RNA transfer mediates platelet-induced hepatocyte proliferation. *Blood*. 2015;
84. Provost P. The clinical significance of platelet microparticle-associated microRNAs. *Clin. Chem. Lab. Med.* 2017;55(5):657–

666.

85. Laffont B, Corduan A, Ple H, et al. Activated platelets can deliver mRNA regulatory Ago2bulletmicroRNA complexes to endothelial cells via microparticles. *Blood*. 2013;122(2):253–261.
86. Semple JW. Platelets deliver small packages of genetic function. *Blood*. 2013;122(2):155–156.
87. Gidlöf O, Van Der Brug M, Öhman J, et al. Platelets activated during myocardial infarction release functional miRNA, which can be taken up by endothelial cells and regulate ICAM1 expression. *Blood*. 2013;121(19):3908–3917.
88. Nilsson RJA, Balaj L, Hulleman E, et al. Blood platelets contain tumor-derived RNA biomarkers. *Blood*. 2011;118(13):.
89. Best MG, Sol N, Kooi I, et al. RNA-Seq of Tumor-Educated Platelets Enables Blood-Based Pan-Cancer, Multiclass, and Molecular Pathway Cancer Diagnostics. *Cancer Cell*. 2015;28(5):666–676.
90. Clancy L, Freedman JE. New paradigms in thrombosis: novel mediators and biomarkers platelet RNA transfer. *J. Thromb. Thrombolysis*. 2014;37(1):12–6.
91. Thompson CB, Eaton KA, Princiotta SM, Rushin CA, Valeri CR. Size dependent platelet subpopulations: relationship of platelet volume to ultrastructure, enzymatic activity, and function. *Br. J. Haematol.* 1982;50(3):509–519.
92. Yakimenko A, Verholomova F, Kotova Y, Ataullakhanov F, Panteleev M. Identification of Different Proaggregatory Abilities of Activated Platelet Subpopulations. *Biophys. J.* 2012;102(10):2261–2269.
93. Corash L, Costa JL, Shafer B, Donlon JA, Murphy D. Heterogeneity of human whole blood platelet subpopulations. III. Density-dependent differences in subcellular constituents. *Blood*. 1984;64(1):185–93.
94. Najean Y, Ardaillou N, Dresch C. Platelet lifespan. *Annu. Rev. Med.* 1969;20:47–62.
95. Ibrahim H, Schutt RC, Hannawi B, et al. Association of immature

platelets with adverse cardiovascular outcomes. *J. Am. Coll. Cardiol.* 64(20):2122–9.

96. Bernlochner I, Goedel A, Plischke C, et al. Impact of immature platelets on platelet response to ticagrelor and prasugrel in patients with acute coronary syndrome. *Eur. Heart J.* 2015;36(45):3202–10.
97. Vaduganathan M, Zemer-Wassercug N, Rechavia E, et al. Relation between ticagrelor response and levels of circulating reticulated platelets in patients with non-ST elevation acute coronary syndromes. *J. Thromb. Thrombolysis*. 2015;40(2):211–217.
98. Hoefer T, Armstrong PC, Finsterbusch M, et al. Drug-Free Platelets Can Act as Seeds for Aggregate Formation During Antiplatelet Therapy. *Arterioscler. Thromb. Vasc. Biol.* 2015;35(10):2122–33.
99. Di Minno MND, Lupoli R, Palmieri NM, et al. Aspirin resistance, platelet turnover, and diabetic angiopathy: a 2011 update. *Thromb. Res.* 2012;129(3):341–4.
100. Himmelfarb J, Holbrook D, McMonagle E, Ault K. Increased reticulated platelets in dialysis patients. *Kidney Int.* 1997;51(3):834–9.
101. Ibrahim H, Nadipalli S, Usmani S, et al. Detection and quantification of circulating immature platelets: agreement between flow cytometric and automated detection. *J. Thromb. Thrombolysis*. 2016;42(1):77–83.
102. Monteagudo Jiménez M, Guedán MJA, Muñoz Martín L, et al. Measurement of reticulated platelets by simple flow cytometry: An indirect thrombocytopoietic marker.
103. Chavda N, Mackie IJ, Porter JB, et al. Rapid flow cytometric quantitation of reticulated platelets in whole blood. *Platelets*. 1996;7(4):189–94.
104. Jiménez MM, Guedán MJA, Martín LM, et al. Measurement of reticulated platelets by simple flow cytometry: An indirect thrombocytopoietic marker. *Eur. J. Intern. Med.* 2006;17(8):541–4.
105. Briggs C, Hart D, Kunka S, Oguni S, Machin SJ. Immature platelet fraction measurement: a future guide to platelet transfusion requirement after haematopoietic stem cell transplantation.

Transfus. Med. 2006;16(2):101–109.

106. van der Linden N, Klinkenberg LJJ, Meex SJR, et al. Immature platelet fraction measured on the Sysmex XN hemocytometer predicts thrombopoietic recovery after autologous stem cell transplantation. *Eur. J. Haematol.* 2014;93(2):150–6.
107. Yamaoka G, Kubota Y, Nomura T, et al. The immature platelet fraction is a useful marker for predicting the timing of platelet recovery in patients with cancer after chemotherapy and hematopoietic stem cell transplantation. *Int. J. Lab. Hematol.* 2010;32(6 PART 1):e208–e216.
108. THE BASICS OF BLEEDING DISORDERS | Steps for Living.
109. Rick ME, Walsh CE, Key NS. Congenital bleeding disorders. *Hematol. Am. Soc. Hematol. Educ. Progr.* 2003;559–74.
110. Shoeb M, Fang MC. Assessing bleeding risk in patients taking anticoagulants. *J. Thromb. Thrombolysis*. 2013;35(3):312–9.
111. Li L, Geraghty OC, Mehta Z, Rothwell PM. Age-specific risks, severity, time course, and outcome of bleeding on long-term antiplatelet treatment after vascular events: a population-based cohort study. *Lancet*. 2017;
112. Collins PW, Chalmers E, Hart DP, et al. Diagnosis and treatment of factor VIII and IX inhibitors in congenital haemophilia: (4th edition). *Br. J. Haematol.* 2013;160(2):153–170.
113. Home - The Haemophilia Society.
114. Laffan MA, Lester W, O'Donnell JS, et al. The diagnosis and management of von Willebrand disease: A United Kingdom Haemophilia Centre Doctors Organization guideline approved by the British Committee for Standards in Haematology. *Br. J. Haematol.* 2014;167(4):453–465.
115. PEYVANDI F, JAYANDHARAN G, CHANDY M, et al. Genetic diagnosis of haemophilia and other inherited bleeding disorders. *Haemophilia*. 2006;12(s3):82–89.
116. Salles II, Feys HB, Iserbyt BF, et al. Inherited traits affecting platelet function. *Blood Rev.* 2008;22(3):155–72.
117. Nurden AT, Freson K, Seligsohn U. Inherited platelet disorders.

Haemophilia. 2012;18 Suppl 4:154–60.

118. Ramasamy I. Inherited bleeding disorders: Disorders of platelet adhesion and aggregation. *Crit. Rev. Oncol. Hematol.* 2004;49(1):1–35.
119. Bolton-Maggs PHB, Chalmers EA, Collins PW, et al. A review of inherited platelet disorders with guidelines for their management on behalf of the UKHCDO.
120. Andrews R, Berndt M. Bernard-Soulier Syndrome: An Update. *Semin. Thromb. Hemost.* 2013;39(6):656–662.
121. Savoia A, Kunishima S, De Rocco D, et al. Spectrum of the mutations in bernard-soulier syndrome. *Hum. Mutat.* 2014;35(9):1033–1045.
122. Nair S, Ghosh K, Kulkarni B, Shetty S, Mohanty D. Glanzmann's thrombasthenia: updated. *Platelets*. 2002;13(7):387–393.
123. Poon M-C, Di Minno G, d?Oiron R, Zotz R. New Insights Into the Treatment of Glanzmann Thrombasthenia. *Transfus. Med. Rev.* 2016;30(2):92–99.
124. Solh T, Botsford A, Solh M. Glanzmann's thrombasthenia: pathogenesis, diagnosis, and current and emerging treatment options. *J. Blood Med.* 2015;6:219–27.
125. Lecchi A, Razzari C, Paoletta S, et al. Identification of a new dysfunctional platelet P2Y12 receptor variant associated with bleeding diathesis. *Blood*. 2015;125(6):1006–1013.
126. Arthur JF, Dunkley S, Andrews RK. Platelet glycoprotein VI-related clinical defects. *Br. J. Haematol.* 2007;139(3):363–372.
127. Watson S, Daly M, Dawood B, et al. Phenotypic approaches to gene mapping in platelet function disorders - identification of new variant of P2Y12, TxA2 and GPVI receptors. *Hamostaseologie*. 2010;30(1):29–38.
128. Sasahara Y. WASP-WIP complex in the molecular pathogenesis of Wiskott-Aldrich syndrome. *Pediatr. Int.* 2016;58(1):4–7.
129. Stewart DM, Tian L, Nelson DL. Mutations that cause the Wiskott-Aldrich syndrome impair the interaction of Wiskott-Aldrich syndrome protein (WASP) with WASP interacting protein. *J.*

Immunol. 1999;162(8):5019–24.

130. Orange JS, Stone KD, Turvey SE, Krzewski K. The Wiskott-Aldrich syndrome. *Cell. Mol. Life Sci.* 2004;61(18):2361–2385.
131. Nurden AT, Nurden P. The gray platelet syndrome: Clinical spectrum of the disease. *Blood Rev.* 2007;21(1):21–36.
132. Blavignac J, Bunimov N, Rivard GE, Hayward CPM. Quebec platelet disorder: Update on pathogenesis, diagnosis, and treatment. *Semin. Thromb. Hemost.* 2011;37(6):713–719.
133. Favier R, Jondeau K, Boutard P, et al. Paris-Trousseau syndrome : clinical, hematological, molecular data of ten new cases. *Thromb. Haemost.* 2003;90(5):893–7.
134. El-Chemaly S, Young LR. Hermansky-Pudlak Syndrome. *Clin. Chest Med.* 2016;37(3):505–511.
135. Lozano ML, Rivera J, Sánchez-Guiu I, Vicente V. Towards the targeted management of Chediak-Higashi syndrome. *Orphanet J. Rare Dis.* 2014;9(1):132.
136. Nisar SP, Jones ML, Cunningham MR, Mumford AD, Mundell SJ. Rare platelet GPCR variants: What can we learn? *Br. J. Pharmacol.* 2015;172(13):3242–3253.
137. Nurden A, Nurden P. Advances in our understanding of the molecular basis of disorders of platelet function. *J. Thromb. Haemost.* 2011;9 Suppl 1:76–91.
138. Lentaigne C, Freson K, Laffan MA, et al. Inherited platelet disorders: toward DNA-based diagnosis. *Blood*. 2016;127(23):2814–2823.
139. Simeoni I, Stephens JC, Hu F, et al. A comprehensive high-throughput sequencing test for the diagnosis of inherited bleeding, thrombotic and platelet disorders. *Blood*. 2016;
140. Jones ML, Murden SL, Bem D, et al. Rapid genetic diagnosis of heritable platelet function disorders with next-generation sequencing: Proof-of-principle with Hermansky-Pudlak syndrome. *J. Thromb. Haemost.* 2012;10(2):306–309.
141. Watson SP, Lowe GC, Lordkipanidzé M, Morgan N V, GAPP consortium. Genotyping and phenotyping of platelet function

disorders. *J. Thromb. Haemost.* 2013;11 Suppl 1:351–63.
142. Westbury SK, Mumford AD. Genomics of platelet disorders. *Haemophilia*. 2016;22:20–24.
143. Westbury SK, Turro E, Greene D, et al. Human phenotype ontology annotation and cluster analysis to unravel genetic defects in 707 cases with unexplained bleeding and platelet disorders. *Genome Med.* 2015;7(1):36.
144. Sivapalaratnam S, Collins J, Gomez K. Diagnosis of inherited bleeding disorders in the genomic era. *Br. J. Haematol.* 2017;179(3):363–376.
145. Gnatenko D V., Dunn JJ, McCorkle SR, et al. Transcript profiling of human platelets using microarray and serial analysis of gene expression. *Blood*. 2003;101(6):2285–2293.
146. Londin ER, Hatzimichael E, Loher P, et al. The human platelet: strong transcriptome correlations among individuals associate weakly with the platelet proteome. *Biol. Direct*. 2014;9(1):3.
147. Liang H, Yan X, Pan Y, et al. MicroRNA-223 delivered by platelet-derived microvesicles promotes lung cancer cell invasion via targeting tumor suppressor EPB41L3. *Mol. Cancer*. 2015;14(1):58.
148. Freedman JE. A platelet transcriptome revolution. *Blood*. 2011;118(14):3760–1.
149. Schneider DJ, Holmes CE, Taatjes-Sommer HS, Sobel BE. Contributions of young platelets and of previously activated platelets to platelet reactivity in patients with coronary artery disease. *Thromb. Res.* 2008;121(4):455–62.
150. Born GVR. Aggregation of blood platelets by adenosine diphosphate and its reversal. *Nature*. 1962;194:927–9.
151. Chan M V, Armstrong PCJ, Papalia F, Kirkby NS, Warner TD. Optical multichannel (optimul) platelet aggregometry in 96-well plates as an additional method of platelet reactivity testing. *Platelets*. 2011;22(7):485–94.
152. Schmittgen TD, Livak KJ. Analyzing real-time PCR data by the comparative CT method. *Nat. Protoc.* 2008;3(6):.
153. Paniccia R, Priora R, Liotta AA, Abbate R. Platelet Function tests: A

Comparative Review. *Vasc. Health Risk Manag.* 2015;11:133–148.
154. Kaiser AFC, Neubauer H, Franken CC, et al. Which is the best anticoagulant for whole blood aggregometry platelet function testing? Comparison of six anticoagulants and diverse storage conditions. *Platelets*. 2012;23(5):359–67.
155. Kalb ML, Potura L, Scharbert G, Kozek-Langenecker SA. The effect of ex vivo anticoagulants on whole blood platelet aggregation. *Platelets*. 2009;20(1):7–11.
156. Wallén NH, Ladjevardi M, Albert J, Bröijersén A. Influence of Different Anticoagulants on Platelet Aggregation in Whole Blood; A Comparison between Citrate, Low Molecular Mass Heparin and Hirudin. *Thromb. Res.* 1997;87(1):151–157.
157. Cattaneo M, Hayward CP, Moffat KA, et al. Results of a worldwide survey on the assessment of platelet function by light transmission aggregometry: a report from the platelet physiology subcommittee of the SSC of the ISTH. *J. Thromb. Haemost.* 2009;7(6):1029.
158. Ames AC, Bamford E. An Appraisal of the Vacutainer System for Blood Collection. *Ann. Clin. Biochem. An Int. J. Biochem. Lab. Med.* 1975;12(1–6):151–155.
159. Cecchetti L, Tolley ND, Michetti N, et al. Megakaryocytes differentially sort mRNAs for matrix metalloproteinases and their inhibitors into platelets: a mechanism for regulating synthetic events. *Blood*. 2011;118(7):1903–11.
160. Mcbane RD, Gonzalez C, Hodge DO, Wysokinski WE. Propensity for young reticulated platelet recruitment into arterial thrombi. *J. Thromb. Thrombolysis*. 2014;37(2):148–154.
161. Hoffmann JJML. Reticulated platelets: analytical aspects and clinical utility. *Clin. Chem. Lab. Med.* 2014;52(8):1107–17.
162. Perl L, Lerman-Shivek H, Rechavia E, et al. Response to prasugrel and levels of circulating reticulated platelets in patients with ST-segment elevation myocardial infarction. *J. Am. Coll. Cardiol.* 2014;63(6):513–517.
163. Kim JH, Bae HY, Kim SY. Clinical marker of platelet hyperreactivity in diabetes mellitus. *Diabetes Metab. J.* 2013;37(6):423–8.

164. Wu Q, Ren J, Hu D, et al. An elevated percentage of reticulated platelet is associated with increased mortality in septic shock patients. *Medicine (Baltimore).* 2015;94(19):e814.
165. Joutsi-Korhonen L, Sainio S, Riikonen S, et al. Detection of reticulated platelets: estimating the degree of fluorescence of platelets stained with thiazole orange. *Eur. J. Haematol.* 2000;65(1):66–71.
166. Cesari F, Marcucci R, Gori AM, et al. Reticulated platelets predict cardiovascular death in acute coronary syndrome patients: Insights from the AMI-florence 2 study. *Thromb. Haemost.* 2013;109(5):846–853.
167. Stratz C, Bömicke T, Younas I, et al. Comparison of Immature Platelet Count to Established Predictors of Platelet Reactivity During Thienopyridine Therapy. *J. Am. Coll. Cardiol.* 2016;68(3):286–293.
168. Brooke MA, Longhurst HJ, Plagnol V, et al. Cryptogenic multifocal ulcerating stenosing enteritis associated with homozygous deletion mutations in cytosolic phospholipase A2-α. *Gut*. 2014;63(1):96–104.
169. Kohoutová D, Bártová J, Tachecí I, et al. Cryptogenic Multifocal Ulcerous Stenosing Enteritis: A Review of the Literature. *Gastroenterol. Res. Pract.* 2013;2013:1–7.
170. Sostres C, Lanas A. Gastrointestinal effects of aspirin. *Nat. Rev. Gastroenterol. Hepatol.* 2011;8(7):385–394.
171. Burke JE, Dennis EA. Phospholipase A2 structure/function, mechanism, and signaling. *J. Lipid Res.* 2009;50 Suppl(Suppl):S237-42.
172. Murakami M, Kudo I. Phospholipase A2. *J. Biochem.* 2002;131(3):285–92.
173. Dennis EA, Cao J, Hsu Y-H, Magrioti V, Kokotos G. Phospholipase A $_2$ Enzymes: Physical Structure, Biological Function, Disease Implication, Chemical Inhibition, and Therapeutic Intervention. *Chem. Rev.* 2011;111(10):6130–6185.
174. Sigal E. The molecular biology of mammalian arachidonic acid

metabolism. *Am.J.Physiol.* 1991;260(2 Pt 1):L13-28.

175. Murakami M, Taketomi Y, Miki Y, et al. Recent progress in phospholipase A2 research: From cells to animals to humans. *Prog. Lipid Res.* 2011;50(2):152–192.
176. Simmons DL, Botting RM, Hla T. Cyclooxygenase isozymes: the biology of prostaglandin synthesis and inhibition. *Pharmacol. Rev.* 2004;56(3):387–437.
177. Rouzer CA, Marnett LJ. Cyclooxygenases: structural and functional insights. *J. Lipid Res.* 2009;50 Suppl(Supplement):S29-34.
178. Ikei KN, Yeung J, Apopa PL, et al. Investigations of human platelet-type 12-lipoxygenase: role of lipoxygenase products in platelet activation. *J. Lipid Res.* 2012;53(12):2546–2559.
179. Adler DH, Cogan JD, Phillips JA, et al. Inherited human cPLA2α deficiency is associated with impaired eicosanoid biosynthesis, small intestinal ulceration, and platelet dysfunction. *J. Clin. Invest.* 2008;118(6):2121–31.
180. Kita Y, Ohto T, Uozumi N, Shimizu T. Biochemical properties and pathophysiological roles of cytosolic phospholipase A2s. *Biochim. Biophys. Acta - Mol. Cell Biol. Lipids*. 2006;1761(11):1317–1322.
181. Armstrong PCJ, Kirkby NS, Chan M V., et al. Novel whole blood assay for phenotyping platelet reactivity in mice identifies ICAM-1 as a mediator of platelet-monocyte interaction. *Blood*. 2015;126(10):e11–e18.
182. Kim D, Pertea G, Trapnell C, et al. TopHat2: accurate alignment of transcriptomes in the presence of insertions, deletions and gene fusions. *Genome Biol.* 2013;14(4):R36.
183. Lin LL, Wartmann M, Lin AY, et al. cPLA2 is phosphorylated and activated by MAP kinase. *Cell*. 1993;72(2):269–78.
184. Kirkby NS, Reed DM, Edin ML, et al. Inherited human group IVA cytosolic phospholipase A2 deficiency abolishes platelet, endothelial, and leucocyte eicosanoid generation. *FASEB J.* 2015;29(11):4568–78.
185. Eno K, Okuno T, Nishi K, et al. Pyrrolidine inhibitors of human cytosolic phospholipase A2. Part 2: Synthesis of potent and

crystallized 4-triphenylmethylthio derivative “pyrrophenone.” *Bioorganic Med. Chem. Lett.* 2001;11(4):587–590.

186. Ono T, Yamada K, Chikazawa Y, et al. Characterization of a novel inhibitor of cytosolic phospholipase A2alpha, pyrrophenone. *Biochem. J.* 2002;363(Pt 3):727–35.
187. Henderson WR, Chi EY, Bollinger JG, et al. Importance of group X–secreted phospholipase A2 in allergen-induced airway inflammation and remodeling in a mouse asthma model. *J. Exp. Med.* 2007;204(4):865–877.
188. Wong DA, Kita Y, Uozumi N, Shimizu T. Discrete role for cytosolic phospholipase A(2)alpha in platelets: studies using single and double mutant mice of cytosolic and group IIA secretory phospholipase A(2). *J. Exp. Med.* 2002;196(3):349–57.
189. Meyer AM, Dwyer-Nield LD, Hurteau GJ, et al. Decreased lung tumorigenesis in mice genetically deficient in cytosolic phospholipase A 2.
190. Yokomizo T, Murakami M. Bioactive lipid mediators : current reviews and protocols.
191. Yoda E, Rai K, Ogawa M, et al. Group VIB Calcium-Independent Phospholipase A2 (iPLA2γ) Regulates Platelet Activation, Hemostasis and Thrombosis in Mice. *PLoS One*. 2014;9(10):e109409.
192. Montrose DC, Kadaveru K, Ilsley JNM, et al. cPLA2 Is Protective Against COX Inhibitor–Induced Intestinal Damage. *Toxicol. Sci.* 2010;117(1):122–132.
193. Bonventre J V, Huang Z, Taheri MR, et al. Reduced fertility and postischaemic brain injury in mice deficient in cytosolic phospholipase A2. *Nature*. 1997;390(6660):622–625.
194. Uozumi N, Kume K, Nagase T, et al. Role of cytosolic phospholipase A2 in allergic response and parturition. *Nature*. 1997;390(6660):618–622.
195. Leslie CC. Properties and regulation of cytosolic phospholipase A2. *J. Biol. Chem.* 1997;272(27):16709–16712.
196. Jin J, Daniel JL, Kunapuli SP. Molecular basis for ADP-induced

platelet activation. II. The P2Y1 receptor mediates ADP-induced intracellular calcium mobilization and shape change in platelets. *J. Biol. Chem.* 1998;273(4):2030–4.

197. Daniel JL, Dangelmaier C, Jin J, et al. Molecular basis for ADP-induced platelet activation. I. Evidence for three distinct ADP receptors on human platelets. *J. Biol. Chem.* 1998;273(4):2024–9.
198. Puri RN, Colman RW, Liberman MA. ADP-Induced Platelet Activation. *Crit. Rev. Biochem. Mol. Biol.* 1997;32(6):437–502.
199. Roberts DE, McNicol A, Bose R. Mechanism of collagen activation in human platelets. *J. Biol. Chem.* 2004;279(19):19421–30.
200. Rittenhouse SE, Allen CL. Synergistic activation by collagen and 15-hydroxy-9 alpha,11 alpha-peroxidoprosta-5,13-dienoic acid (PGH2) of phosphatidylinositol metabolism and arachidonic acid release in human platelets. *J. Clin. Invest.* 1982;70(6):1216–24.
201. Pollock WK, Rink TJ, Irvine RF. Liberation of [3H]arachidonic acid and changes in cytosolic free calcium in fura-2-loaded human platelets stimulated by ionomycin and collagen. *Biochem. J.* 1986;235(3):869–77.
202. Ollivier V, Syvannarath V, Gros A, et al. Collagen can selectively trigger a platelet secretory phenotype via glycoprotein VI. *PLoS One*. 2014;9(8):e104712.
203. Purchase M, Dusting GJ, Li DM, Read MA. Physiological concentrations of epinephrine potentiate thromboxane A2 release from platelets in the isolated rat heart. *Circ. Res.* 1986;58(1):172–6.
204. Dunlop PC, Leis LA, Johnson GJ. Epinephrine correction of impaired platelet thromboxane receptor signaling. *Am. J. Physiol. Cell Physiol.* 2000;279(6):C1760-71.
205. Alanko J, Riutta A, Mucha I, et al. Adrenaline stimulates thromboxane and inhibits leukotriene synthesis in man. *Eicosanoids*. 1992;5(3–4):169–75.
206. Paul BZS, Jin J, Kunapuli SP. Molecular Mechanism of Thromboxane A 2 -induced Platelet Aggregation.
207. Donato R, Cannon BR, Sorci G, et al. Functions of S100 proteins. *Curr. Mol. Med.* 2013;13(1):24–57.

208. Donato R. S100: A multigenic family of calcium-modulated proteins of the EF-hand type with intracellular and extracellular functional roles. *Int. J. Biochem. Cell Biol.* 2001;33(7):637–668.
209. Sedaghat F, Notopoulos A. S100 protein family and its application in clinical practice. *Hippokratia*. 2008;12(4):198–204.
210. Donato R. Functional roles of S100 proteins, calcium-binding proteins of the EF-hand type. *Biochim. Biophys. Acta*. 1999;1450(3):191–231.
211. Schiopu A, Cotoi OS. S100A8 and S100A9: DAMPs at the crossroads between innate immunity, traditional risk factors, and cardiovascular disease. *Mediators Inflamm.* 2013;2013:1–10.
212. Healy AM, Pickard MD, Pradhan AD, et al. Platelet expression profiling and clinical validation of myeloid-related protein-14 as a novel determinant of cardiovascular events. *Circulation*. 2006;113(19):2278–2284.
213. Morrow DA, Wang Y, Croce K, et al. Myeloid-related protein 8/14 and the risk of cardiovascular death or myocardial infarction after an acute coronary syndrome in the Pravastatin or Atorvastatin Evaluation and Infection Therapy: Thrombolysis in Myocardial Infarction (PROVE IT-TIMI 22) trial. *Am. Heart J.* 2008;155(1):49–55.
214. Lood C, Tydén H, Gullstrand B, et al. Platelet-Derived S100A8/A9 and Cardiovascular Disease in Systemic Lupus Erythematosus. *Arthritis Rheumatol.* 2016;68(8):1970–1980.
215. Tyden H, Lood C, Gullstrand B, et al. Increased serum levels of S100A8/A9 and S100A12 are associated with cardiovascular disease in patients with inactive systemic lupus erythematosus. *Rheumatology*. 2013;52(11):2048–2055.
216. Wang Y, Fang C, Gao H, et al. Platelet-derived S100 family member myeloidrelated protein-14 regulates thrombosis. *J. Clin. Invest.* 2014;124(5):2160–2171.
217. Santilli F, Paloscia L, Liani R, et al. Circulating Myeloid-Related Protein-8/14 is Related to Thromboxane-Dependent Platelet Activation in Patients With Acute Coronary Syndrome, With and

Without Ongoing Low-Dose Aspirin Treatment. *J. Am. Heart Assoc.* 2014;3(4):e000903–e000903.

218. Larsen SB, Grove EL, Pareek M, et al. Calprotectin and Platelet Aggregation in Patients with Stable Coronary Artery Disease. *PLoS One*. 2015;10(5):e0125992.
219. Abbas A, Aukrust P, Dahl TB, et al. High Levels of S100A12 Are Associated With Recent Plaque Symptomatology in Patients With Carotid Atherosclerosis. *Stroke*. 2012;43(5):1347–1353.
220. Haas MJ. S100A9—clot not, bleed not. *Sci. Exch.* 2014;7(21):.
221. Bouzidi F, Doussiere J. Binding of arachidonic acid to myeloid-related proteins (S100A8/A9) enhances phagocytic NADPH oxidase activation. *Biochem. Biophys. Res. Commun.* 2004;325(3):1060–1065.
222. Karim S, Habib A, Lévy-Toledano S, Maclouf J. Cyclooxygenase-1 and -2 of endothelial cells utilize exogenous or endogenous arachidonic acid for transcellular production of thromboxane. *J. Biol. Chem.* 1996;271(20):12042–8.
223. Franke B, Akkerman JWN, Bos JL. Rapid Ca2+-mediated activation of Rap1 in human platelets. *EMBO J.* 1997;16(2):252–259.
224. Jung SM, Ohnuma M, Watanabe N, et al. Analyzing the mechanism of Rap1 activation in platelets: Rap1 activation is related to the release reaction mediated through the collagen receptor GPVI. *Thromb. Res.* 2006;118(4):509–521.
225. Frische EW, Zwartkruis FJT. Rap1, a mercenary among the Ras-like GTPases. *Dev. Biol.* 2010;340(1):1–9.
226. Schultess J, Danielewski O, Smolenski AP. Rap1GAP2 is a new GTPase-activating protein of Rap1 expressed in human platelets. *Blood*. 2005;105(8):3185–3192.
227. Neumüller O, Hoffmeister M, Babica J, et al. Synaptotagmin-like protein 1 interacts with the GTPase-activating protein Rap1GAP2 and regulates dense granule secretion in platelets. *Blood*. 2009;114(7):1396–1404.
228. Doumas S, Kolokotronis A, Stefanopoulos P. Anti-inflammatory and

antimicrobial roles of secretory leukocyte protease inhibitor. *Infect. Immun.* 2005;73(3):1271–4.

229. NIHR BioResource – Rare Diseases.
230. Genotyping and Phenotyping of Platelets - University of Birmingham.
231. Watson SP, Lowe GC, Lordkipanidzé M, Morgan N V. Genotyping and phenotyping of platelet function disorders. *J. Thromb. Haemost.* 2013;11 Suppl 1:351–63.
232. Williams CS, Mann M, DuBois RN. The role of cyclooxygenases in inflammation, cancer, and development. *Oncogene*. 1999;18(55):7908–16.
233. Perneby C, Wallén NH, Rooney C, Fitzgerald D, Hjemdahl P. Dose- and time-dependent antiplatelet effects of aspirin. *Thromb. Haemost.* 2006;95(4):652–8.
234. Awtry EH, Loscalzo J. Aspirin. *Circulation*. 2000;101(10):1206–1218.
235. Vane JR, Botting RM. The mechanism of action of aspirin. *Thromb. Res.* 2003;110(5–6):255–258.
236. Catella-Lawson F, Reilly MP, Kapoor SC, et al. Cyclooxygenase Inhibitors and the Antiplatelet Effects of Aspirin. *N. Engl. J. Med.* 2001;345(25):1809–1817.
237. Patrono C, Ciabattoni G, Patrignani P, et al. Clinical pharmacology of platelet cyclooxygenase inhibition. *Circulation*. 1985;72(6):1177–84.
238. FitzGerald GA. Mechanisms of platelet activation: Thromboxane A2 as an amplifying signal for other agonists. *Am. J. Cardiol.* 1991;68(7):B11–B15.
239. Rauzi F, Kirkby NS, Edin ML, et al. Aspirin inhibits the production of proangiogenic 15(S)-HETE by platelet cyclooxygenase-1. *FASEB J.* 2016;30(12):4256–4266.
240. Kemperman RFJ, Horvatovich PL, Hoekman B, et al. Comparative Urine Analysis by Liquid Chromatography−Mass Spectrometry and Multivariate Statistics: Method Development, Evaluation, and Application to Proteinuria. *J. Proteome Res.* 2007;6(1):194–206.

241. Goodeve A, James P. von Willebrand Disease. 1993.
242. Federici AB. Current and emerging approaches for assessing von Willebrand disease in 2016. *Int. J. Lab. Hematol.* 2016;38(S1):41–49.
243. Rodeghiero F. von Willebrand disease: Still an intriguing disorder in the era of molecular medicine. *Haemophilia*. 2002;8(3):292–300.
244. Castaman G, Linari S. Diagnosis and Treatment of von Willebrand Disease and Rare Bleeding Disorders. *J. Clin. Med.* 2017;6(4):.
245. Gadisseur A, Hermans C, Berneman Z, et al. Laboratory Diagnosis and Molecular Classification of von Willebrand Disease. *Acta Haematol.* 2009;121(2–3):71–84.
246. Detera SD, Becerra SP, Swack JA, Wilson SH. Studies on the Mechanism of. *J. Insect Physiol.* 1959;3(2):219–229.
247. Ghoshal K, Bhattacharyya M. Overview of Platelet Physiology: Its Hemostatic and Nonhemostatic Role in Disease Pathogenesis. *Sci. World J.* 2014;2014:1–16.
248. Estcourt LJ, Stanworth SJ, Doree C, et al. Comparison of different platelet count thresholds to guide administration of prophylactic platelet transfusion for preventing bleeding in people with haematological disorders after myelosuppressive chemotherapy or stem cell transplantation. *Cochrane database Syst. Rev.* 2015;11(11):CD010983.
249. Rendu F, Brohard-Bohn B. The platelet release reaction: granules' constituents, secretion and functions. *Platelets*. 2001;12(5):261–273.
250. SMYTH SS, MCEVER RP, WEYRICH AS, et al. Platelet functions beyond hemostasis. *J. Thromb. Haemost.* 2009;7(11):1759–1766.
251. Ware J, Corken A, Khetpal R. Platelet function beyond hemostasis and thrombosis. *Curr. Opin. Hematol.* 2013;20(5):451–456.
252. Beaulieu LM, Vitseva O, Tanriverdi K, et al. Platelet functional and transcriptional changes induced by intralipid infusion. *Thromb. Haemost.* 2016;115(6):1147–1156.
253. Plé H, Maltais M, Corduan A, et al. Alteration of the platelet transcriptome in chronic kidney disease. *Thromb. Haemost.*

2012;108(4):605–15.
254. GRAIL | Combining Science, Tech and Clinical Studies to Reveal Cancer.
255. Aravanis AM, Lee M, Klausner RD, et al. Next-Generation Sequencing of Circulating Tumor DNA for Early Cancer Detection. *Cell*. 2017;168(4):571–574.
256. Best MG, Sol N, Kooi I, et al. RNA-Seq of Tumor-Educated Platelets Enables Blood-Based Pan-Cancer, Multiclass, and Molecular Pathway Cancer Diagnostics. *Cancer Cell*. 2015;28(5):666–676.
257. Nilsson RJA, Karachaliou N, Berenguer J, et al. Rearranged EML4-ALK fusion transcripts sequester in circulating blood platelets and enable blood-based crizotinib response monitoring in non-small-cell lung cancer. *Oncotarget*. 2015;7(1):1066–1075.
258. Hayward CPM, Moffat K a., Raby A, et al. Development of North American consensus guidelines for medical laboratories that perform and interpret platelet function testing using light transmission aggregometry. *Am. J. Clin. Pathol.* 2010;134(6):955–963.
259. Christie DJ, Avari T, Carrington LR et al. Platelet function testing by aggregometry: Approved Guideline. Clinical and Laboratory Standards Institute, Wayne, PA: 2008.
260. Kleiman NS. Are Immature Platelets Growing Up?: Toward a New Marker of Antiplatelet Drug Resistance∗. *J. Am. Coll. Cardiol.* 2016;68(3):294–296.
261. Balduini CL, Noris P, Spedini P, et al. Relationship between size and thiazole orange fluorescence of platelets in patients undergoing high-dose chemotherapy.
262. Grove EL, Hvas A-M, Kristensen SD. Immature platelets in patients with acute coronary syndromes. *Thromb. Haemost.* 2009;101(1):151–6.
263. Lakkis N, Dokainish H, Abuzahra M, et al. Reticulated platelets in acute coronary syndrome: A marker of platelet activity. *J. Am. Coll. Cardiol.* 2004;44(10):2091–2093.

264. Lee EY, Kim SJ, Song YJ, Choi SJ, Song J. Immature platelet fraction in diabetes mellitus and metabolic syndrome. *Thromb. Res.* 2013;132(6):692–695.
265. Liu M, Li X-C, Lu L, et al. Cardiovascular disease and its relationship with chronic kidney disease. *Eur. Rev. Med. Pharmacol. Sci.* 2014;18(19):2918–26.
266. Armstrong PC, Hoefer T, Knowles RB, et al. Newly Formed Reticulated Platelets Undermine Pharmacokinetically Short-Lived Antiplatelet TherapiesHighlights. *Arterioscler. Thromb. Vasc. Biol.* 2017;37(5):949–956.
267. Lawrence MJ, Sabra A, Thomas P, et al. Fractal dimension: A novel clot microstructure biomarker use in ST elevation myocardial infarction patients. *Atherosclerosis*. 2015;240(2):402–407.
268. Knowles RB, Lawrence MJ, Ferreira PM, et al. Platelet reactivity influences clot structure as assessed by fractal analysis of viscoelastic properties. *Platelets*. 2017;1–9.
269. Sabra A, Lawrence MJ, Aubrey R, et al. Characterisation of clot microstructure properties in stable coronary artery disease. *Open Hear.* 2017;4(2):e000562.
270. Nesbitt WS, Westein E, Tovar-Lopez FJ, et al. A shear gradient–dependent platelet aggregation mechanism drives thrombus formation. *Nat. Med.* 2009;15(6):665–673.
271. JACKSON SP, NESBITT WS, WESTEIN E. Dynamics of platelet thrombus formation. *J. Thromb. Haemost.* 2009;7:17–20.
272. Swieringa F, Baaten CCFMJ, Verdoold R, et al. Platelet Control of Fibrin Distribution and Microelasticity in Thrombus Formation Under FlowSignificance. *Arterioscler. Thromb. Vasc. Biol.* 2016;36(4):692–699.
273. Whyte CS, Swieringa F, Mastenbroek TG, et al. Plasminogen associates with phosphatidylserine-exposing platelets and contributes to thrombus lysis under flow. *Blood*. 2015;125(16):2568–2578.
274. Munnix ICA, Cosemans JMEM, Auger JM, Heemskerk JWM. Platelet response heterogeneity in thrombus formation. *Thromb.*

Haemost. 2009;102(6):1149–56.

275. Agbani EO, van den Bosch MTJ, Brown E, et al. Coordinated Membrane Ballooning and Procoagulant Spreading in Human Platelets. *Circulation*. 2015;132(15):1414–24.
276. Polanowska-Grabowska R, Gibbins JM, Gear ARL. Platelet Adhesion to Collagen and Collagen-Related Peptide Under Flow: Roles of the 2 1 Integrin, GPVI, and Src Tyrosine Kinases. *Arterioscler. Thromb. Vasc. Biol.* 2003;23(10):1934–1940.
277. Ruggeri ZM. Platelet adhesion under flow. *Microcirculation*. 2009;16(1):58–83.
278. Moroi M, Jung SM, Shinmyozu K, et al. Analysis of platelet adhesion to a collagen-coated surface under flow conditions: the involvement of glycoprotein VI in the platelet adhesion. *Blood*. 1996;88(6):2081–92.
279. Nagy M, Heemskerk JWM, Swieringa F. Use of microfluidics to assess the platelet-based control of coagulation. *Platelets*. 2017;28(5):441–448.
280. Sally Davies et al. Annual Report of the Chief Medical Officer 2016. London: 2017.
281. Roberts M. Chief medical officer calls for gene testing revolution. *BBC News*. 2017;1.
282. Feero WG. Clinical Application of Whole-Genome Sequencing Proceed With Care. *JAMA*. 2014;311(10):1017–1019.
283. Bainbridge MN, Wiszniewski W, Murdock DR, et al. Whole-Genome Sequencing for Optimized Patient Management. *Sci. Transl. Med.* 2011;3(87):87re3-87re3.
284. Witney AA, Gould KA, Arnold A, et al. Clinical application of whole-genome sequencing to inform treatment for multidrug-resistant tuberculosis cases. *J. Clin. Microbiol.* 2015;53(5):1473–83.
285. Stavropoulos DJ, Merico D, Jobling R, et al. Whole-genome sequencing expands diagnostic utility and improves clinical management in paediatric medicine. *npj Genomic Med.* 2016;1(1):15012.
286. Turro E, BioResource N. Whole Genome Sequencing of 10,000

Rare Disease Patients Reveals Digenic Inheritance of Blood Disorders. *Blood*. 2016;128(22):.